2011

Characterisation of Metallo-Cyclodextrins for Chiral Separations

Gary Hessman
Technological University Dublin, Ireland

Characterisation of Metallo-Cyclodextrins for Chiral Separations

By

Gary Hessman BSc.

A Thesis Submitted to the Dublin Institute of Technology,
for the Degree of Doctor of Philosophy.

Supervised by Dr. Mary McNamara

School of Chemical and Pharmaceutical Sciences
Dublin Institute of Technology
Kevin Street, Dublin 8.

2011

Abstract

Almost half of commercial pharmaceuticals are chiral and therefore effective analytical techniques to detect and quantify enantiomers are important in the pharmaceutical sector to ensure drug safety and efficacy.

In this work copper(II) complexes of aminoalkane derivatives of *β*-cyclodextrin (CDEn, CDPn and CDBn) were investigated to determine if they provide a versatile solution for the direct separation of the enantiomers of DOPA, benserazide and carbidopa using capillary electrophoresis. Tyrosine was used as a model compound.

Electronic spectroscopy was used in order to determine if copper(II) coordinates to the amino-CDs and to determine if further coordination to the guest species occurs. Decreases in λ_{max} for the d-d transitions on coordination of the metal ion suggest the formation of a CuCDAm binary complex with CDEn and CDPn acting as bidentate ligands and CDBn acting as a monodentate ligand. A further blue shift on the introduction of a guest species suggests further coordination of copper(II) and formation of ternary complexes of tyrosine and DOPA with all three metallo-complexes of the aminoalkane derivatives. A ternary complex also formed between CuCDEn and L-carbidopa. No coordination was evident with benserazide. These results suggest that the use of these metallo-cyclodextrin derivatives for enantioselection may be guest specific if ternary complex formation is required for separation.

Cicular dichroism (c.d.) can show the differential inclusion of enantiomers in cyclodextrin cavities and therefore was used here to determine if the metallo-cyclodextrins can differentiate between enantiomers. Increases in intensity of the bands in the spectra indicate deeper inclusion of a guest in the CD cavity. From the results obtained in this study it can be shown that the binary complex CuCDEn is the most

enantioselective material of those studied towards both tyrosine and DOPA. CuCDPn and CuCDBn showed no enantioselection.

The stoichiometry of all complexes was determined using electronic spectroscopy and Job's method of continuous variation. A 1:1 binary complex formed between Cu(II) and CDEn. It was also shown that CuCDEn formed a 1:1 ternary complex with tyrosine and a 2:1 complex with DOPA. Results also suggested that both 1:1 and 2:1 complexes of CuCDEn and L-carbidopa were formed.

Using CE in normal polarity mode and a background electrolyte (BGE) at pH 6.8, separation of the enantiomers of DOPA was not achieved using CuCDEn as a chiral selector. The stability of the binary complex is limited by pH and therefore CDEn alone was used as the chiral selector. Separation of L-DOPA from L-carbidopa was achieved using CDEn in a BGE at pH 2.5 and a resolution of 2.36 was obtained. However it was still not possible to separate the isomers of DOPA. An alternative charged CD derivative, sulfated-β-cyclodextrin was investigated and was found to successfully separate the enantiomers of D,L-DOPA in a BGE of pH 2.5 and a resolution of 3.62 was obtained.

These results suggest that amino-cyclodextrin derivatives are guest specific for chiral separations in capillary electrophoresis and do not represent a universal method for separations required for regulatory compliance. Since separations were obtained using the anionic sulfated derivatives it is suggested that host molecules with a permanent charge are more useful and therefore inclusion is not the only factor needed for separation to be successful.

Declaration

I certify that this thesis, which I now submit for examination for the award of PhD, is entirely my own work and has not been taken from the work of others save and to the extent that such work has been cited and acknowledged within the text of my work.

This thesis was prepared according to the regulations for postgraduate study by research of the Dublin Institute of Technology and has not been submitted in whole or in part for an award in any other Institute or University.

The work reported on in this thesis conforms to the principles and requirements of the Institute's guidelines for ethics in research.

The Institute has permission to keep, to lend or to copy this thesis in whole or in part, on condition that any such use of the material of the thesis be duly acknowledged.

Signature_____ Date_____

Gary Hessman

Acknowledgements

Throughout the course of my PhD I owe many people sincere thanks for their help and support. This thesis would not have become a reality without them.

Firstly I would like to thank my supervisor Dr Mary McNamara for her guidance, support and insight during the project. From her I have learned that no problem is insurmountable and with patience and hard work any puzzle can be unravelled.

Sincere thanks must also be attributed to Professor John Cassidy and Dr Antonino Mazzaglia for their work as internal and external readers on the revision of the thesis.

To Professor Hugh Byrne and the staff of the Focas Institute thank you for providing such a welcoming and unique place to work. Since 2005 I have worked there as a summer student and postgrad and it has become a home from home where I have undoubtedly made friends for life. To the technical staff, thank you Theresa and Andrew (sorry for infecting my PC more than once!). Special thanks to Luke and Anne for not only their support on the instruments but for when times were hard there was always a cup of coffee a biscuit and a listening ear in their office.

I must also show my appreciation to the members of the MSA lab for providing a friendly atmosphere in which to work. To the original crew, Dr Ciarán Potter and Dr Paddy Lynch thank you for taking a young Padawan under your wing! Thank you to Aja, Catriona, Mark 1 and Mark 2, Crystal, Raj, Andrew and Zlata also. To those who have become fast friends Nick, Mim and Damo I cannot fully express my appreciation to you. Without you I would have either gone mad or given up, cheers pals! For long winded rants and chats over pints and United games thank you to my oldest friend and Best man Dave.

Thank you to my family both immediate and extended. This thesis has been a mystery to you all and now that it is finished please don't ask me to explain it again! And no I

cannot write out your prescriptions sorry. To my Mam and Dad, yes I have finally finished school!! Thank you for all the packed lunches, ironed shirts, lifts after late labs and the countless things you have both done for me. To Tracy and Jason thank you for keeping me grounded, there was absolutely no chance of me getting a big head with you two around!

To my little Pocket Granny R.I.P. You didn't get to see me become a doctor but I know you are proud of me. Thank you for knitted jumpers, plasters over scraped knees, endless dinners and all your prayers. I will miss that welcoming smile every time I came in the door. You will never be forgotten.

I must also acknowledge the best madra in the world Jessie, my little shadow who sat under my feet while I wrote this thesis. She proved a dog really is a man's best friend!

Most importantly I would like to thank the person who has been the greatest influence in my life, my wife Anne. You had the most thankless task supporting the lifelong student! From sitting up late at night helping me memorise formulae in third year to never letting me wander off the path when times got tough. Yet again we will be standing in a church holding hands in October! Your unwavering dedication, devotion, enthusiasm and love have seen us through some very hard times and it is impossible to sum up all you have done for me. You are my everything, I love you Bee.

Dedication

I dedicate this thesis to my loving wife Anne and to the memory of my Grandmother Mona Hanway (1922-2011) R.I.P.

"Done is better than perfect"

Scott Allen

List of Abbreviations

AAB	Ammonium Acetate Buffer
ACN	Acetonitrile
APD	Anti- Parkinson's Disease
B_0	Applied Magnetic Field
BH	Benesi-Hildebrand
BGE	Background Electrolyte
Boc	*N-tert*-Butoxycarbonyl-*β*-Alanylhistamine
Bn	1,4-Diaminobutane
BP	Butyl *p*-Hydroxybenzoate
c.d.	Circular Dichroism
CD	Cyclodextrin
CDAm	Diaminoalkane Cyclodextrin Derivatives
CDBn	6-Deoxy-6-[1-(4-Amino)Butylamino]-*β*-Cyclodextrin
CDEn	6-Deoxy-6-[1-(2-Amino)Ethylamino]-*β*-Cyclodextrin
CDPn	6-Deoxy-6-[1-(3-Amino)Propylamino]-*β*-Cyclodextrin
CDTs	6-*O*-Monotosyl-6-Deoxy-*β*-Cyclodextrin
CD-CZE	Cyclodextrin Modified Capillary Zone Electrophoresis

CD-EKC	Cyclodextrin Modified Electrokinetic Chromatography
CD-MEKC	Cyclodextrin Modified Micellar Electrokinetic Chromatography
CE	Capillary Electrophoresis
CGE	Capillary Gel Electrophoresis
CIEF	Capillary Isoelectric Focusing
CIP	Cahn Ingold Prelog
CITP	Capillary Isotachophoresis
CZE	Capillary Zone Electrophoresis
δ	Chemical Shift
Δε	Molar Extinction Coefficient in Circular Dichroism
DMSO	Dimethylsulphoxide
DNS	Dansyl
D_2O	Deuterium Oxide
DOPA	3,4-dihydroxyphenylalanaine
DOS	Degree of Substitution
ε	Molar Extinction Coefficient in Absorption Spectroscopy Dielectric Constant in CE
EKC	Electrokinetic Chromatography
En	1,2-Diaminoethane

EOF	Electroosmotic Flow
FDA	Food and Drug Administration
FIR	Far-Infrared
GC	Gas Chromatography
HPLC	High Performance Liquid Chromatography
HSQC	Heteronuclear Single Quantum Coherence
i.c.d.	Induced Circular Dichroism
i.d.	Internal Diameter
LEC	Ligand Exchange Chromatography
LECE	Ligand Exchange Capillary Electrophoresis
NMR	Nuclear Magnetic Resonance
MEKC	Micellar Electrokinetic Chromatography
MeOH	Methanol
MPA	Mobile Phase Additive
μ	Mobility in CE / Nuclear Magnetic Moment in NMR
NSAIDs	Non-Steroidal Anti-Inflammatory Drugs
v	Velocity
PAHs	Polyaromatic Hydrocarbons
PD	Parkinson's Disease

Phe	Phenylalanine
Pn	1,3-Diaminopropane
R_s	Resolution
S	Selectivity
SDS	Sodium Dodecyl Sulphate
θ	Ellipticity
TMS	Tetramethylsilane
Ts	Tosyl
Tyr	Tyrosine
VAT	Value Added Tax
ζ	Zeta Potential

Table of Contents

List of Figures

List of Tables

List of Schemes

1. Introduction

1.1 Introduction

Chiral molecules lack an internal plane of symmetry and have non-superimposable mirror images. They are extremely important in the pharmaceutical industry with 56 % of drugs currently in use being chiral compounds and a further 88% of these chiral drugs being used as racemates.[1] An example of such a racemate is D,L-sotalol (D-sotalol is an anti-arrhythmic while L-sotalol is a beta-blocker).[2]

1.1.1 Isomerism

The renowned French chemist Louis Pasteur is credited with the discovery of the existence of molecular chirality and isomerism. He found that the sodium ammonium salt of racemic tartaric acid crystallised as a mixture of two different crystals, which he separated using a microscope and tweezers.[3] He postulated that the isomers have different three-dimensional arrangements of atoms, and are non-superimposable mirror images of one another, both on a macro scale and on a micro scale.

Isomers are compounds with the same molecular formula, but vary in the orientation or connectivity of atoms and can be divided into two classes, constitutional isomers and stereoisomers. Constitutional isomers have the same molecular formula but differ in the way their atoms are connected. Examples of constitutional isomers 1-propanol, 2-propanol and ethyl methyl ether can be seen in Figure 1.1.

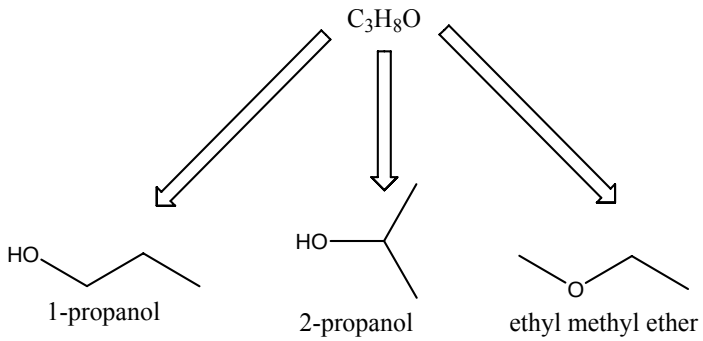

Figure 1.1 Constitutional isomers of C_3H_8O

Unlike the atoms in constitutional isomers, the atoms in stereoisomers have the same connectivity but are different in their three-dimensional orientation in space. Stereoisomers can be further subdivided into two distinct groups, enantiomers and diastereoisomers.[4]

Enantiomers are defined as stereoisomers with the same molecular formula that are non-superimposable mirror images i.e. chiral molecules. They possess identical physical properties such as melting point, boiling point and solubility. Enantiomers behave in the same manner when reacted with an achiral molecule, but react differently to one another when reacted with another chiral compound. Diastereoisomers are stereoisomers that have the same molecular formula but are not mirror images of each other and unlike enantiomers they do have different physical properties. Figure 1.2 gives an overview of isomerism.

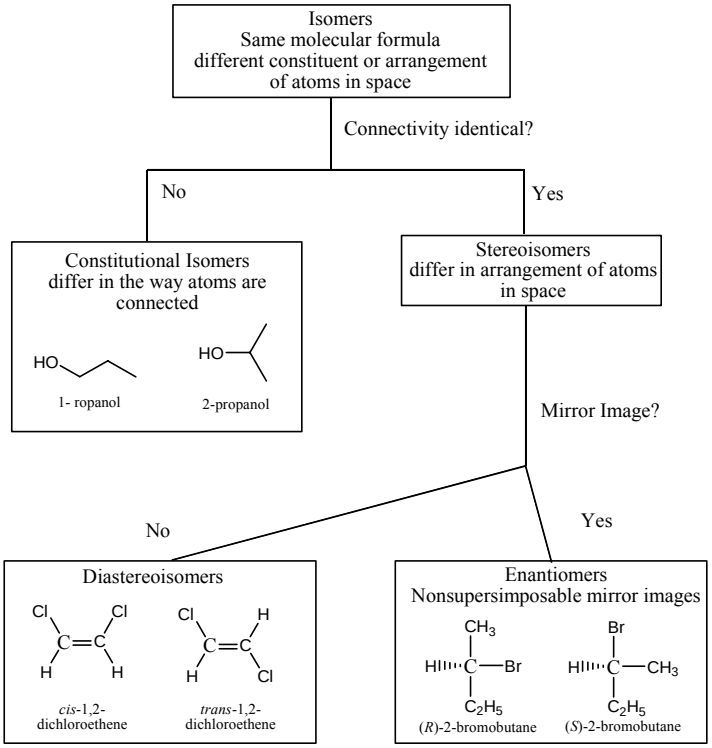

Figure 1.2 Overview of isomerism[5]

The most important difference between enantiomers is their interaction with plane polarised light. Plane polarised light oscillates in one plane only and when passed through a solution of one pure enantiomer of a compound it is rotated, the angle of rotation being an inherent property of the material. Therefore enantiomers are also called optical isomers. One of the enantiomers will rotate the plane clockwise to the right and is labelled the (+) enantiomer, while the other enantiomer will rotate the plane by an equivalent angle to the left and is labelled (-). A racemic solution contains the same concentration of the two enantiomers and will give no overall rotation of the plane polarised light.

1.1.2 Designating Isomers

Chiral molecules were named initially using (+) and (-) signs or *d* (dextro) and *l* (levo) indicating the direction in which the enantiomers rotate the plane of polarised light. *d* or

(+) denotes rotation to the right (clockwise) and *l* or (-) rotation to the left (anti-clockwise). However there is the possibility of confusion with the designation D or L used for amino acids and carbohydrates.

Emil Fischer is credited with the designation of isomers of both carbohydrates and amino acids. By drawing a molecule of glyceraldehyde in a two-dimensional form (Fischer Projection) he defined one isomer as being D on the basis that the hydroxyl group attached to C2 is on the right hand side of the molecule. The other enantiomer is defined as L because the hydroxyl group is situated on the left hand side of the molecule.

D-glyceraldehyde L-glyceraldehyde

Figure 1.3 Fischer projections of the isomers of glyceraldehyde with carbon atoms numbered

This notation was also extended to the assignment of amino acids. L enantiomers are those in which the amino group is on the left hand side of the Fischer projection (when the carboxyl group appears at the top). Conversely the D enantiomers are those in which the amino group is on the right hand side.

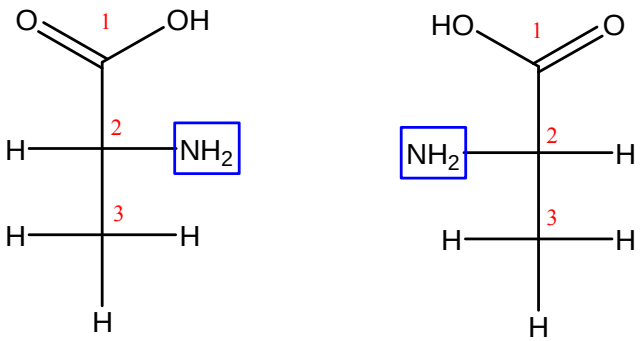

D-alanine L-alanine

Figure 1.4 Fischer projections of the isomers of alanine

The drawback to all these systems of nomenclature is that they either only relate to optical activity or are somewhat ambiguous for definitive structural configuration. To overcome these difficulties the Cahn–Ingold–Prelog system was introduced.

Cahn-Ingold-Prelog notation (CIP notation) provides an unambiguous description of a stereoisomer of a compound. The assignment of *R* or *S* according to CIP notation follows a sequence of rules shown in Figure 1.5. In step 1 the groups are prioritised on the basis of the decrease in the atomic number of the atoms directly bonded to the centre of chirality. In cases where two or more of these atoms are identical, the next bonded atoms have to be considered and then eventually the third bonded atoms and so on. The branch containing the atom with the highest atomic number has the highest priority. In step 2 the group of lowest priority is rotated to the back. Finally the *R* configuration is determined as the structure, where the increasing order of priority (1 to 4) is clockwise. The *S* configuration shows the increasing order of priority in a counter-clockwise direction. It is important to note however, that the designation of *R* and *S* is independent of the direction the isomers rotate plane polarised light.

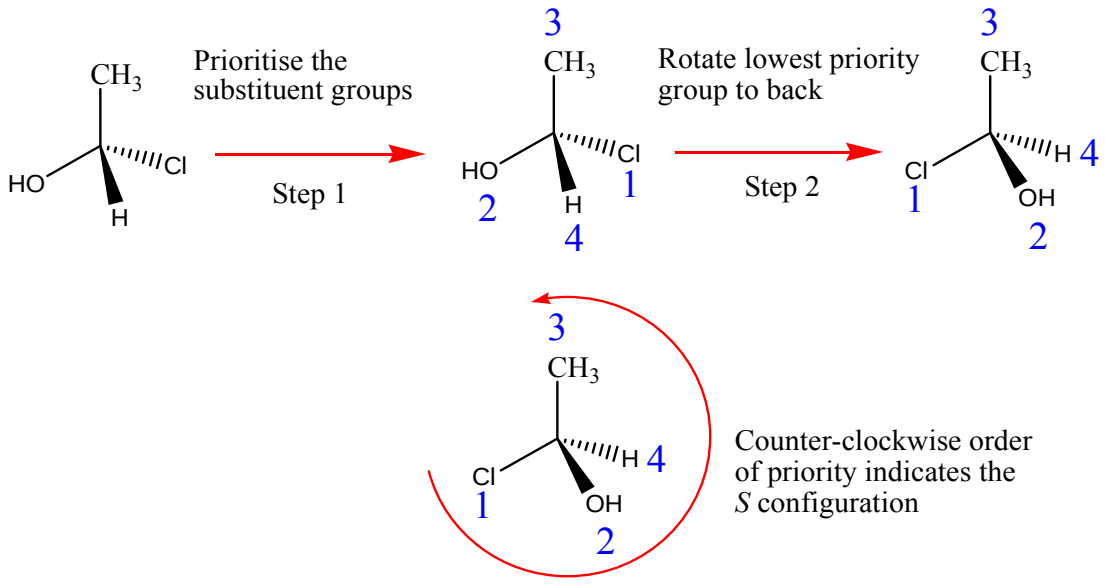

Figure 1.5 Selection rules for Cahn-Ingold-Prelog notation

1.1.3 Chiral Pharmaceuticals

The majority of racemic pharmaceuticals have one major bioactive enantiomer (eutomer) and a less bioactive enantiomer (distomer). The distomer can be toxic or even exert a totally undesired pharmacological affect.[6] It is also possible for racemic drugs to have equally bioactive enantiomers. Cyclophosphamide (anti-neoplastic), flecainide (anti-arrhythmic) and fluoxetine (anti-depressant) are among this latter group.[7]

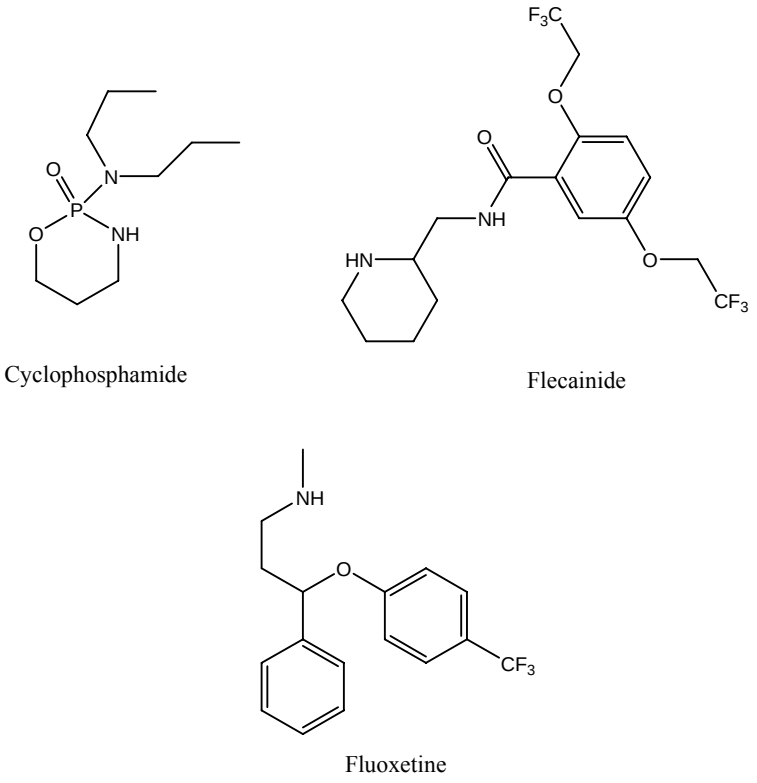

Cyclophosphamide

Flecainide

Fluoxetine

Figure 1.6 Structures of cyclophosphamide, flecainide and fluoxetine

A third group of racemic drugs also exists, where chiral inversion can take place. This can happen in two ways, unidirectional and bidirectional conversion. Ibuprofen falls into the category of unidirectional conversion, where only the *S* enantiomer is active (analgesic / anti-inflammatory) but a significant amount of the *R* enantiomer is converted to *S* (and not *vice versa*) *in vivo*.

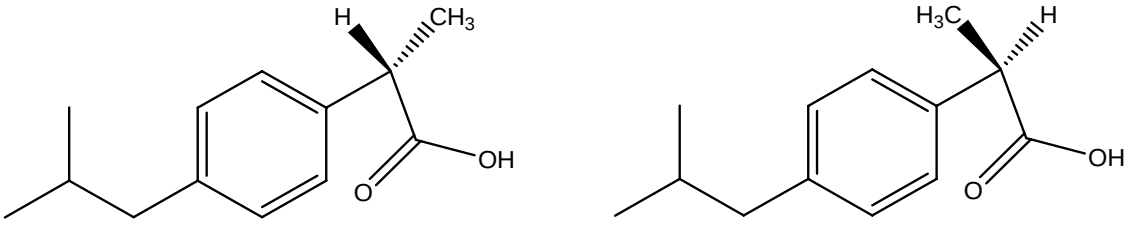

S-Ibuprofen *R*-Ibuprofen

Figure 1.7 Structures of *S* and *R*-ibuprofen

Therefore, even when ibuprofen is administered in racemic form, the drug exhibits 75% of the activity of the pure *S* form at the same dose level.[8]

Thalidomide is a famous example of bidirectional conversion (racemisation). Thalidomide was a racemic sedative removed from the market in the 1960s due to severe teratogenic side-effects. It was discovered that the *S* enantiomer was responsible for these ill effects. However administration of the *R* enantiomer alone would have made no difference as the thalidomide enantiomers can interconvert. It was this case that started the drive to treat the undesirable enantiomer as an unwanted component or indeed an impurity which must be eliminated.

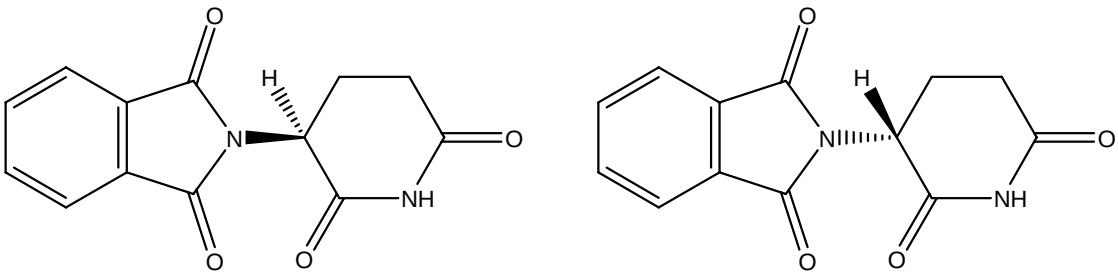

S-Thalidomide *R*-Thalidomide

Figure 1.8 Structures of *S* and *R*-thalidomide

The drug studied in this work is dihydroxyphenylalanine (DOPA) which is the most effective drug at present for Parkinson's disease which results from reduced levels of dopamine in the brain. L-DOPA is the active isomer and is converted to dopamine *via* decarboxylation catalysed by L-amino acid decarboxylase (L-DOPA decarboxylase). D-

DOPA is inactive. Dopamine itself cannot be used to treat the disease since it cannot cross the blood-brain barrier. L-DOPA however can undergo extracerebral decarboxylation to dopamine and is therefore administered in conjunction with the inhibitor carbidopa. Benserazide can also inhibit decarboxylation. Both inhibitors do not cross the blood-brain barrier and therefore do not inhibit conversion of L-DOPA to dopamine in the brain. The amino acid tyrosine is used as a simpler model compound in this work and is also a precursor in the synthesis of L-DOPA. The structures of the compounds studied are given in Figure 1.9.

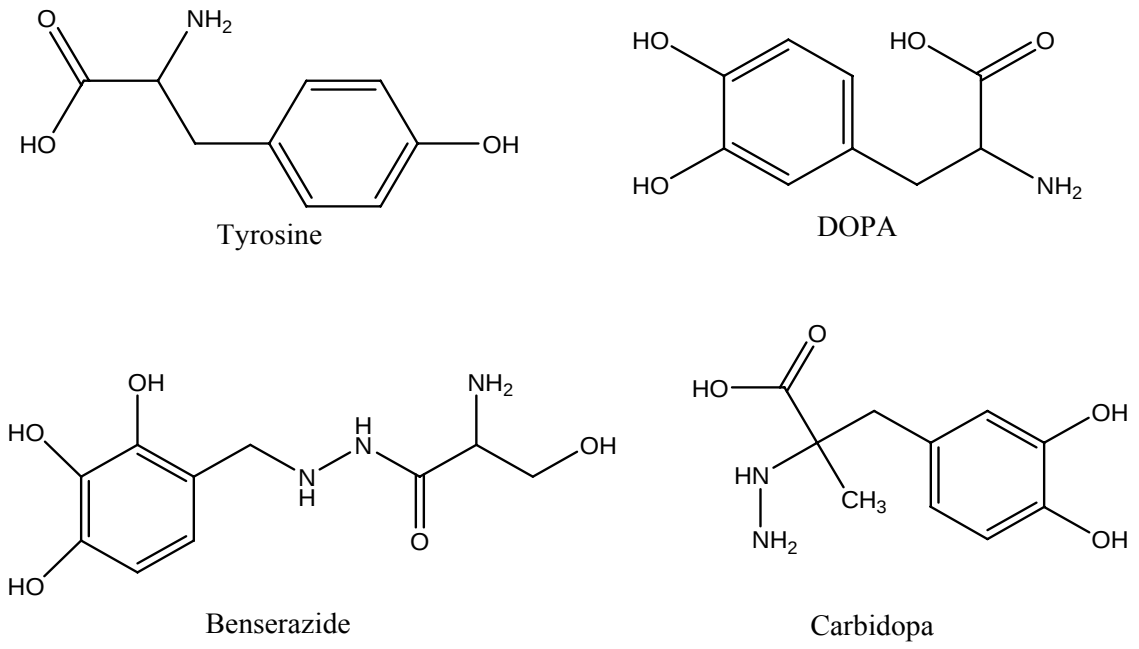

Figure 1.9 Structures of tyrosine, DOPA, benserazide and carbidopa

In 1992 the Food and Drug Administration (FDA) issued a policy statement encouraging pharmaceutical companies to use recent advances in synthetic and separation techniques to develop single enantiomeric drugs.

"The stereoisomeric composition of a drug with a chiral centre should be known and the quantitative isomeric composition of the material used in pharmacologic,

toxicologic, and clinical studies should be known. Specifications for the final product should assure identity, strength, quality, and purity from a stereochemical viewpoint".[2] *"When the drug product is a racemate and the pharmacokinetic profiles (what the body does to the drug) of the isomers are different, manufacturers should monitor the enantiomers individually to determine such properties as dose linearity and the effects of altered metabolic or excretory function and drug-drug interactions".*[2]

Therefore there is a need for methods for the separation and analysis of chiral materials. BCC Market Research has predicted that the market for chiral synthesis, resolution and analysis of products will grow at 2.8 per cent per year and reach $5.1 billion by 2014. Much of this growth is due to the pharmaceutical industry's development of chirally pure drugs, encouraged by FDA policies.[9]

1.1.4 Current Separation Methods for Chiral Pharmaceuticals

Enantiomers share many of the same characteristic properties *e.g.* boiling point, melting point, solubility, molecular weight and size, therefore making their separation difficult. Clearly the ideal way to obtain a pure single enantiomeric drug would be to employ enantioselective synthesis. However this is not always a practical or cost effective option. Therefore, the separation of racemic mixtures of intermediates or final products is a common practice. To carry out enantiomeric separation a number of chromatographic techniques exist including, high performance liquid chromatography (HPLC), gas chromatography (GC), supercritical fluid chromatography (SFC) and thin layer chromatography (TLC).[10] More recently several electrophoretic techniques have become popular such as capillary electrophoresis (CE).[11,12] A review by Timothy J. Ward and Karen D. Ward of chiral separations publications from 2008 to 2010 showed that HPLC and CE are the most widely used techniques in the field. Of the two

techniques HPLC is by far the most used with a conservative estimate of 1000 publications on chiral separations appearing in the two year period.[13]

Chiral separations by CE and HPLC can be broken down into two classifications, indirect and direct separation. Indirect separation involves reaction of the enantiomers with an enantiomerically pure reagent followed by the separation of the diastereomeric derivatives by HPLC or CE. This approach can be particularly advantageous if strongly UV absorbing or fluorescent derivatives are produced, which can lead to an increase in the limit of detection by electronic absorption or fluorescence. However using this method requires reagents of high stereochemical purity and includes extra synthetic steps leading to an increase in cost and time of analysis. Examples of some derivatisation reagents include (+)-1(9-fluorenyl)ethyl chloroformate (FLEC), 2,3,4,6-tetra-*O*-acetyl-*β*-D-glucopyranosyl isothiocyanate (GITC) and Marfey's reagent which are used in the separation and detection of amino acids.[14]

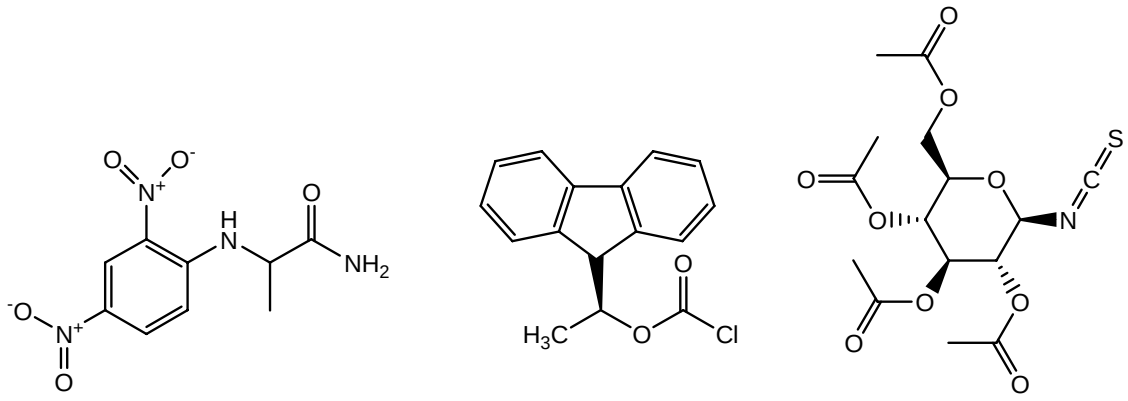

Figure 1.10 Structures of some chiral derivitisation reagents

Direct separations require the presence of a chiral selector which is able to form transient diastereomeric complexes with the analyte enantiomers. In CE the selector can be added to the background electrolyte (BGE), while in HPLC the selector can be dissolved in the mobile phase. It is also possible to have the chiral selector present in the

packing material of the column *i.e.* chiral stationary phase (CSP). Examples of some chiral selectors are cyclodextrins and their derivatives, chiral crown ethers and macrocyclic antibodies. Molecularly imprinted polymers are also used to a lesser extent.[13]

HPLC is considered the industry standard for analytical separations. However there are many economic disadvantages associated with the method such as the initial cost of the instruments and the cost of large volumes of solvents. Also indirect chiral separations generally require derivatisation of the analyte under investigation which can be time consuming and can lead to longer analysis times due to the extra sample preparation step. Direct methods for chiral separations, which are becoming more popular with advances in column manufacturing, use specialised column packing. Here cyclodextrins have found a role, but the disadvantage is that these columns are expensive and have low versatility. Take for example a Phenomenex Chirex column, containing D-penicillamine with a metal ion linker which can be used for ligand exchange chiral separations. This column costs in the region of €1,400 to €1,560 (excluding VAT) depending on column dimensions, which compares to ~ €300 for a commonly used C18 column. The versatility of many these chiral columns can be quite poor whereby they are only effective for one class of analytes.

Capillary electrophoresis (CE) on the other hand consists of simpler less expensive equipment, uses millilitre quantities of solvent (usually inexpensive aqueous buffers) and milligram quantities of chiral selectors. Also capillaries cost in the region of €60 each (excluding VAT) and have theoretical plate numbers measured in the hundreds of thousands compared to thousands for HPLC. Disadvantages of CE include its inability to perform preparative scale separations, issues with reproducibility and poor limits of detection due to a short optical path through the capillary for detection.

1.1.5 Cyclodextrins

Cyclodextrins (CDs) are neutral and water soluble cyclic oligosaccharides of several glucopyranose units which can be used as chiral selectors. They are chiral due to the presence of asymmetric carbon atoms on the glucose units and glycosidic bridges between the glucose units. Figure 1.11 gives the structures of the three most widely used cyclodextrins. Cyclodextrins are named by the number of repeating glucopyranose units in their structure. α-CD has 6, β-CD has 7 and γ-CD has 8 glucose units. They are produced from the degradation of starch by the enzyme glycosyltransferase.[15] The process involves the cleavage of a turn of the starch helix followed by intramolecular cyclisation.[16] CDs have a characteristic truncated cone structure with a cavity of different dimensions depending on CD type (α being the smallest). The external surface of a CD is hydrophilic due to it containing hydroxyl groups, while its inner cavity is hydrophobic as it is lined with ether-like anomeric oxygen atoms. It is this cavity that makes CDs such useful tools, as they are capable of including guest molecules of different types, particularly those with non-polar groups. Among all the potential hosts available today, (*e.g*. dendrimers and crown ethers) cyclodextrins are significant, due to the following reasons:[17]

- CDs are semi-natural products as they are produced from a renewable source (starch) by a relatively simple enzymatic conversion.
- They are produced on an industrial scale (thousands of tons per year) by environmentally friendly technologies.
- The scale of their production has reduced their initially high prices to a level acceptable for most industrial applications.
- Their inclusion ability can be significantly altered by derivatisation and is already widely used in many industrial products, technologies and analytical

methods. Indeed worldwide there are 30-40 different drugs marketed as cyclodextrin complexes.[18, 19, 20]

- Any of their toxic effects are of secondary character and can be eliminated by selecting the appropriate CD type or derivative.

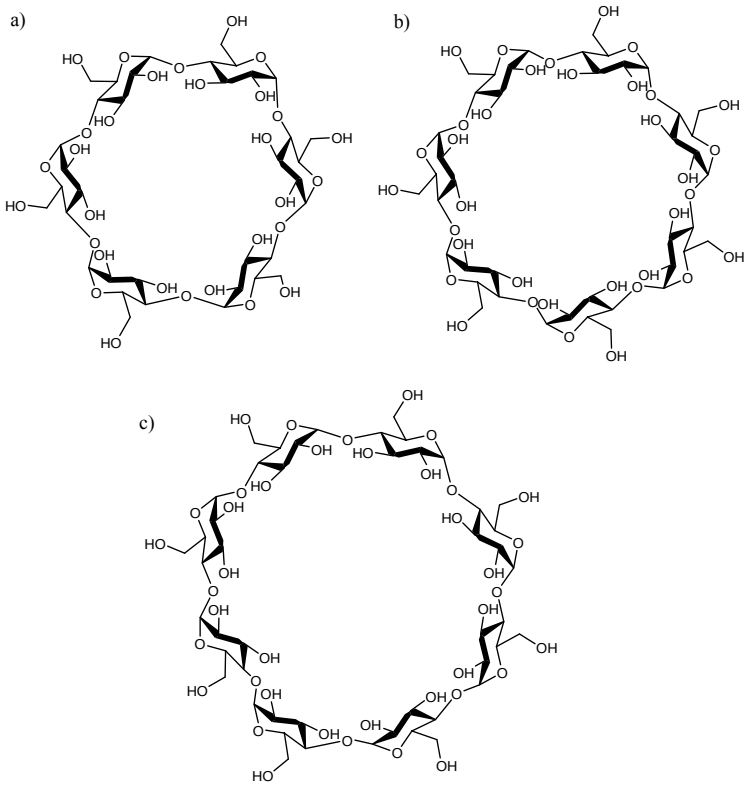

Figure 1.11 Structures of a) *α*-CD, b) *β*-CD and c) *γ*-CD, viewed from the secondary hydroxyl group face

1.1.6 Inclusion Complexes

In aqueous solutions, the less polar cavity of cyclodextrins is occupied by water molecules. Due to polar-apolar interaction this is energetically unfavourable and in the presence of a less polar molecule the water molecules are replaced by the guest molecule. The most frequent and simplest host:guest ratio is 1:1. However 2:1, 1:2, 2:2 and higher order equilibria can exist.[17] The formation of the inclusion complexes can be described by the following thermodynamic equilibrium where G is the guest molecule,

$$CD + G \rightleftharpoons CD.G$$

$$K_{1:1} = \frac{[CD.G]}{[CD][G]}$$ Equation 1.1

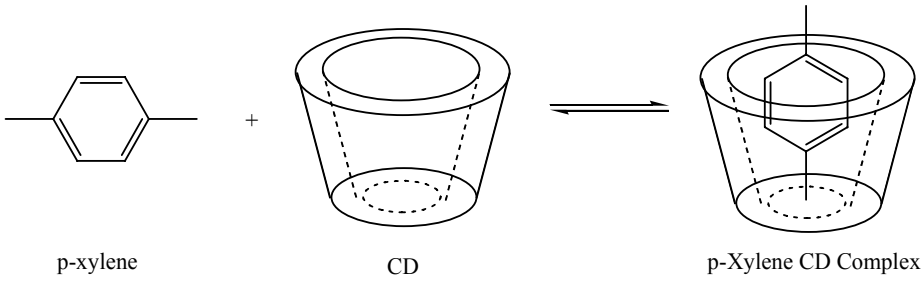

Figure 1.12 Schematic representation of inclusion of *p*-xylene by CD; solvent is omitted for clarity

It is the inclusion ability of CDs that is exploited in this work and more crucially their ability to discriminate between enantiomers. Native cyclodextrins however are poor chiral discriminating agents.[21] Literature suggests that the presence of a metal ion centre, introducing further structural restrictions on any complex formed, can greatly enhance chiral discrimination particularly in the cases of some amino acids.[22] However CDs are also inefficient coordinating ligands because of intramolecular hydrogen bonding. This function can be enhanced by modifying the cyclodextrin which has the dual effect of increasing solubility and coordinating ability.[23]

The choice of CD is a very important factor and is the first step in creating a chiral selector. This choice is essentially dependant on the enantiomers to be resolved. As the aim of this project is to investigate chiral selectors based on metallo-CDs for the separation of the enantiomers of tyrosine and DOPA, a cyclodextrin with the appropriate cavity size must be selected. If the cavity is too small no inclusion will be

possible and if the cavity is too large, it is reasonable to assume that the non-covalent bonds responsible for inclusion will not be strong enough to hold the guest in place.

α-CD has been shown to include low molecular weight molecules or compounds with aliphatic side chains. β-CD can include aromatic compounds and heterocycles while γ-CD is more suited to inclusion of macrocycles and steroids.[24] β-CD was chosen as the ideal candidate in this work as its cavity dimensions are the appropriate size for the inclusion of benzene ring-based molecules.[25] These dimensions are shown in Figure 1.13 while Table 1.1 shows some of the physical properties of cyclodextrins.

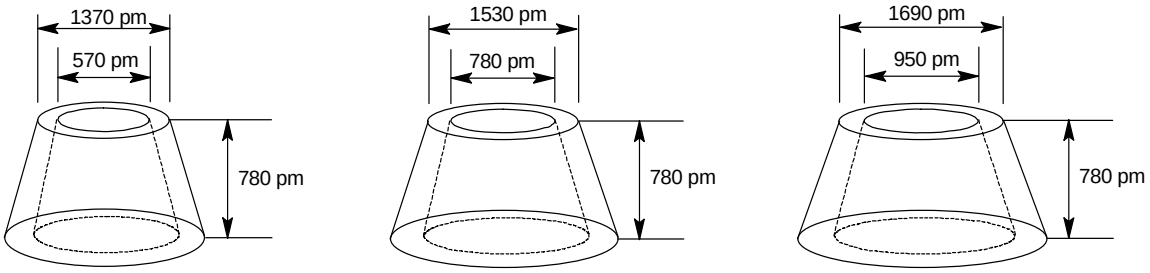

Figure 1.13 Cyclodextrin dimensions

Table 1.1 Physical properties of α-CD, β-CD and γ-CD

	α-CD	β-CD	γ-CD
Number of glucopyranose units	6	7	8
Molecular weight (anhydrous)	972.85	1134.99	1297.14
Solubility in H_2O at room temp. ($g/100\ cm^3$)	14.50	1.85	23.20
Annular diameter measured from the C5 hydrogens (pm)	470	600	750
Annular diameter measured from the C3 hydrogens (pm)	520	640	830
Annular depth from the primary to the secondary hydroxyl groups (pm)	~800	~800	~800
Annular volume, pm^3	17400	26200	42700
Partial molar volume ($cm^3\ mol^{-1}$)	611.4	703.8	801.2
$[\alpha]_D$ at 25 °C	+150.5	+162.5	+177.4
pK_a at 25 °C	12.33	12.20	12.08

1.1.7 Cyclodextrins and Metal Ions

As metal ions behave as Lewis acids (electron pair acceptors), they have the ability to bond with a vast number of both organic and inorganic molecules. To facilitate this bonding one condition is that the molecules must have one or more electron pairs available for donation *i.e.* Lewis bases. The resulting species is called a coordination complex and the electron pair donors are called ligands. The Irving-Williams series allows selection of a metal ion that forms the most stable metal-ligand complexes. From the series it is clear that Cu^{2+} has the highest stability constant and is therefore used in this work.[26]

$$Mn^{2+} < Fe^{2+} < Co^{2+} < Ni^{2+} < Cu^{2+} > Zn^{2+}$$

$\longrightarrow$ Increasing ionic potential and stability constant

Figure 1.14 Irving Williams series

Cyclodextrins can behave as first sphere or second sphere ligands. They can also behave simultaneously as both first and second sphere ligands. It was Alfred Werner in 1893 who proposed that the coordinating influence of many transition metal complexes extends beyond their covalently bound first sphere ligands to noncovalently bound species in the second sphere.[27]

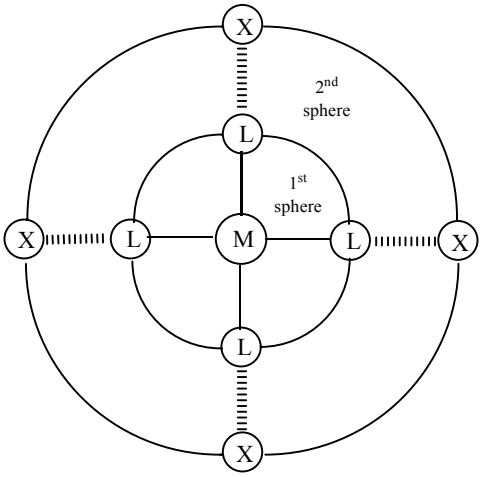

Figure 1.15 Representation of first and second sphere coordination where M is the metal ion, L is the first sphere ligand and X is the second sphere ligand

Costes *et al.* demonstrated the first use of second sphere coordination by molecular receptors using crown ethers, which formed adducts with transition metal complexes containing aqua ligands.[28] Crown ethers have also been shown to form adducts with transition metal amine complexes.[29] In these complexes strong hydrogen bonds are formed between the oxygen atoms of the crown ether and the protons of the neutral first sphere ligands.

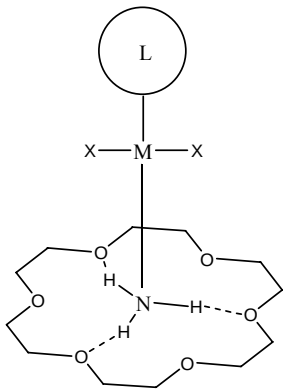

Figure 1.16 Second sphere coordination of a metal amine complex by 18-crown-6 where L = organic ligand and X = inorganic ligand

Some of the earliest work on CDs as second sphere coordination ligands was carried out by Siegel and Breslow using CD-ferrocene coordination complexes.[30] Harada and Takahashi also investigated crystalline samples of ferrocene and CDs and found that for α-CD a 2:1 complex was formed whereas β-CD and γ-CD each formed a 1:1 complex with ferrocene.[31] (Figure 1.17)

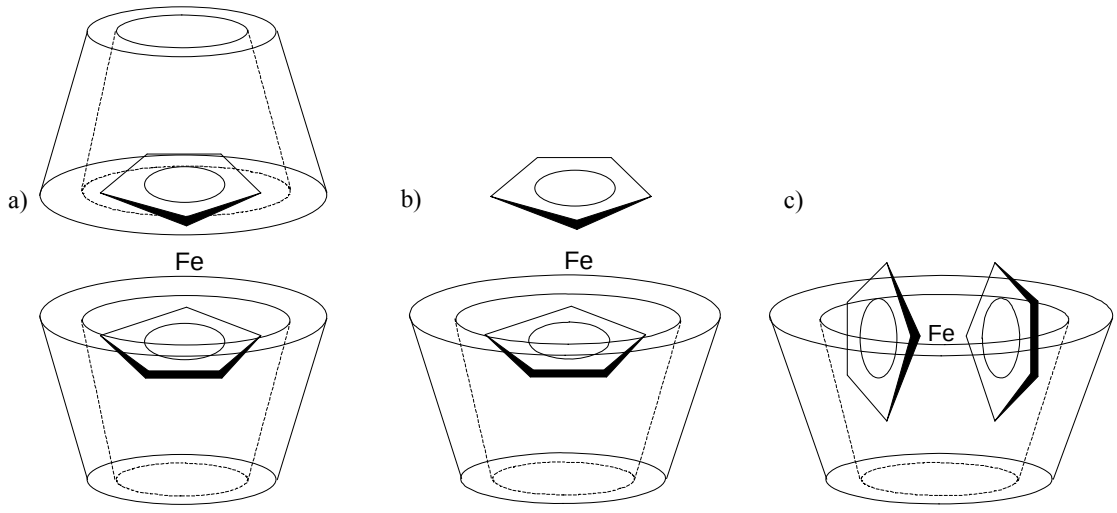

Figure 1.17 Proposed structures of ferrocene inclusion complexes of a) α-CD, b) β-CD and c) γ-CD using second sphere coordination

Critical to the work reported here is the ability of cyclodextrins to act as first sphere ligands. CDs are inefficient first sphere ligands, but this can be improved by

deprotonation of the hydroxyl groups at high pH. Matsui *et al.* were the first to report the formation of a metal-CD complex with the metal ion coordinated directly to the cyclodextrin.[32] Figure 1.18 shows the proposed binuclear hydroxyl-bridged structure for this complex. Nair and Dismukes prepared a complex of *β*-CD with Mn(III) with a Mn:CD ratio of 2:1.[33] A bridged structure similar to that proposed by Matsui was supported by electronic and vibrational spectroscopy results.

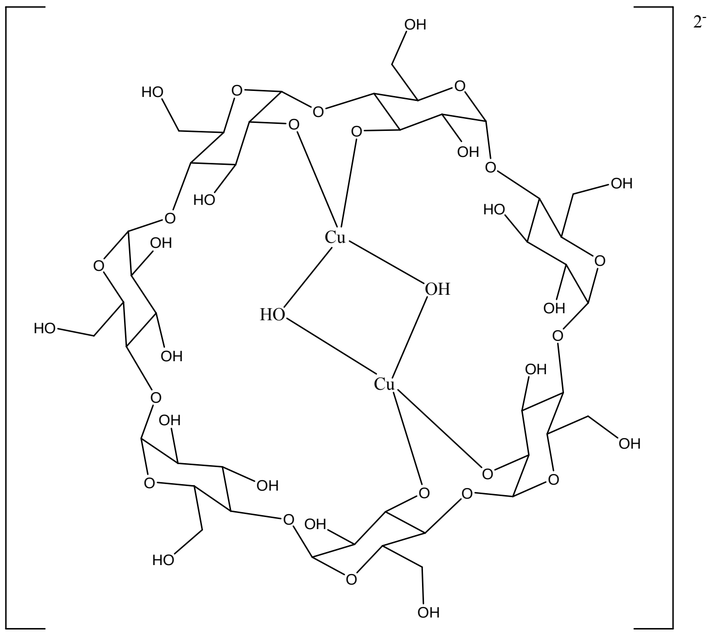

Figure 1.18 Proposed binuclear bridged structure of the $[Cu_2(OH)_2$-*β*-$CD]^{2-}$ complex

The possibility of simultaneous second sphere interaction in this complex was proposed by Stoddart and Zarycki.[34] They postulated that hydrogen bonding could link the secondary hydroxyl groups of the CD with the hydroxyl groups of the bridged structure. This suggestion that cyclodextrins may act as both first and second sphere ligands simultaneously was supported by vibrational spectroscopy studies carried out by Russell and McNamara.[35] Further studies from this group showed that similar complexes are formed by a range of metal ions with *β*-CD such as Mn(III), Cr(III), Fe(III), Co(II) and Cu(II).[36]

Modifying cyclodextrins can also allow them to act as first sphere ligands for metal coordination. These derivatised CDs have been used as metallo-enzyme mimics and as catalysts. Breslow and Overman prepared the nickel(II) chelate of an *α*-CD ester of pyridine-2,5-dicarboxylic acid (Figure 1.19).[23] The electron donating nitrogen and oxygen atoms allow for the coordination of the metal ion. This derivative was further developed by Szejtli and Pagington resulting in "Breslow's Enzyme" which increased the rate of hydrolysis of *p*-nitrophenylacetate over 1000-fold.[37]

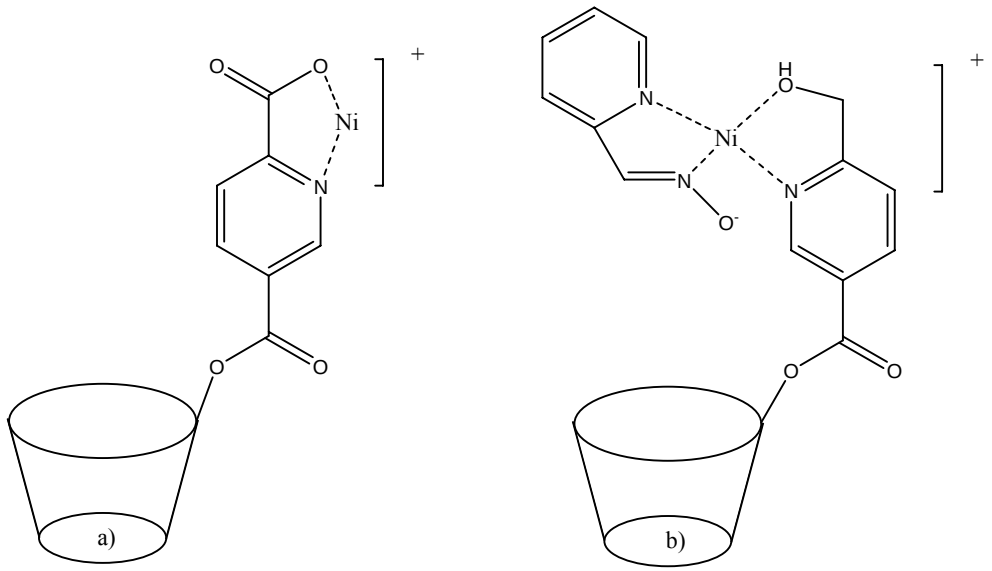

Figure 1.19 Proposed structures of a) Ni(II) chelate coordinated to *α*-CD ester of pyridine-2,5-dicarboxylic acid and b) Breslow's Enzyme

Nitrogen-modified cyclodextrins have been reported to be particularly efficient ligands for first sphere coordination of various metal ions. Matsui *et al.* reported the synthesis of the 6-deoxy-6-[1-(2-amino)ethylamino]-*β*-cyclodextrin (CDEn) derivative which was shown to form a complex with Cu(II) at a pH of 10.5.[38] Figure 1.20 shows the proposed structure of the complex.

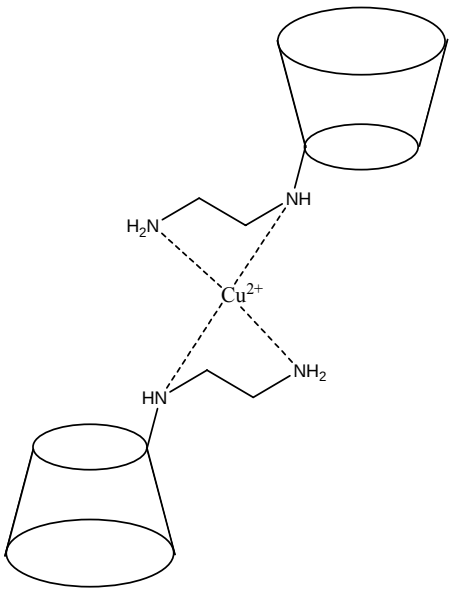

Figure 1.20 Proposed structure of the Cu(II) complex with the diaminoethane-*β*-CD derivative CDEn

Bonomo *et al.* showed that at a pH of 7.8 a 1:1 complex of CDEn and Cu(II) formed and that this complex displayed some enantiomeric stereoselectivity towards amino acids.[39] Brown *et al.* reported similar selectivity using a range of metal centres (Co(II), Ni(II), Cu(II) and Zn(II)) with a diaminopropane derivative of *β*-CD, CDPn.[40] Work previously carried out by this group demonstrated how the choice of metal centre can enhance the enantioselectivity of a hydroxylethylamine-CD derivative (CDea).[41]

Therefore critical to this work is the selective modification of the primary hydroxyl group on the C6 position of *β*-CD to take advantage of the metal ion coordination properties of amino CDs.

1.1.8 Functionalised Cyclodextrins

There are many different functional groups, for example methyl and hydroxypropyl groups, which can be introduced onto the cyclodextrin molecule by reaction of the hydroxyl groups lining the upper and lower ridges of the toroid. The result is a large number of possible positional and optical isomers since each hydroxyl group differs in its chemical reactivity and the resultant cyclodextrin products are amorphous.

Theoretically a cyclodextrin molecule can have up to 3(n) substituents, where n is the number of glucopyranose units that comprise the CD molecule. This is called the degree of substitution (DOS) and refers to substituents other than hydrogen.

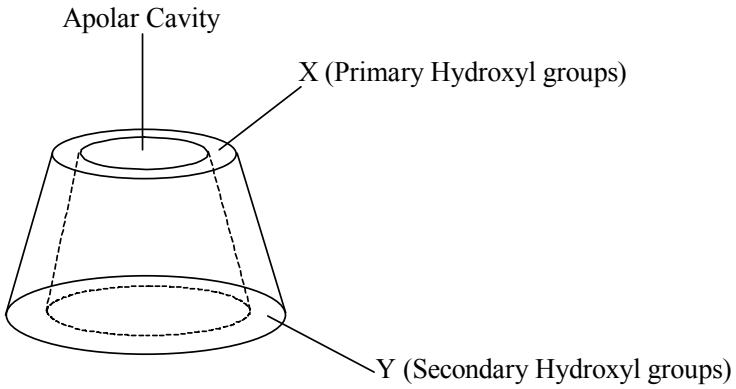

Figure 1.21 Cyclodextrin substituents

Figure 1.21 shows substituent X, following the replacement of one C6 hydroxyl group whereas substituent Y involves replacement of one of the C2 or C3 hydroxyl groups. The multiple numbers of hydroxyls on cyclodextrins enables many possible modifications. This was highlighted in 1998 by Cyclodextrin News, which stated that more than 1500 new derivatives were reported from 1985 to 1997.[42]

1.1.9 Modification Involving the C6 Primary Hydroxyl Group

Selective modification of the C6 hydroxyl groups on the CD is assisted by the fact that the primary face of the torus suffers less steric hindrance than the secondary. In addition there is less hydrogen bonding between the hydroxyls at C6 than those at C2 and C3. Also the primary hydroxyl groups of CDs are the most basic and most nucleophilic and can be selectively modified through reaction with an electrophilic species.

Amino derivatives of CDs can be prepared by an indirect approach. For example hemispherodextrins shown in Figure 1.22 have been reported by Cucinotta *et al*. These capped cyclodextrins namely, 6A,6D-dideoxy-6A,6D-[6,6'-dideoxy-6,6'-di(S-cysteamine)-α,α'-trehalose]-β-CD (THCMH) [43], 6A,6D-dideoxy-6A,6D-N-[6,6'-di-(β-alanylamino)-6,6'-dideoxy-α,α'-trehalose]-β-CD (THALA)[44] and 6A,6D-(6,6'-diamino-α,α'-trehalose)-6A,6D-dideoxy-β-CD (THAMH)[45] which have been shown to be effective chiral selectors for amino acids using Capillary Electrophoresis were synthesised from the 6A,6D-dideoxy-6A,6D-diiodo-β-cyclodextrin intermediate.

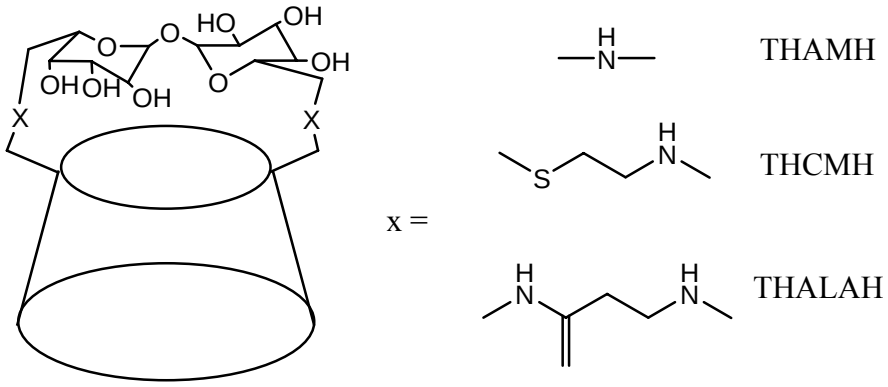

Figure 1.22 Schematic structures of hemispherodextrins

A more widely used intermediate is mono-6-deoxy-6-tosyl-*β*-cyclodextrin (CDTs). A common method for preparation of CDTs involves reaction of *β*-CD with excess *p*-toluenesulphonyl chloride, with recrystallisation from water.[46] Due to the importance of these sulphonates acting as intermediates for the further synthesis of other modified CDs, there exist many other methods of preparation.[47, 48, 49, 50] For instance CDTs can be prepared by the reaction of *β*-CD with *p*-toluenesulphonyl chloride in pyridine.[48] This route has the disadvantage that the product is obtained in poor yield and must be separated from multitosylated by-products by chromatography along with the inherent

difficulties of using pyridine as a solvent. The synthesis used in this study is a slightly modified version of an aqueous-based method reported by Brady *et al.*[49]

Monoamine derivatives of CDs have been prepared by the treatment of the corresponding tosylate with ammonia.[46] Analogous reactions of primary and secondary amines have also been reported as a method for attaching amino groups at the C6 position of a CD.[51] These materials can then be exploited for further modification, since the amino groups are substantially more nucleophilic than the CD hydroxyl groups. Matsui *et al.* published a synthesis route for 6-deoxy-6-[1-(2-amino)ethylamino]-*β*-cyclodextrin (CDEn) in 1976.[38] A modified version of Matsui's synthesis was also reported by Singh *et al*.[52] The diaminoalkane derivatives 6-deoxy-6-[1-(2-amino)ethylamino]-*β*-cyclodextrin (CDEn), 6-deoxy-6-[1-(3-amino)propylamino]-*β*-cyclodextrin (CDPn) and 6-deoxy-6-[1-(4-amino)butylamino]-*β*-cyclodextrin (CDBn), prepared here follow a modified synthesis of the route proposed by Singh *et al*.

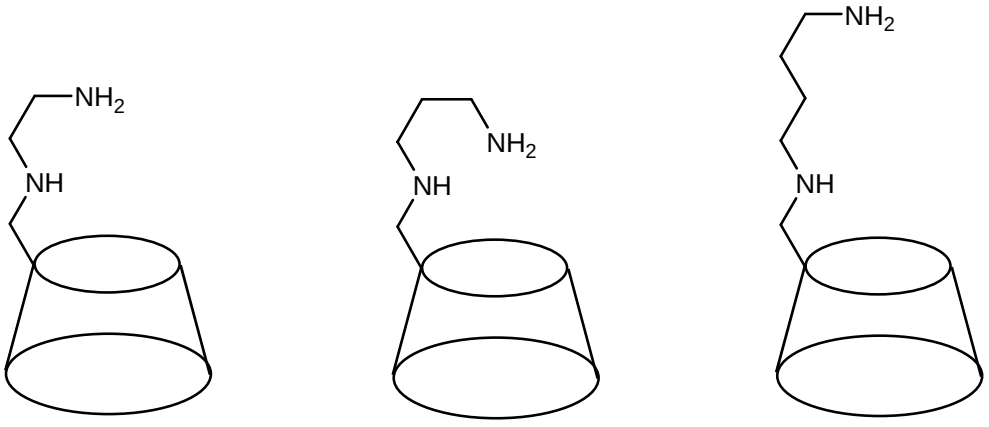

1 2 3

Figure 1.23 Structures of 1) CDEn, 2) CDPn and 3) CDBn

1.2 Aims and Objectives

In a review of charged CD derivatives, Cucinotta *et al.* have shown that functionalised cyclodextrins can be used as efficient chiral selectors for a range of enantiomeric species.[53] Many cyclodextrin derivatives have been studied including anionic sulfated cyclodextrins (SCDs) and neutral or cationic amino-cyclodextrins (CDAm). However mechanistic studies are still required in order to determine a mode of action if these selectors. It has been suggested that anionic selectors are very effective due to electrostatic interactions with cationic analytes.[54] It has also been suggested that binary metallo-CD complexes can act in a multi-site recognition manner, using the inclusion properties if the CD cavity in cooperation with the coordination ability of the metal ion.[55] Therefore the aim of this work is to determine if copper(II) complexes of amino-CD derivatives provide a more versatile solution than sulfated cyclodextrins for the direct separation of enantiomers in capillary electrophoresis.

To this end the objectives of this work are as follows:

1. Electronic Spectroscopy Study of Binary and Ternary Complexes.

In chapter two the results of an electronic spectroscopy study of the metallo-complexes of the amino-cyclodextrins CDEn, CDPn and CDBn are presented. Electronic spectroscopy was used in order to determine if Cu(II) coordinates to the amino-CDs and to determine if further coordination to guest species such as tyrosine, DOPA, carbidopa and benserazide occurs.

2. Circular Dichroic Study of Binary and Ternary Complexes.

In chapter three the results of a circular dichroic (c.d.) spectroscopic study of the Cu(II) complexes of CDEn, CDPn and CDBn are presented. The formation of ternary

complexes with tyrosine and DOPA is also studied. c.d. spectroscopy can show the differential inclusion of enantiomers in cyclodextrin cavities and therefore was used here to determine if the metallo-cyclodextrins can act as chiral selectors for the enantiomers of tyrosine and DOPA.

3. Stoichiometry of Binary and Ternary Complexes.

The stoichiometry of the complexes formed by Cu(II) and CDEn, tyrosine, DOPA and carbidopa were investigated using Job's method of continuous variation, and the results are presented in chapter four.

4. Separation by Capillary Electrophoresis

The chiral selector identified in the c.d. study was used in the background electrolyte to determine if it is a versatile and effective chiral selector for a range of separations. Chapter five details the development of a method for the separation of L-DOPA from L-carbidopa along with a method for the chiral separation of the enantiomers of DOPA in a Chiral Ligand Exchange Capillary Electrophoresis experiment.

Chapter six presents the conclusions arising from this work. The synthetic methods and characterisation techniques used in this work are summarised in chapter seven.

1.3 References

[1] K.M. Rentsch: *J. Biochem. Biophys. Methods,* **54**, (2002) 1

[2] http://www.fda.gov/cder/guidance/stereo.htm

[3]L. Pasteur: *Comp. Rend. Hebd. Seances Acad. Sci.* **26** (1848) 535

[4] P. Y. Bruice: *Organic Chemistry*, Prentice Hall, (2004) p. 182

[5] A. V. Eckhaut, Y. Michotte: *Chiral Separations by Capillary Electrophoresis*, Chromatographic Series, CRC Press, Volume 100 (2010) p. 2

[6] L. A. Nguyen, H. He and C. Pham-Huy: *Int. J. Biomed. Sci.* **2**, (2006) 85

[7] N. M. Davies and X. V. Teng: *Adv. Pharm.* **1**, (2003) 242

[8] S. Houlton: *Manuf. Chem.*, **73**, (2002) 28

[9] http://www.bccresearch.com/report/BIO012E.html accessed on 15/03/11

[10] V. A. Davankov: *Pure Appl. Chem.* **69**, (1997) 1469

[11] S. Finali: *J. Chromatogr A,* **792**, (1997) 229

[12] B. Chankvetadze: *J. Chromatogr A,* **792**, (1997) 269

[13] T.J. Ward and K.D. Ward: *Anal. Chem,* **82**, (2010) 4712

[14] G. Subramanian: *Chiral Separation Techniques: A Practical Guide*, 3rd Edition, Wiley-VCH (2007)

[15] F. Schardinger: *Wien. Klin. Wochenschr.* **17**, (1904) 207; F. Schardinger: *Zentralbl. Bakteriol. Parasitenkd. Infektionskr.* **14**, (1905) 772

[16] W. Saenger: *Angew. Chem. Int. Ed. Engl.* **19**, (1980) 344

[17] J. Szejtli: *Chem Rev.* **98**, (1998) 1743

[18] T. Loftsson, M.E. Brewster and M. Masson: *Am. J. Drug Deliv.* **2**, (2004) 261

[19] T. Loftsson, P. Jarho, M. Masson and T. Jarvinen: *Expert Opin. Drug Deliv.* **2**, (2005) 235

[20] J. Szejtli: *Pure Appl. Chem.,* **76**, (2004) 1825

[21] T. Kitae, T. Nakayama and K. Kano: *J. Chem. Soc. Perkin Trans.* **2**, (1998) 207

[22] C.A. Haskard, C.J. Easton, B.L. May and S.F. *Lincoln: Inorg. Chem*. **35**, (1996) 1059

[23] R. Breslow and L.E. Overman: *J. Am. Chem. Soc*. **92**, (1970) 1075

[24] E.M.M. Del Valle: *Process Biochem*. **39**, (2004) 1033

[25] Wacker Chemie product specification sheet

[26] D. Nicholls: *Complexes and First-Row Transition Elements*, 2nd Edition, MacMillan Education Ltd. (1991)

[27] A. Werner: Z. *Anorg. Chemie*., **3**, (1893) 267

[28] R.M. Costes, G. Folcher, K. Keller, P. Plurien and P. Rigny: *Inorg. Nuc. Chem. Lett*. **11**, (1975) 469

[29] H.M. Colquhoun and J.F. Stoddart: *J. Chem. Soc., Chem. Commun*. **612** (1981)

H.M. Colquhoun, J.F. Stoddart and D.J. Williams: *J. Chem. Soc., Chem. Commun*. **847, 849, 851** (1981)

[30] B. Siegel and R. Breslow: *J. Am. Chem. Soc*. **97**, (1975) 6869

[31] A. Harada and S. Takahashi: *J. Inclusion Phenom*. **2**, (1984) 791

[32] Y. Matsui, T Kurita, Y. Date: *Bull. Chem. Soc. Jpn*: **45**, (1972) 3229; Y. Matsui, T. Kurita, M. Yagi, T. Okayama, K. Mochida and Y. Date: *Bull. Chem. Soc. Jpn*: **48**, (1975) 2187; Y. Matsui and D. Suemitsu: *Bull. Chem. Soc. Jpn*: **58**, (1984) 1658

[33] B.U. Nair and G.C. Dismukes: *J. Am. Chem. Soc.* **105**, (1983) 124

[34] J.F. Stoddart and R. Zarzycki: *Recl. Trav. Chim. Pays-Bas*. **107**, (1989) 455

[35] N.R. Russell and M. McNamara: *J. Inclusion Phenom. Mol. Recogn. Chem*. **7**, (1989) 455

[36] M. McNamara and N.R. Russell: *J. Inclusion Phenom. Mol. Recogn. Chem*. **10**, (1991) 485

[37] J. Szejtli and J. Pagington: *Cyclodextrin News* **5**, (1991) 153

[38] Y. Matsui, Y. Yokoi and K. Mochid: *Chem. Lett*. **10**, (1976) 1037

[39] R.P. Bonomo, V. Cucinotta, F. D'Allessandro, G. Imellizzeri, G. Maccarrone and E. Rizzarelli: *J. Inculsion Phenom. Mol. Recog. Chem*. **15**, (1993) 167

[40] S.E. Brown, J.H. Coates, C.J. Easton and S.F. Lincoln: *J. Chem. Soc. Faraday Trans*. **90**, (1994) 739

S.E. Brown, C.A. Haskard, C.J. Easton and S.F. Lincoln: *J. Chem. Soc. Faraday Trans*. **91**, (1995) 1013

[41] N.van Hoof, N.R. Russell, M. McNamara and R. Darcy: *J. Inclusion Phenom. Macrocyclic Chem.* **36**, (2000) 179

[42] Cyclodextrin News, monthly abstracting news letter edited and published by Cyclolab Ltd., Budapest, Jan. (1998).

[43] V. Cucinotta, A. Giuffrida, G. Grasso, G. Maccarrone, A. Mazzaglia and G. Vecchio: *Fresenius J. Anal. Chem.* **370,** (2001) 363

[44] V. Cucinotta, A. Giuffrida, G. Maccarrone, M. Messina, A. Puglisi and G. Vecchio: *Electrophoresis,* **28,** (2007) 2580

[45] V. Cucinotta, A. Giuffrida, G. Grasso, G. Maccarrone, A. Mazzaglia, M. Messina and G. Vecchio: *J. Sep. Sci,* **34**, (2011) 70

[46] S.E. Brown, J.H. Coates, D.R. Coglan, C.J. Easton, S.J. van Eyk, W. Janoski, A. Lepore, S.F. Lincoln, Y. Luo, B.L. May, D.S. Schiesser, P. Wang and M.L. Williams: *Aust. J. Chem*. **46**, (1993) 953

[47] C. Bertolla, L. Pochet and B Masereel: *Proceedings of the 12th International Cyclodextrin Symposium*, Montpellier, France, May 2004.

[48] N. Zhong, H.S. Byun and R. Bittman: *Tet. Lett*. **39**, (1998) 2919

[49] B. Brady, N. Lynam, T. O' Sullivan, C. Ahern and R. Darcy: *Org. Syn*. **77**, (2000) 220

[50] H.S Byun, N. Zhong and R. Bittman: *Org. Syn*. **77**, (1999) 225

[51] C.J. Easton and S.F. Lincoln: *Modified Cyclodextrins; Scaffolds and Templates for Supramolecular Chemistry*, Imperial College Press, London (1999)

[52] A.P. Singh, P.R. Cabrer, E. Alvarez-Parrilla, F. Meijide and J.V. Tato: *J. Incl. Phenom. Macro:* **35**, (1999) 335

[53] V. Cucinotta, A. Contino, A. Giuffrida, G. Maccarrone, M. Messina: *J. Chromatogr A,* **1217**, (2010) 953

[54] M-Y. Tong and D.W. Armstrong: *PACE Setter,* **12**(2), (2008) 5

[55] C.F. Potter, N.R. Russell and M. McNamara: *J. Inclusion Phenom. Macrocyclic Chem.* **56**, (2006) 395

2. Electronic Spectroscopic Study of Binary and Ternary Complexes

2.1 Introduction

The use of electronic spectroscopy in the detection of first sphere coordination of transition metal ions with cyclodextrins and their derivatives is well established.[1, 2, 3] A shift in the maximum wavelength of absorption λ_{max} indicates a change in the strength of the ligand while a change in intensity of absorption can give an insight into the nature of the electronic transition occurring and structural symmetry of the complex. This is particularly useful in this work as an increase in absorption intensity with respect to the aquated copper(II) ion, measured in terms of the molar extinction coefficient ε, indicates a lowering in symmetry of the coordination sphere of the metal ion. Furthermore a decrease in λ_{max} indicates replacement of the aqua ligands in the copper(II) complex by stronger amino-cyclodextrin ligands (CDAm). Electronic spectroscopy is therefore employed to obtain an understanding of the coordination between transition metal ions and the cyclodextrin derivatives and guest molecules.

Matsui *et al.* investigated first sphere metallo-cyclodextrin complexes using electronic spectroscopy and reported a shift in λ_{max} from ~800 nm for the aqueous copper(II) ion to 667 nm for the aqueous solutions of metallo-CD complex at pH 10.5.[4] A binuclear hydroxy-bridged structure was proposed with two copper ions coordinated to the O2 and O3 groups of adjacent glucopyranose units and bridged by two hydroxyl groups. Russell and McNamara also proposed a binuclear bridge structure through the use of FTIR and Raman spectroscopies.[1] The proposed structure is given in Figure 2.1.

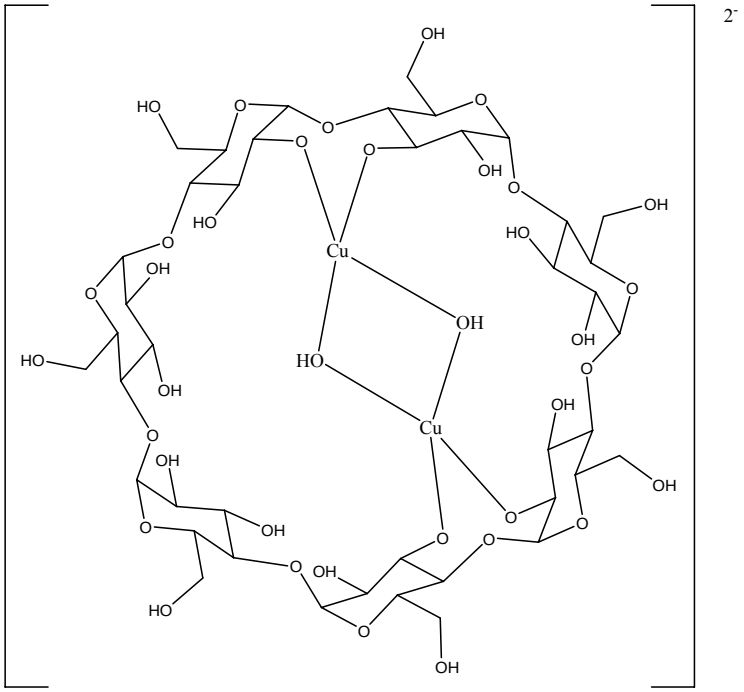

Figure 2.1 Proposed binuclear hydroxy-bridged structure of the $[Cu_2(OH)_2$-β-$CD]^{2-}$ complex

Norkus *et al*. studied complexes of β-CD and copper as well as a range of other transition metals.[5] They observed the failure of these complexes to form at an acidic or neutral pH. Also reported was the formation of a light blue $[CuCD(OH)_2]^{2-}$ precipitate in the pH range 8-10, whereas a dark blue solution and no precipitate was seen at a higher pH, the result of the formation of the Cu(II) binuclear hydroxy-bridged complex. All of these studies suggest that cyclodextrins have poor coordination properties that can be improved at high pH values due to deprotonation of the hydroxyl groups. Coordination can also be improved by derivatising the cyclodextrin.

Matsui *et al.* reported the formation of a Cu(II) complex with the CD derivative 6-deoxy-6-[1-(2-amino)ethylamino]-β-cyclodextrin (CDEn).[2] Electronic spectroscopy was also employed for the characterisation of this complex at a pH of 10.5. There was an observed shift in λ_{max} from ~800 nm to 570 nm and the authors suggested the formation of a 1:2 complex between the Cu(II) ion and CDEn at this pH (Figure 2.2).

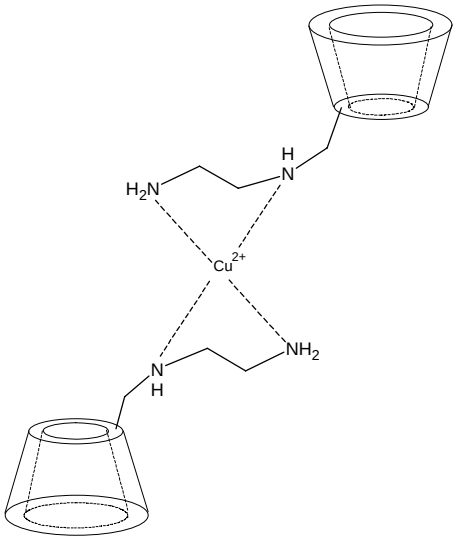

Figure 2.2 Proposed structure of the diaminoethane-*β*-CD derivative coordinated to Cu(II) at high pH.

Electronic spectroscopy has also been used to study the ternary complexes of metallo-CDs with amino acids. Bonomo and Cucinotta *et al.* have shown the coordination of copper to various CD derivatives, such as CDEn, 3A,3B-dideoxy-3A,3B-diamino-2A(S),2B(S),3A(R),3B(R)-β-CD ($AB3NH_2$), and 6-mono-deoxy-6-[4-(2-aminoethyl)imidazolyl]-*β*-CD (CDmh).[6,7,9] The binary complexes were shown to form ternary complexes with various guest species. For example, Cucinotta *et al.* showed the coordination of $CuAB3NH_2$ to tyrosine by a shift in the *d-d* transition of Cu(II) from 656 nm for the binary complex to 625 nm for the ternary complex.[9] Potter *et al.* also utilised electronic spectroscopy to verify coordination of a metal ion to CDAm derivatives such as CDEn, 6-deoxy-6-[1-(3-amino)propylamino]-*β*-cyclodextrin (CDPn) and 6-deoxy-6-[1-(4-amino)butylamino]-*β*-cyclodextrin (CDBn). Further coordination to guest species was also discussed.[3] For example coordination of copper to CDEn was demonstrated by a hypsochromic shift in the d-d transition of copper from 810 nm to 671 nm. A further shift (671 to ~635 nm) was observed when the ternary complex with tyrosine was formed through further coordination of the metal ion. The structure proposed for the ternary complex is shown in Figure 2.3.

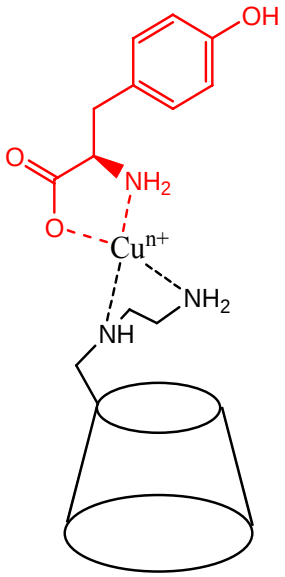

[L-TyrCuCDEn]$^{n+}$

Figure 2.3 Proposed CuCDEn(Tyr) structure

In this work electronic spectroscopy is used to study the binary Cu(II) complexes of 6-deoxy-6-[1-(2-amino)ethylamino]-*β*-cyclodextrin (CDEn), 6-deoxy-6-[1-(3-amino)propylamino]-*β*-cyclodextrin (CDPn) and 6-deoxy-6-[1-(4-amino)butylamino]-*β*-cyclodextrin (CDBn) and their ternary complexes with D,L- tyrosine (Tyr), 3,4-dihydroxy-L-phenylalanine (L-DOPA), 3,4-dihydroxy-D-phenylalanine (D-DOPA), D,L-serine-2-(2,3,4-trihydroxybenzyl)hydrazide (benserazide) and *S*-(−)-*α*-hydrazino-3,4-dihydroxy-2-methylbenzenepropanoic acid (L-carbidopa).

2.2 Theory

At room temperature the majority of molecules will exist in their vibrational and electronic ground states. Upon the absorption of visible or ultraviolet (UV) radiation it is possible for electronic transitions from this ground state to a higher excited electronic state. Such transitions can only occur if the incident radiation corresponds in magnitude to the energy gap between these two states. This is given by the following relationship,

$$\Delta E = E_f - E_i = h\nu = hc/\lambda \qquad \textbf{Equation 2.1}$$

where E_f and E_i are the energies of the final and initial electronic states respectively, h is Planck's constant and ν is the frequency of the radiation. λ is the maximum wavelength of absorption and c is the velocity if light.

The absorbance (A) at λ_{max} can be related to the molar extinction coefficient ε by the Beer Lambert Law:

$$A = \varepsilon.c.l \qquad \textbf{Equation 2.2}$$

where c is the concentration of the absorbing species in mol dm^{-3} and l is the path length in cm.

Pathways for the absorption of electromagnetic radiation by molecules and the corresponding return to the ground state can be illustrated using a Jablonski Diagram (Figure 2.4).

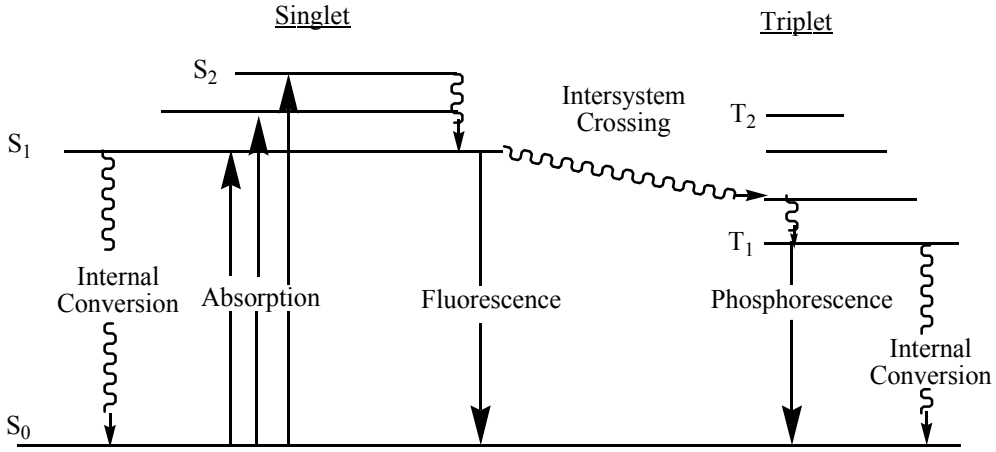

Figure 2.4 Jablonski diagram showing electronic absorption and emission

The area of interest in this work is the electronic spectra of metallo-complexes, which show absorption bands occurring from a variety of electronic transitions including,

- Transitions involving π, σ or n electrons of the ligands or counter ions.
- Transitions involving charge transfer between metal and ligand orbitals or *vice versa*.

- Transitions between metal d orbitals, known as "d-d" transitions.

As a result of selection rules charge transfer causes very intense absorption bands which occur at high energy usually in the UV region. On the other hand d-d transitions tend to give weaker and broader signals at lower energies from the near IR to near UV. The selection rules for these processes are the Laporte Rule and the Spin Forbidden Rule.

- Spin Forbidden Rule:

Transitions in which the total spin of the electrons remains fixed are spin allowed transitions *i.e.* $\Delta S = 0$ where S is the total spin quantum number. Therefore there can be no change in the number of parallel electron spins, during the transition.

- Laporte Rule:

Transitions involving the redistribution of electrons within a single energy level are forbidden, *i.e.* s→p or p→d transitions are allowed but d→d transitions are forbidden. However relaxation of the Laporte Rule can occur. Any phenomenon which alters the symmetry of the d orbitals has the effect of relaxing the Laporte rule. In tetrahedral complexes d orbitals are in an asymmetric environment and therefore tetrahedral complexes have 'built-in' relaxation of the Laporte rule. In octahedral complexes the Laporte rule is relaxed by a vibronic mechanism. Vibrational coupling alters the symmetry of the d orbitals so that transitions are no longer purely d-d but rather d → partially d. The Laporte rule is also relaxed by changes in the symmetry of complexes. Therefore as the symmetry is reduced the Laporte rule is more relaxed and the extinction coefficient will increase.

In this work we use electronic spectroscopy to determine if Cu(II) ions form binary complexes with CDAm derivatives and then further form ternary complexes with amino acids and drugs such as tyrosine, DOPA, benserazide and carbidopa.

2.3 Experimental

Electronic spectra were measured at room temperature using a Perkin Elmer Lambda 900 UV/Vis/NIR Spectrometer. The spectrometer is a double-beam, double monochromator ratio recording system with pre-aligned tungsten-halogen and deuterium lamps as sources. The wavelength range is from 175-3300 nm with an accuracy of 0.08 nm in the UV-visible region and 0.3 nm in the NIR region. It has a photometric range of +/-6 in absorbance. Parameters used in this work were: Range: 200-800 nm, Slit Width: 0.1 nm, Accumulation: 1. Spectra were taken using 10 mm quartz cells and 1 mm cells at higher wavelengths to compensate for molar extinction coefficients being smaller. The resultant spectra were combined for analysis.

Solutions used for recording the electronic spectra were as follows:

- CD derivative and guest solutions were prepared by dissolution of the appropriate moiety (0.010 mol dm^{-3}) in a KH_2PO_4/NaOH buffer that was made using 500 cm^3 of KH_2PO_4 (0.100 mol dm^{-3}) added to 347 cm^3 of NaOH (0.100 mol dm^{-3}) and diluted to 1000 cm^3 with deionised water to give a resulting pH of 7.2.
- Binary and ternary complex solutions were prepared by addition of 2 cm^3 of aqueous $CuSO_4.5H_2O$ (0.010 mol dm^{-3}), 2 cm^3 of the amino CD (0.010 mol dm^{-3} in buffer) and 2 cm^3 of the guest (0.010 mol dm^{-3} in buffer), when appropriate, to a 10 cm^3 volumetric flask and dilution to the mark using the KH_2PO_4/NaOH buffer resulting in an overall complex concentration of 0.002 mol dm^{-3}.
- The ternary complex solutions containing tyrosine were made to 0.001 mol dm^{-3} due to the poor solubility of tyrosine. The concentration of CDAm and $CuSO_4.5H_2O$ was adjusted accordingly.

2.4 Results

Figure 2.5 shows the electronic absorption spectrum of the hexaquacopper(II) ion. Figure 2.6 shows the spectra obtained from the electronic spectroscopic study of the binary complexes of Cu(II) with CDEn, CDPn and CDBn at a pH of 7.2. Figures 2.7 to 2.11 show the electronic spectra for the corresponding ternary complexes, with L and D tyrosine, L and D-DOPA and L-carbidopa as guest molecules. Table 2.1 summarises the data obtained. Spectra of amino CDs and guests are given in Appendix 8.1.

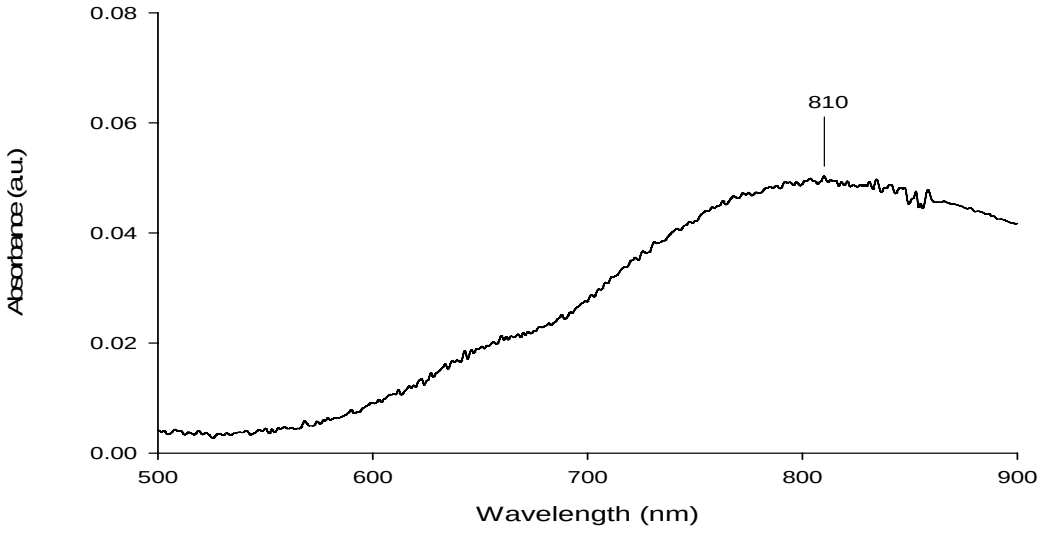

Figure 2.5 Electronic absorption spectrum of $[Cu(H_2O)_6]^{2+}$

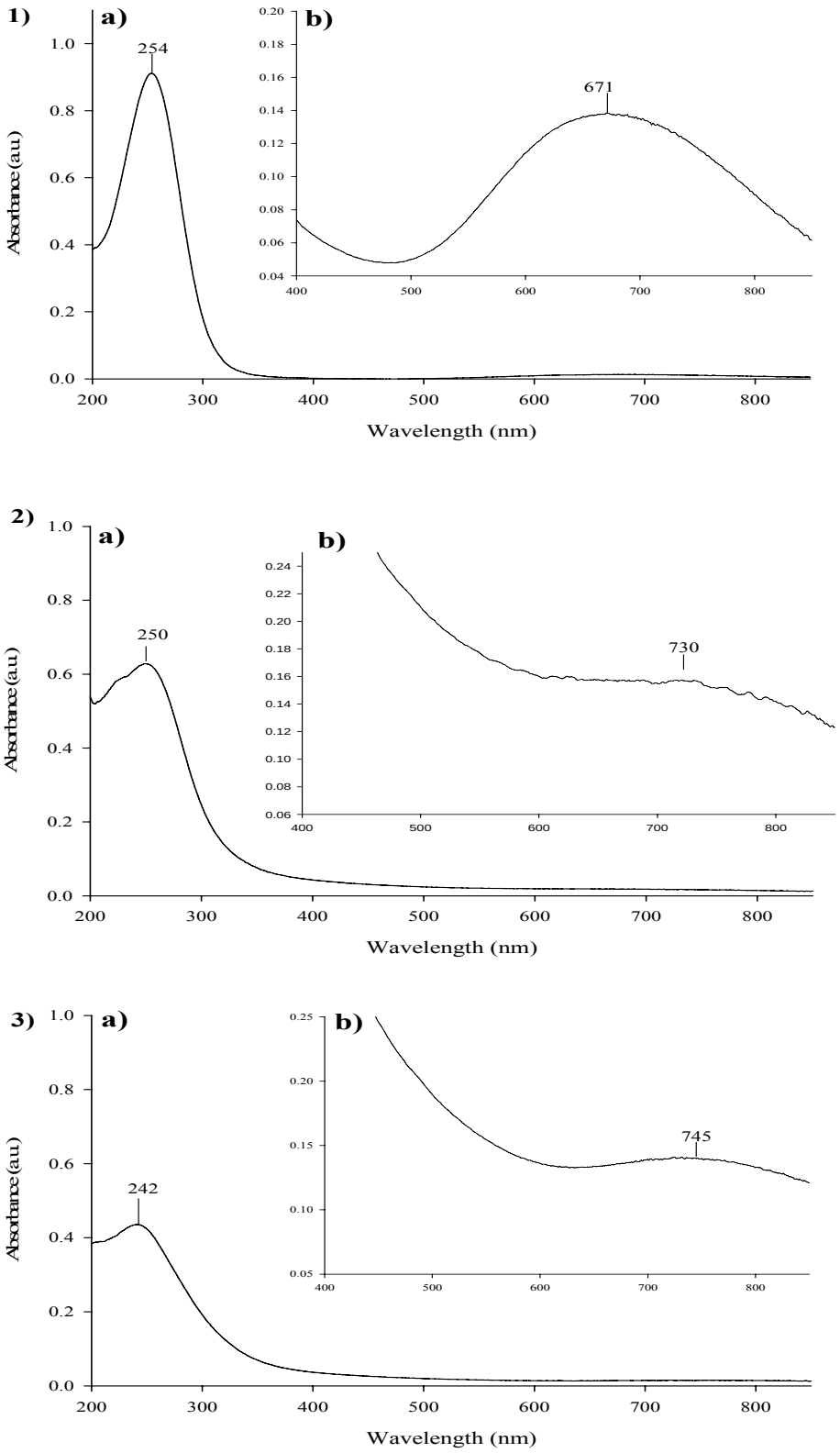

Figure 2.6 Electronic absorption spectra of binary complexes of Cu(II) with 1) CDEn 2) CDPn 3) CDBn in a) 1 mm cell and b) 10 mm cell

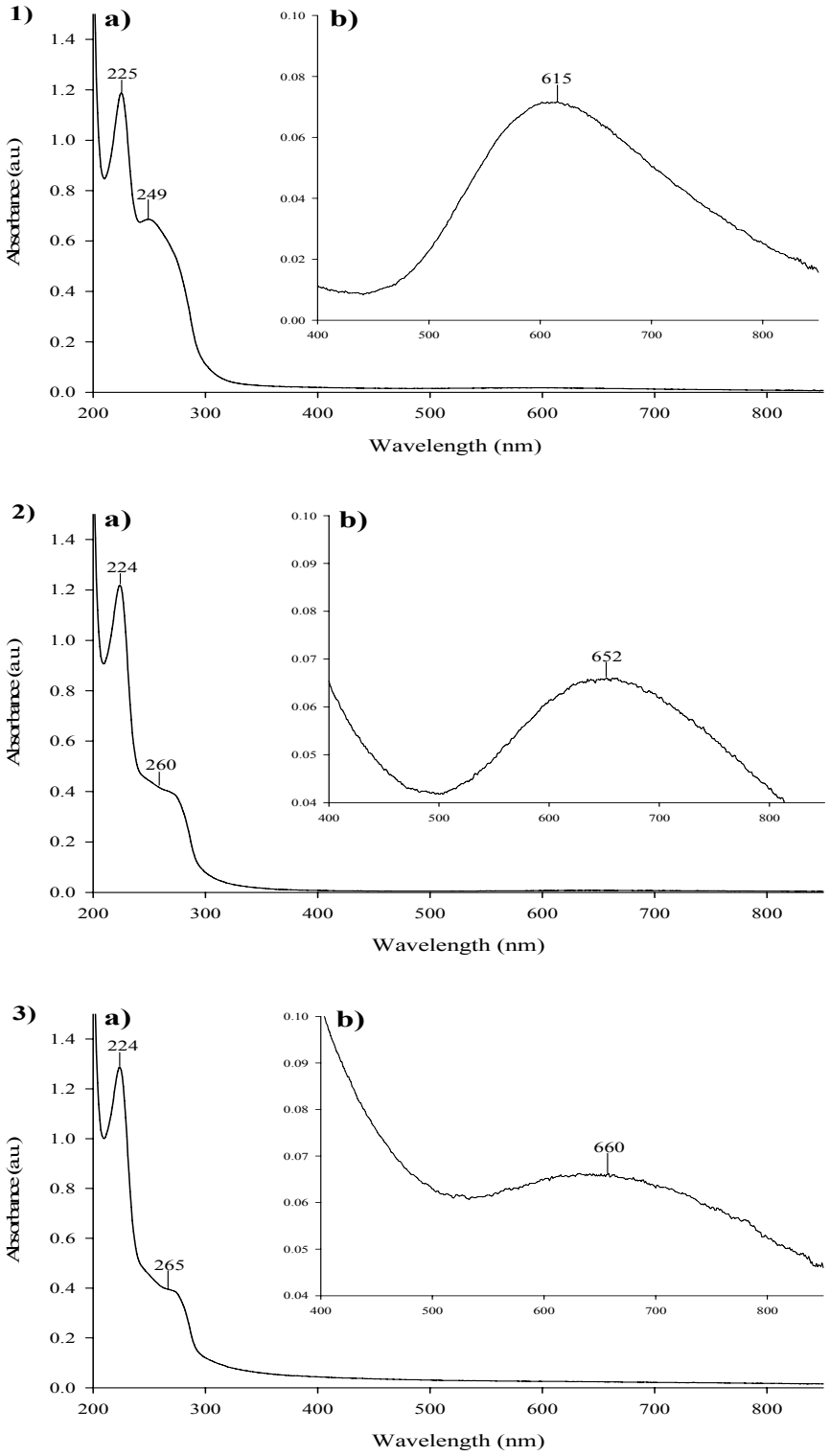

Figure 2.7 Electronic absorption spectra of the ternary complexes of L-Tyr with Cu(II) and 1) CDEn 2) CDPn and 3) CDBn in a) 1 mm cell and b) 10 mm cell

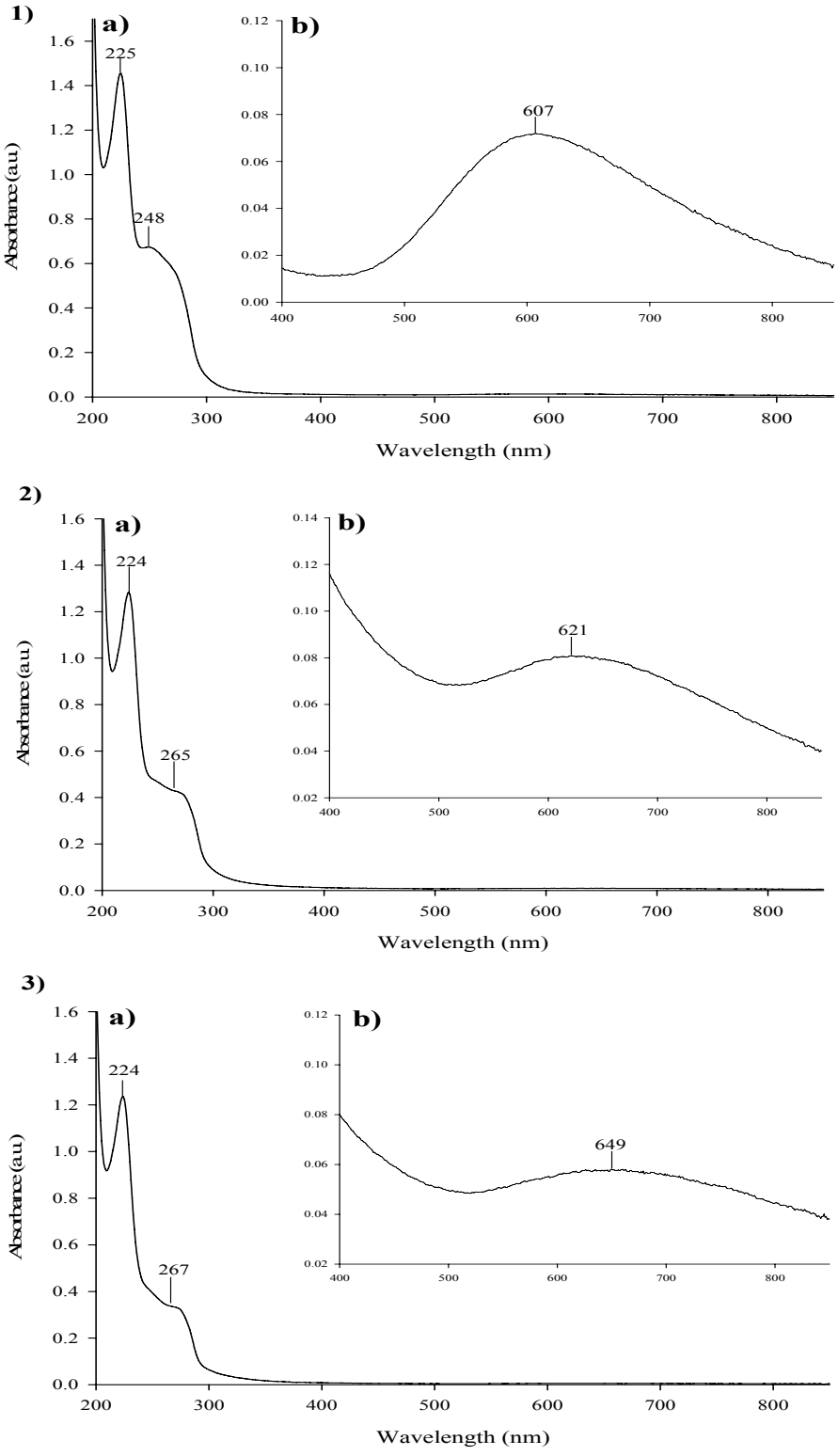

Figure 2.8 Electronic absorption spectra of the ternary complexes of D-Tyr with Cu(II) and 1) CDEn 2) CDPn and 3) CDBn in a) 1 mm cell and b) 10 mm cell

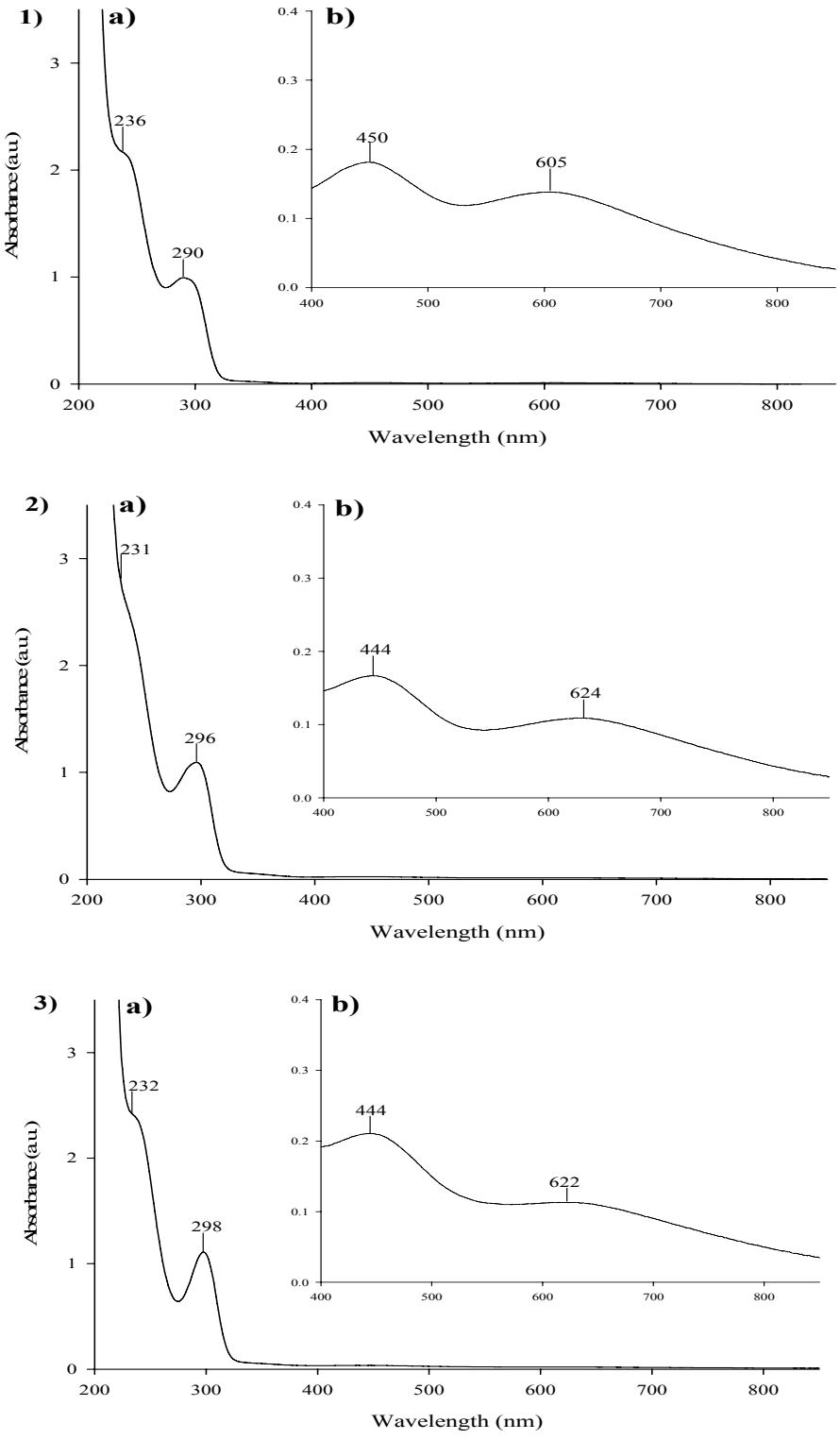

Figure 2.9 Electronic absorption spectra of the ternary complexes of L-DOPA with Cu(II) and 1) CDEn 2) CDPn and 3) CDBn in a) 1 mm cell and b) 10 mm cell

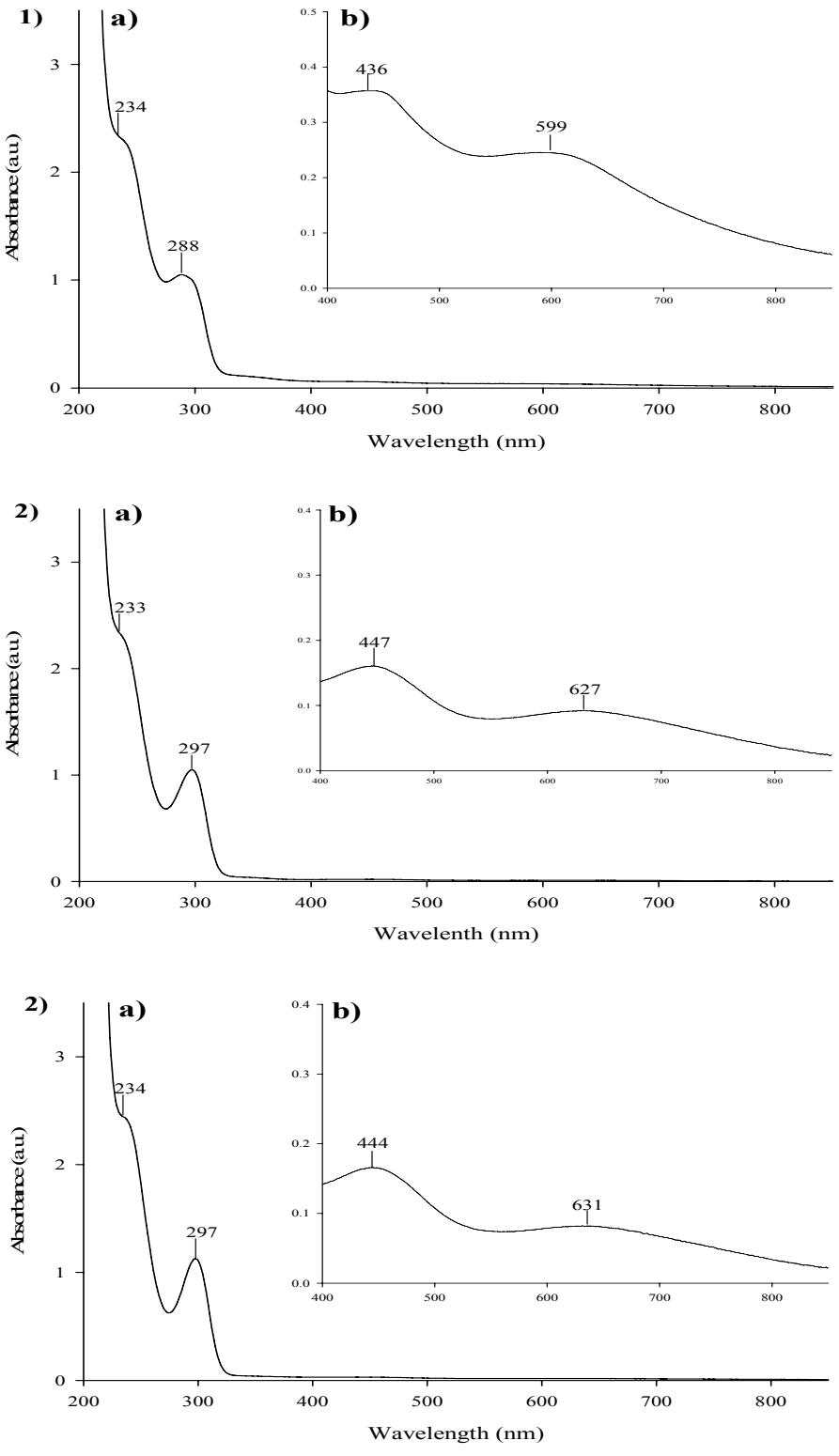

Figure 2.10 Electronic absorption spectra of the ternary complexes of D-DOPA with Cu(II) and 1) CDEn 2) CDPn and 3) CDBn in a) 1 mm cell and b) 10 mm cell

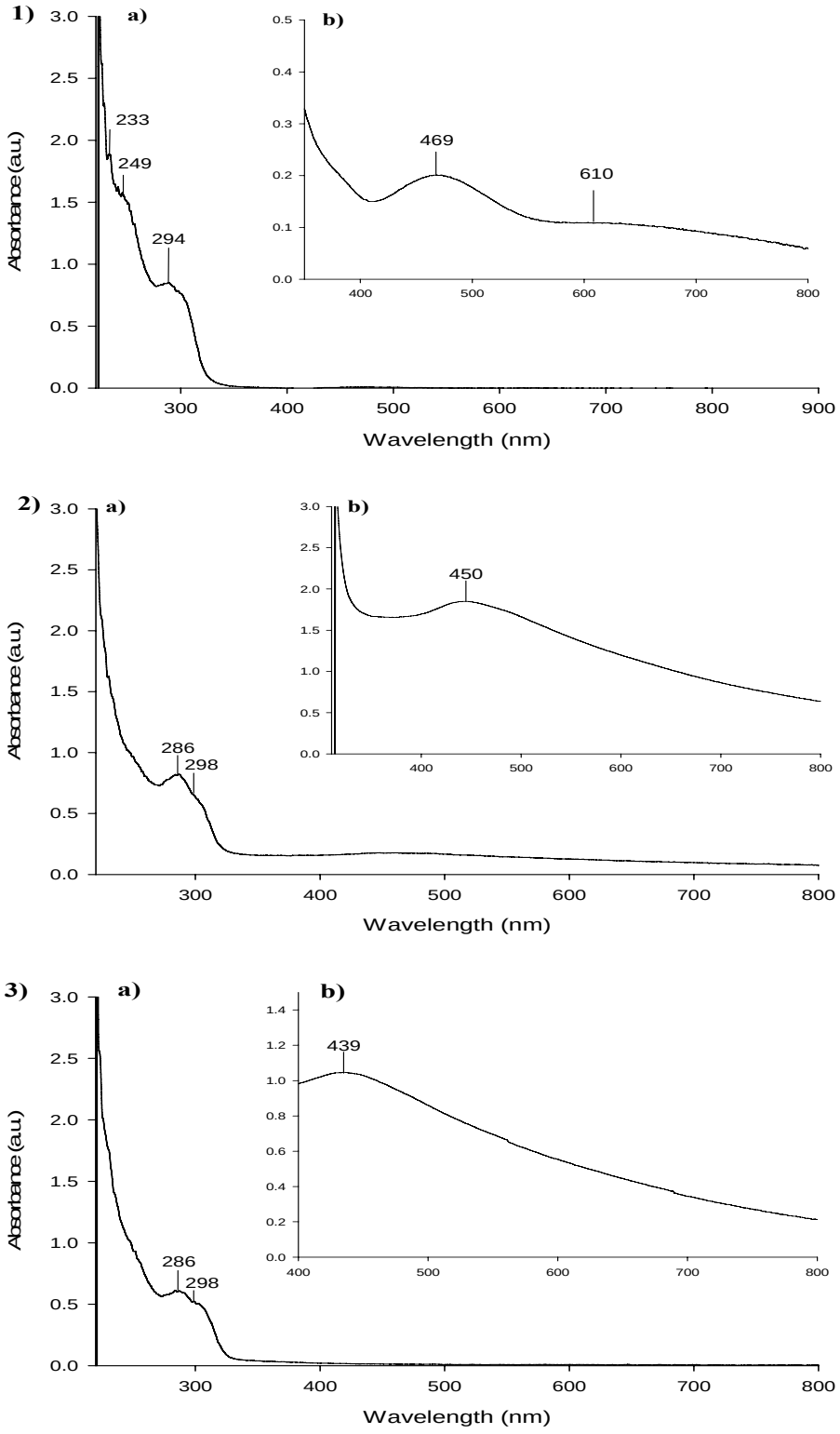

Figure 2.11 Electronic absorption spectra of the ternary complexes of L-carbidopa with Cu(II) and 1) CDEn 2) CDPn and 3) CDBn in a) 1 mm cell and b) 10 mm cell

Table 2.1 Electronic Absorption Data for Binary and Ternary Cu(II) Complexes at pH 7.2

	Binary Complexes	
	λ (nm)	*ε (± 0.01 mol^{-1} dm^3 cm^{-1})*
[Cu(H$_2$O)$_6$]$^{2+}$	810	25
[CuCDEn]$^{n+}$	671 254	69 4557
[CuCDPn]$^{n+}$	730 250	79 3143
[CuCDBn]$^{n+}$	745 242	70 2179

	Ternary Complexes *λ nm* *(ε)* (± 0.01 mol^{-1} dm^3 cm^{-1})		
Guest	**Cu(CDEn)**	**Cu(CDPn)**	**Cu(CDBn)**
L-Tyr	615 (72) 249 (6861) 225 (11878)	652 (66) 260 (4133) 224 (12194)	660 (66) 265 (3977) 224 (12877)
D-Tyr	607 (72) 248 (6735) 225 (14560)	621 (81) 265 (4283) 224 (12847)	649 (58) 267 (3366) 224 (12367)
L-DOPA	605 (69) 450 (91) 290 (4968) 236 (10895)	624 (55) 443 (83) 296 (5466) 231 (13497)	622 (57) 444 (105) 298 (5553) 232 (12195)
D-DOPA	599 (123) 436 (179) 288 (5250) 234 (11680)	627 (46) 447 (80) 297 (5251) 233 (11803)	631 (41) 444 (83) 297 (5641) 234 (12229)
L-Carbidopa	610 (54) 469 (100) 294 (4965) 249 (7765) 234 (9385)	- 450 (920) 298 (3365) 289 (3970) 234 (7200)	- 439 (520) 299 (2600) 290 (2950) 236 (6850)
D,L-Benserazide	-	-	-

2.5 Discussion

2.5.1 Binary Complexes

The spectra of the binary complexes of Cu(II) with the amino cyclodextrin derivatives all show a band in the visible region assigned to the d-d transition of the metal centre. Bands in the UV region are assigned to electronic transitions of the CD moiety. The Cu(II) hexaqua ion $[Cu(H_2O)_6]^{2+}$ has a d-d transition at ~ 810 nm. However for the binary complexes $[CuCDEn]^{n+}$, $[CuCDPn]^{n+}$ and $[CuCDBn]^{n+}$ a hypsochromic shift can be observed in each case, to 671, 730 and 745 nm respectively, suggesting that the CDAm ligands are stronger than aqua ligands. The order in which the ligand field strength increases (CDBn < CDPn < CDEn) is significant as it indicates the shorter the diaminoalkane moiety the higher the field strength. Previous publications by our group also reported similar values.[3] In all cases there is also an increase in the value of the molar extinction coefficient when compared to the value of 25 mol^{-1} dm^3 cm^{-1} obtained for the Cu(II) hexaqua ion. This indicates a lowering in symmetry of the coordination sphere around the metal ion as expected for these complexes. There is very little change in the spectra in the UV region compared to spectra of the ligands alone, except for a slight broadening of bands.

Matsui *et al.* observed a shift to 570 nm for the $[Cu(CDEn)_2]^{2+}$ complex at pH 10.5 (Figure 2.2).[8] Cucinotta *et al.* reported a shift from 810 nm for the Cu(II) hexaqua ion to 656 nm at a pH of 7 for the Cu(II) complex of a $3^A,3^B$-diamine-3^A, 3^B-dideoxy-β-cyclodextrin ($AB3NH_2$) where A and B represent adjacent pyranose units of β-CD.[9] Similar complexes of $6^A,6^B$-diamino-6^A, 6^B-dideoxy-β-cyclodextrin ($ABNH_2$) exhibit a shift in λ_{max} to 680 nm.[10] These authors suggested this could be due to coordination of the metal ion to two nitrogen atoms of the ligands which are shown in Figure 2.12.

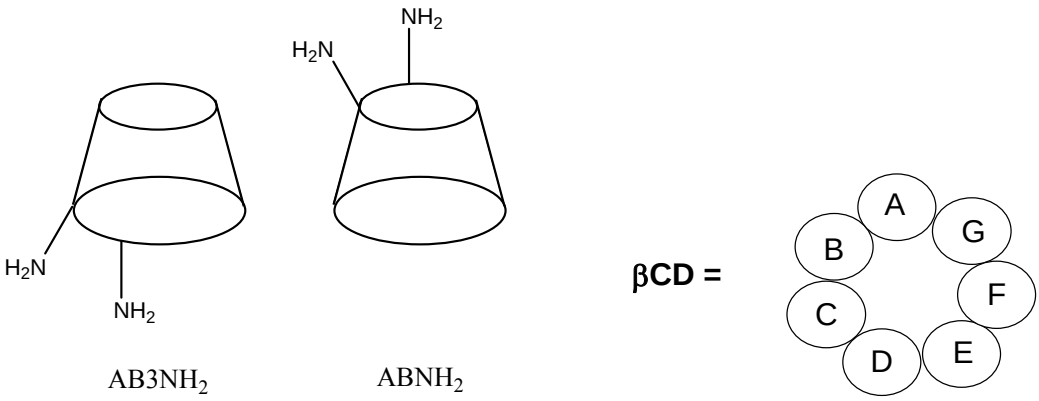

AB3NH$_2$ ABNH$_2$

Figure 2.12 Representations of AB3NH$_2$ and ABNH$_2$ and diagram representing the labelling system used for disubstituted derivatives by Cucinotta[4] and Bonomo[5]

The results in this work are obtained in aqueous solution and the complexes do not crystallise. Therefore structural information is not available from X-ray crystallography. However some structural information can be inferred by comparison with the electronic absorption data for other complexes that have been shown to have aminoalkane ligands acting in a bidentate manner. For example it is reported that the complex $[Cu(en)_2Cl_2].H_2O$ has two bands in its electronic spectrum at 667 nm and 535 nm.[11] Therefore the results obtained here suggest that the two nitrogen atoms of CDEn have replaced two water molecules and the octahedral coordination sphere of Cu(II) may be completed by aqua ligands. The decrease in λ_{max} suggests that CDEn and CDPn are acting as bidentate ligands through this coordination *via* the two nitrogen atoms of the diaminoalkane moiety. The decrease in λ_{max} is much less for the $[CuCDBn]^{n+}$ complex. It is possible that in this case the metal ion may only be coordinated to one of the nitrogen atoms, as the longer alkane chain prevents access to the other amino group. The structures proposed are given in Figure 2.13.

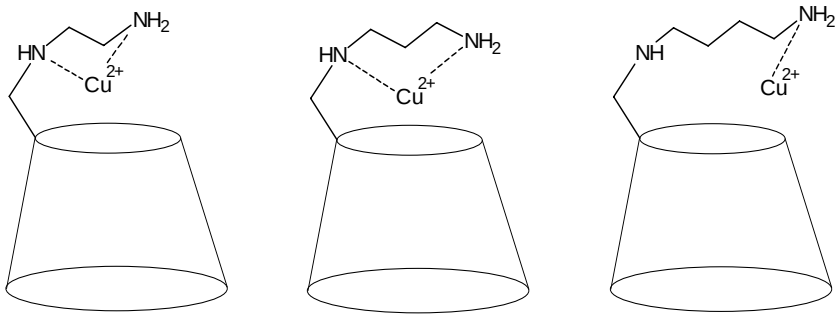

Figure 2.13 Proposed structures of the binary complexes of Cu(II) CDEn, CDPn and CDBn (aqua ligands are omitted for clarity)

2.5.2 Ternary Complexes

Ternary complexes are formed when the binary complexes react with guest species such as amino acids. The ternary complexes formed in this work again display characteristic bands in the visible region of their electronic absorption spectra synonymous with the d-d transitions of the copper metal centre. Bands in the UV region are difficult to assign as transitions in this region are complicated by the presence of the guest molecules which also absorb in this region. By collecting absorption data separately for the guest molecules it is possible to identify bands due solely to their transitions. From these spectra (Appendix 8.1) it is possible to assign the bands at ~225 nm to a transition of tyrosine while the band at 250–265 nm is assigned to transitions of both the amino acid and the CDAm species. Again when DOPA is the guest species, bands at ~280 nm can be assigned to transitions of the drug while absorption in the ~ 235 nm region is assigned to transitions of both the drug and CDAm species. When using carbidopa as the guest species bands at ~ 280 nm can be assigned to transitions of the drug while absorption in the 230-250 nm is assigned to both the drug and CDAm species.

For the ternary complexes of tyrosine, DOPA and carbidopa a further hypsochromic shift in the d-d absorption band is observed when compared to the binary complexes. For example the band at 671 nm for $[Cu(CDEn)]^{2+}$ is shifted to 615 nm for

$[Cu(CDEn)(L\text{-}Tyr)]^{n+}$. Again this suggests further coordination of the metal ion to the guest molecule. Coordination would most likely take place to the amine and carboxylic acid groups of the amino acid/drug as both contain oxygen and nitrogen atoms with lone pairs available for donation to the metal centre.

The results obtained for tyrosine and DOPA agree with work carried out by this group previously.[3] There are no other reported electronic spectroscopy studies of tyrosine interaction with CuCDPn and CuCDBn. However parallels can be drawn from similar work with other cyclodextrin derivatives. Cucinotta *et al.* reported λ_{max} values for complexes of tyrosine and the copper complex of $AB3NH_2$ at ~ 270 and 624 nm (ε = ~ 4900 and ~ 207 mol^{-1} dm^3 cm^{-1}).[9] Bonomo *et al.* report λ_{max} values for the d-d transition between 598-616 nm for both L and D enantiomers of tyrosine with the Cu(II) complexes of $ABNH_2$.[7] The results presented here compare favourably with these authors.

The spectrum for the ternary complex of L-carbidopa with CuCDEn shows a further hypsochromic shift in the visible region indicating further coordination of the metal centre to the carbidopa guest. However stable complexation with CuCDPn and CuCDBn was not achieved. Upon mixing the solutions containing these chiral selectors a green solution is formed initially, which quickly becomes brown and a yellow/brown precipitate is formed, which is likely to be copper(I) oxide. Electronic absorption data is collected immediately on formation of the green solution. However as these ternary complexes are not stable, CDPn and CDBn are deemed unsuitable as chiral selectors for separations involving carbidopa.

To the best of the author's knowledge there are no reports on the coordination of carbidopa to a metallo-cyclodextrin.

It was not possible to investigate the coordination of benserazide to any of the metallo-cyclodextrin derivatives, due to the formation of a precipitate. It is therefore concluded that the chiral selectors $[CuCDEn]^{n+}$, $[CuCDPn]^{n+}$ and $[CuCDEn]^{n+}$ are not appropriate for separations involving this drug. The formation of any precipitate during either an electrophoretic or chromatographic separation could block the columns and terminate the analysis. Pecanac *et al.* investigated the determination of L-DOPA in the presence of benserazide in the medication Madopar by UV spectrophotometric micro-determination.[12] This was accomplished by complexing DOPA with copper and measuring changes in transitions in the UV region. Pecanac suggested that there was no interaction between copper and benserazide at the concentrations found in the medication as the presence of benserazide did not interfere with the determination of DOPA in the study.

2.6 Conclusion of Electronic Spectroscopy Study

From the increase in the molar extinction coefficient seen in the spectra of the binary and ternary Cu(II) complexes of aminocyclodextrins as compared to the hexaqua complex $[Cu(H_2O)_6]^{2+}$ it can be concluded that there is a lowering in symmetry of the first coordination sphere of the metal ion. There is also a decrease in λ_{max} for the d-d transitions on coordination of the metal ion to the amino cyclodextrins (CDAm). The results suggest the formation of a CuCDAm binary complex with CDEn and CDPn acting as bidentate ligands coordinating to the metal ion through the two nitrogen atoms of the diaminoalkane. CDBn acts as a monodentate ligand coordinating through just one nitrogen on the diaminoalkane chain. A further blue shift on the introduction of a guest species to the system suggests a further coordination of the Cu(II) ion to the guest creating a ternary complex. This was observed for tyrosine and DOPA with all three chiral selectors and for $[CuCDEn]^{n+}$ and carbidopa. No coordination was evident with

benserazide. This result suggests that the use of these metallo-CD derivatives for enantioselection may be guest specific.

Very few regular octahedral (O_h point group) Cu(II) complexes exist due to Jahn Teller distortion of the d^9 ground state. Jahn Teller theory states that any non-linear molecule with a spatially degenerate electronic ground state will undergo a geometrical distortion that removes that degeneracy. Therefore Cu(II) complexes are normally tetragonal which results in a slight splitting of the degenerate e_g level resulting in two possible electronic transitions. For example $[Cu(en)_2Cl_2]$ is assigned to the D_{2h} point group and has a pseudo-octahedral structure which gives rise to two bands in the electronic absorption spectrum at 667 and 535 nm.[11] Spectra of the ternary complexes of CuCDEn with DOPA and carbidopa as guests also show two bands in the visible region at 600-610 and ~ 430-470 nm. This suggests highly distorted or *pseudo*-octahedral structures. However at this stage it is not possible to propose definite structures for these ternary complexes. Further information concerning the enantioselective properties of CuCDEn must be obtained (Chapter 3) and the stoichiometry of the complexes formed must be determined (Chapter 4).

2.7 References

[1] N.R. Russell and M. McNamara: *J. Inclusion Phenom. Mol. Recogn. Chem.* **7**, (1989) 455; M. McNamara and N.R. Russell: *J. Inclusion Phenom. Mol. Recogn. Chem.* **10**, (1991) 485; M. McNamara and N.R. Russell: *J. Inclusion Phenom. Mol. Recogn. Chem.* **13**, (1992) 145

[2] Y. Matsui, T. Yokoi and K. Mochida: *Chem. Lett.* **10,** (1976) 1037

[3] C.F. Potter, N.R. Russell and M. McNamara: *J. Inclusion Phenom. Macrocyclic Chem.* **56**, (2006) 395

[4] Y. Matsui, T. Kurita and Y. Date: *Bull. Chem. Soc. Jpn.* **45**, (1972) 3229

[5] E. Norkus, G. Grinciene, T. Vuorinen and R. Vaitkus: *J. Inclusion Phenom. Macrocyclic Chem.* **48**, (2004) 147

[6] R.P. Bonomo, V. Cucinotta, G. Maccarrone, E. Rizzarelli, G. Vecchio: *J. Chem. Soc. Dalton Trans.* (2001) 1366

[7] R.P. Bonomo, S. Pedotti, G. Vecchio and E. Rizzarelli: *Inorg. Chem*. **16**, (1996) 6873

[8] Y. Matsui, T. Yokoi and K. Mochida: *Chem. Lett.* **10**, (1976) 1037

[9] V. Cucinotta, A. Giuffrida, G. Maccarrone, M. Messina, A. Puglisi, E. Rizzarelli and G. Vecchio, *Dalton Trans.* **16**, (2005) 2731

[10] R.P. Bonomo, S. Pedotti, G. Vecchio and E. Rizzarelli: *Inorg. Chem*. **16**, (1996) 6873

[11] B.J. Hathaway, D.E. Billing, P. Nicholls and I.M. Proctor: *J. Chem. Soc. (A)*. **2**, (1969) 319

[12] D. Pecanac, K. Karljikovic-Rajic and D. Radulovic: *Anal. Lett.* **30,** (1997) 1833

3. Circular Dichroic Study of Binary and Ternary Complexes

3.1 Introduction

The electronic spectroscopy study presented in the previous chapter showed that the copper(II) complexes of amino-CDs can form ternary complexes with tyrosine, DOPA and carbidopa. However electronic spectroscopy cannot be used to determine the chiral recognition properties of the metallo-CDs. Therefore the circular dichroic properties of the binary and ternary complexes were investigated.

Circular dichroism (c.d.) is a form of spectroscopy based on the differential absorption of left and right circularly polarised light. It is used to examine the optical properties of molecules. The technique has been used for the characterisation of pharmaceuticals. For example Bowen *et al.* report its use as an "Alternative Method for Drug Analysis", claiming that the method has advantages in its simplicity, speed and reproducibility.[1] The technique is ideally suited to the detection of an optically active material present in a mixture of impurities that show no optical activity. Examples of applications studied by Bowen's group include the determination of opium alkaloids,[2] cocaine[3] and heroin.[4] Due to their chiral nature circular dichroism has been increasingly applied in the study of cyclodextrins. The method has found great use in the measurement of the extent of inclusion of a species within the cyclodextrin cavity. Donzé *et al.* studied the inclusion of L-tryptophan with various CD derivatives. Intensity changes in the spectra suggested the successful inclusion of the guest within the cavity of the CD derivatives, with increasing intensities for the different derivatives suggesting increasing degrees of inclusion.[5] Impellizzeri *et al.* used c.d. spectroscopy as a complimentary technique to NMR spectroscopy to study a *N*-*tert*-butoxycarbonyl-*β*-alanylhistamine (Boc) group self-including within a CD cavity.[6] Similar examples of c.d. spectroscopy used as evidence of inclusion are given by Ramusino *et al.*[7] and Tarnai *et al.*[8]

Circular dichroism spectroscopy has also been applied to measurements involving metals and metal complexes. Czarnecki and Margerum showed the c.d. spectra of copper and nickel complexes of tetra- and pentapeptides with c.d. signals in the d-d transition range. The authors concluded that the involvement of the metal centre in chelation or its location immediately adjacent to the asymmetric centre is not essential for the resulting c.d. peak.[9]

Bonomo *et al.* used both electronic spectroscopy and circular dichroism to examine the ternary complexes of copper, CDEn and amino acids.[10] This is of particular relevance to the work reported here. Bonomo reported no inclusion of the amino acid alanine in the CD, but inclusion of the aromatic amino acids phenylalanine and tryptophan was seen, with the L enantiomer demonstrating stronger c.d signals. The same group studied other similar systems, for example the Cu(II) complex of the derivative 6-deoxy-6-*N*-(2-methylaminopyridine)-β-cyclodextrin $[Cu(CDampy)]^{2+}$ and the Cu(II) complex of a histamine monofunctionalised β-cyclodextrin $[Cu(CDhm)]^{2+}$ with similar results.[6] Studies carried out by Corradini *et al.* using metallo-CDs, also found that no stereoselectivity was observed towards aliphatic amino acids, whereas enantiomeric discrimination was observed for aromatic amino acids.[11]

It is for this reason that c.d. spectroscopy was chosen to study the inclusion of tyrosine and DOPA enantiomers within the cavity of the derivatised CDs. Carbidopa was not included in this study since only the L-enantiomer is commercially available. Benserazide was also excluded since the electronic spectroscopy study demonstrated that it does not form a ternary complex with the metallo-CDs.

3.2 Theory

A light beam is made up of electromagnetic waves that oscillate in all possible planes perpendicular to its path. Polarised light is produced by passing normal light through a polarising material such as a Nicol prism (crystalline calcium carbonate) or the material Polaroid (iodoquinine sulphate embedded in nitrocellulose film). Linearly plane polarised light oscillates in one single plane passing along the path of propagation. Circularly polarised light consists of two linearly plane polarised electromagnetic waves that are superimposed at an orientation of 90º to each other, both with an identical amplitude and frequency and which are out of phase by $\pi/2$ ($\lambda/4$). The resulting vector propagates in a full circle during each cycle, similar to the shape of a screw thread, as seen in Figure 3.1. Circular dichroism is the differential absorption of right and left circularly polarised light. The absorption coefficients of the two circularly polarised components differ due to the fact that they travel through the medium at different velocities and hence are absorbed to differing degrees by the substance. Circular dichroism can be measured as electronic circular dichroism in the spectral regions where electronic transitions occur (UV-Vis) or as vibrational circular dichroism in infrared spectral regions. All measurements made in this study are in terms of electronic circular dichroism.

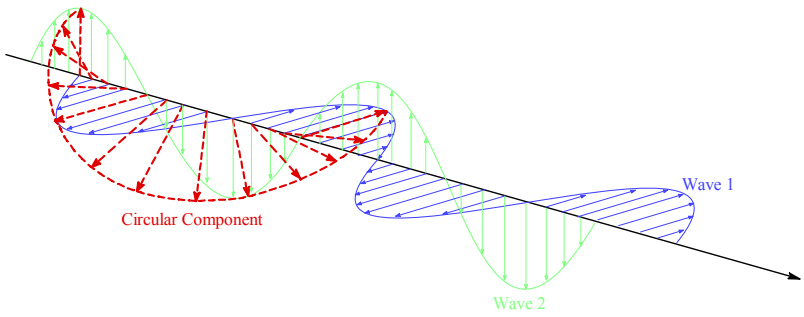

Figure 3.1 Generation of Circularly Polarised Light by Superposition of Electric Components of Two Linearly Polarised Light Beams with a Phase Difference of a Quarter Wavelength

Therefore at a given wavelength,

$$\Delta A = A_L - A_R \qquad \textbf{Equation 3.1}$$

where ΔA is the difference between the absorbance of left circularly polarised (A_L) and right circularly polarised (A_R) light. Applying the Beer-Lambert law gives,

$$\Delta A = (\varepsilon_L - \varepsilon_R)cl \qquad \textbf{Equation 3.2}$$

where ε_L and ε_R are the molar extinction coefficients for left and right circularly polarised light respectively, c is the molar concentration and l is the pathlength in cm. Thus the molar circular dichroism (Δε) can be described as

$$\Delta\varepsilon = (\varepsilon_L - \varepsilon_R) \qquad \textbf{Equation 3.3}$$

Circular dichroism also causes another effect, called ellipticity. As the absorptions of the left circularly polarised light and the right circularly polarised light are different, the light exiting the sample is now elliptically polarised. Ellipticity is given by the angle θ and is defined as the tangent of the ratio of the minor to major elliptical axis as shown in Figure 3.2.

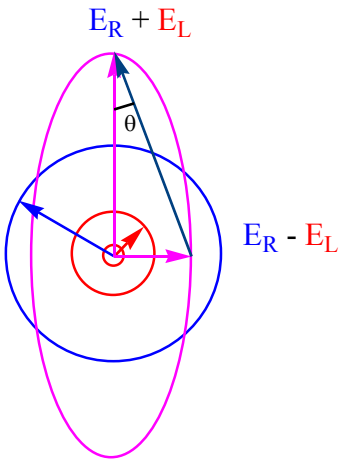

Figure 3.2 Elliptically polarised light (purple) is composed of unequal contributions of right and left circularly polarised light

C.d. instruments measure the difference in absorbance and results are normally reported in degrees or millidegrees of ellipticity. When θ is in degrees,

$$\Delta A = \frac{4\pi\theta}{180\ln 10} \qquad \textbf{Equation 3.4}$$

and when θ is in millidegrees

$$\Delta A = \frac{\theta}{3298} \qquad \textbf{Equation 3.5}$$

Combining equations (3.2) and (3.5) gives,

$$\Delta\varepsilon = \frac{\theta}{(32982cl)} \qquad \textbf{Equation 3.6}$$

where θ is ellipticity (mdeg), c is molar concentration (mol dm^{-3}) and l is the pathlength of the cell (cm).

In this work c.d. spectroscopy is used to determine if the binary Cu(II) complexes of CDEn, CDPn and CDBn include the two enantiomers of the guests tyrosine and DOPA to varying degrees, with a view to using the binary complexes for enantiorecognition.

3.3 Experimental

Circular dichroic spectra were measured at 25 ºC using a Jasco J-810 Spectropolarimeter. The Jasco J-810 spectropolarimeter allows measurement of both circular dichroism and optical rotary dispersion. The system uses a 150 W air-cooled Xenon arc lamp as the light source and has an operating range from 163 to 900 nm with a wavelength accuracy of approximately 0.2 nm. A NIR sensitive photomultiplier tube (PMT) allows measurements out to 1100 nm. Up to four channels can be acquired

simultaneously. Two channels have been incorporated for external signals such as temperature probes, pH meters *etc.* The internal signal can be chosen from circular dichroism or optical rotatory dispersion.

Calibration of the c.d. instrument was performed with a 0.06 % w/v ammonium *d-camphor*-10-sulfonate solution in water using a 1 cm cell. The spectrum was recorded between 350-250 nm and a c.d. peak value of +190.4 mdeg at 291 nm was found, which agreed well with reported values.[12]

Parameters used for the rest of the study were: Range: 900-200 nm, Sensitivity: Standard (100 mdeg), Data Pitch: 0.1-0.5 nm, Scanning Mode: continuous, Scanning Speed: 50 nm/ min, Response: 1, Bandwidth: 1 nm, Accumulation: 6-8.

For the circular dichroic study, spectra were recorded from 900 to 350 nm using a 10 mm cell and from 450 to 200 nm using a 1 mm cell, unless otherwise stated, since the molar extinction coefficients are smaller in the higher wavelength region. The resultant spectra were combined for analysis. It should be noted that the concentrations of the solutions used for the circular dichroism study were the same as those used for recording the electronic absorption spectra in Chapter 2.

3.4 Results and Discussion of Circular Dichroic Study

3.4.1 Binary Complexes

Figure 3.3 shows the spectra obtained from the c.d. spectroscopic study of the binary complexes of copper and CDEn, CDPn and CDBn. Table 3.1 summarises the results obtained.

Table 3.1 Results of the c.d spectroscopic study of CuCDEn, CuCDPn and CuCDBn

Binary Complex	λ (nm)	$\Delta\varepsilon$ ($mol^{-1}dm^3$ $cm^{-})^1$
CuCDEn	680	0.040

	529	-0.01
	308	0.026
	262	-0.207
	223	0.275
CuCDPn	615	0.035
	296	0.762
	250	-0.251
	217	-0.030
CuCDBn	381	0.001
	288	-0.060
	245	0.007

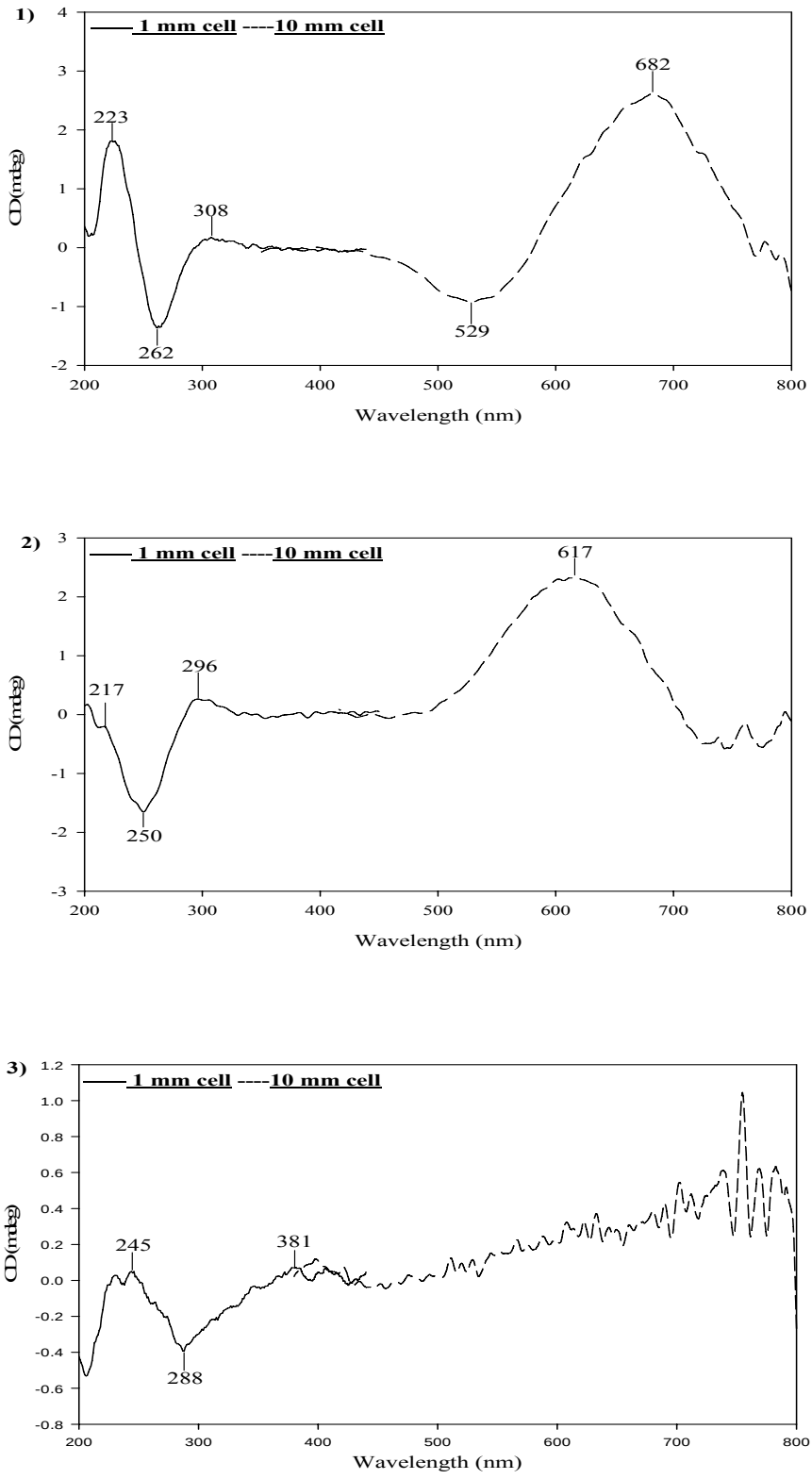

Figure 3.3 Circular dichroic spectra of Cu(II) with 1) CDEn 2) CDPn and 3) CDBn

The c.d. spectrum of $[CuCDEn]^{n+}$ shows bands at 308 nm (0.026 mol^{-1} dm^3 cm^{-1}), 262 nm (- 0.207 mol^{-1} dm^3 cm^{-1}) and 223 nm (0.275 mol^{-1} dm^3 cm^{-1}) while the spectrum of the $[CuCDPn]^{n+}$ system contains bands in the UV region at 296 nm (0.762 mol^{-1} dm^3 cm^{-1}), 250 nm (- 0.251 mol^{-1} dm^3 cm^{-1}) and 217 nm (-0.03 mol^{-1} dm^3 cm^{-1}). The c.d. spectrum of the $[CuCDBn]^{n+}$ system shows bands at 381 nm (0.001 mol^{-1} dm^3 cm^{-1}), 288 nm (-0.060 mol^{-1} dm^3 cm^{-1}) and 245 (0.007 mol^{-1} dm^3 cm^{-1}).

Corradini *et al.* assigned the c.d. band found in the spectra of the binary complexes of Cu(II) with CD derivatives at ~ 250 nm to charge transfer transitions from the two highest occupied π-orbitals of the CD moiety to the vacant copper(II) d-orbital.[11] However since CDAm ligands also give bands in this region, it is difficult to confirm assignments. Therefore it is probably more appropriate to broadly assign bands in the UV region to some transition of the CD group. The band in the visible region of the spectra is assigned to d-d transitions of the metal ion.

The binary complexes $[CuCDEn]^{n+}$ and $[CuCDPn]^{n+}$ give c.d spectra showing a broad band in the visible region (~ 680 nm for $[CuCDEn]^{n+}$ and ~ 615 nm for $[CuCDPn]^{n+}$). However this band is not evident in the c.d spectrum of $[CuCDBn]^{n+}$ most likely due to poor coordination of CDBn to the Cu(II) ion. This result confirms the results seen in the electronic absorption study which showed poorer coordination of CDBn acting as a monodentate ligand.

3.4.2 Ternary Complexes

As was the case in the electronic spectroscopy study, bands present in the UV region of the c.d. spectra of the ternary complexes are assigned to transitions of the CD moiety and the amino acids and bands in the visible region are due to d-d transitions of the metal ion. Therefore to investigate the inclusion of the guests in the CD cavity it was important to concentrate on bands in the UV region.

Figures 3.4-3.5 show the spectra for the ternary complexes of D/L-tyrosine and D/L-DOPA with CuCDEn, CuCDPn and CuCDBn at pH 7.2. Table 3.2 summarises the results obtained.

Increases in $\Delta\varepsilon$ arise from an increase in the depth of inclusion of the aromatic ring of an amino acid within the CD cavity.[10] Therefore the circular dichroic spectra of all complexes were compared by calculating $\Delta(\Delta\varepsilon)$ where $\Delta(\Delta\varepsilon) = |\Delta\varepsilon(D)| - |\Delta\varepsilon(L)|$) at ~ 228 nm for tyrosine and 250 nm for DOPA. Table 3.3 summarises the results obtained.

Table 3.2 Spectral data for tyrosine and DOPA ternary complexes at pH 7.2

Guest	**Ternary Complex** λ **(nm)** $(\Delta\varepsilon)$ **(mol^{-1} dm^3 cm^{-1})**		
	$[CuCDEn]^{2+}$	**$[CuCDPn]^{2+}$**	**$[CuCDBn]^{2+}$**
D-Tyrosine	228 (2.71) 277 (-0.41) 298 (0.22)	228 (3.08) 270 (-2.00) 295 (-0.02)	227 (2.85) 269 (-1.15) 299 (0.43)
L-Tyrosine	225 (-0.89) 270 (0.45) 298 (-0.05)	227 (-2.44) 270 (0.62) 295 (-0.02)	228 (-2.40) 269 (0.97) 299 (-0.24)
D-DOPA	251 (-3.93) 295 (-1.33)	250.4 (-3.8) 295 (-2.76)	249.6 (-3.14) 295 (-2.52)
L-DOPA	251 (1.96) 295 (1.30)	250.4 (3.72) 295 (2.82)	249.6 (3.47) 295 (2.65)

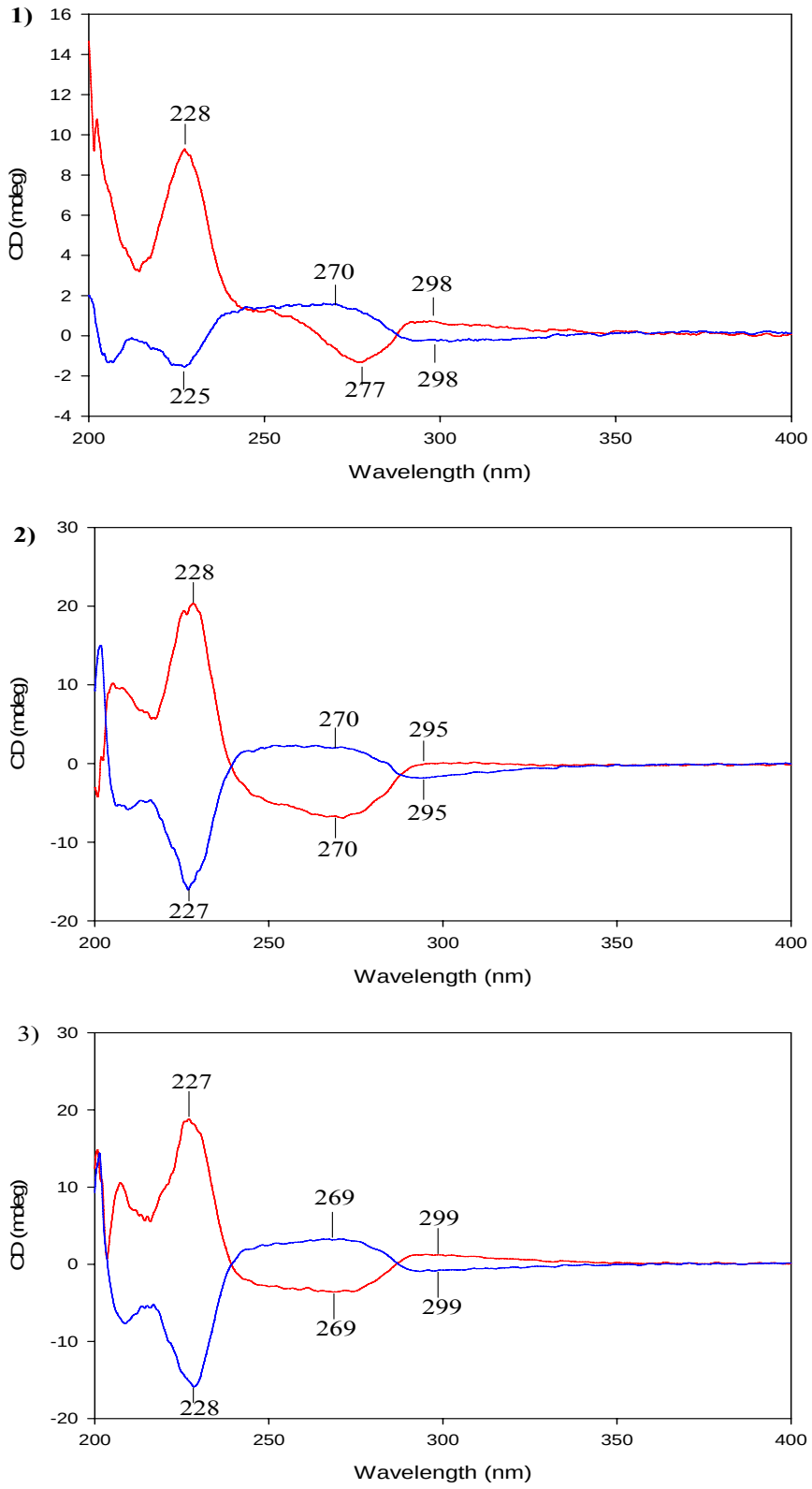

Figure 3.4 Circular dichroic spectra of ternary complexes of Cu(II) and D-tyrosine in red and L-tyrosine in blue with 1) CDEn, 2) CDPn and 3) CDBn

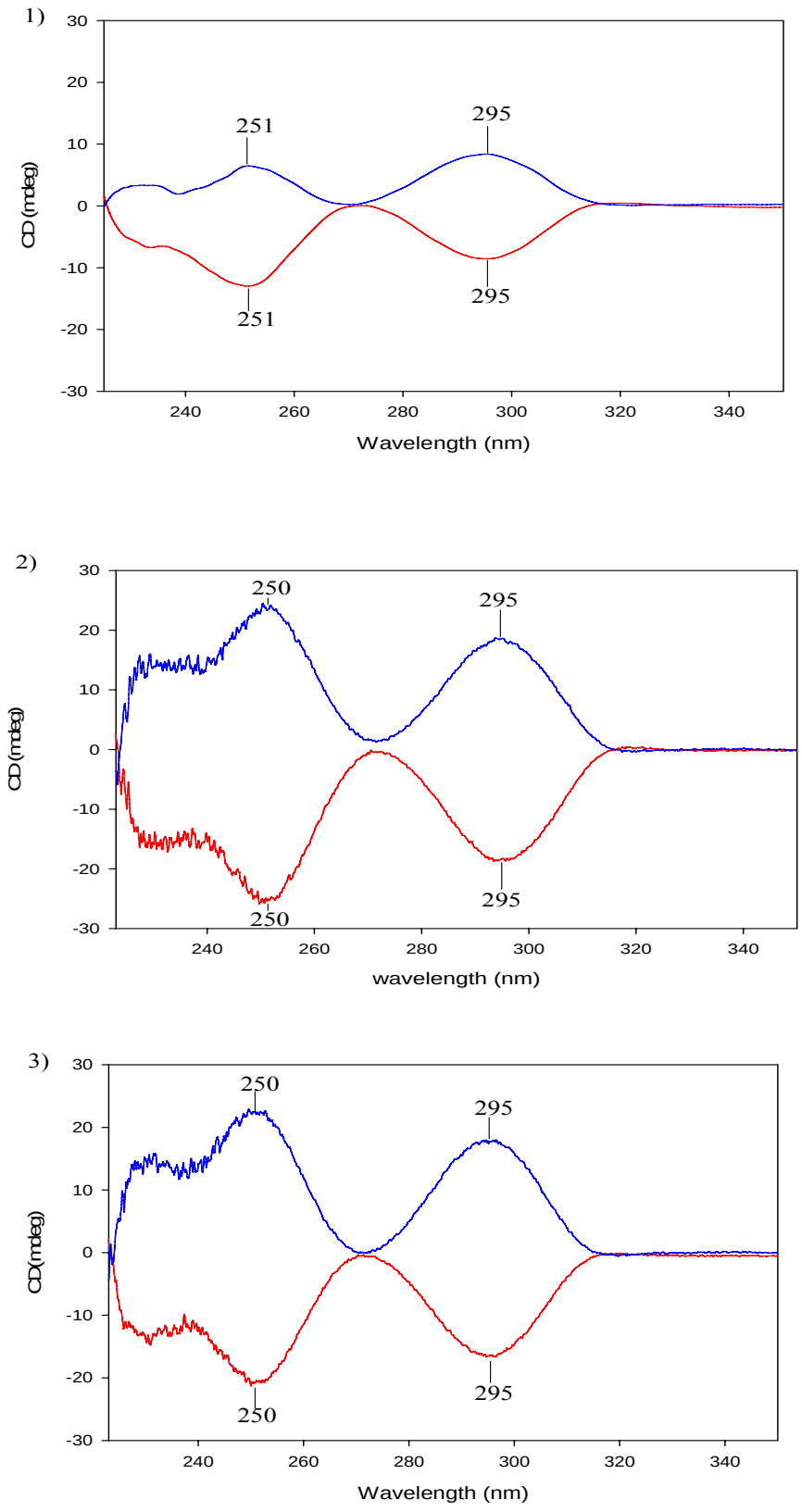

Figure 3.5 Circular dichroic spectra of ternary complexes of Cu(II) and D-DOPA in red and L-DOPA in blue with 1) CDEn, 2) CDPn and 3) CDBn

Table 3.3 Comparison of $\Delta(\Delta\varepsilon)$ values in the UV region for the ternary complexes of CuCDAm with tyrosine and DOPA

Guest	$[CuCDEn]^{2+}$	$[CuCDPn]^{2+}$	$[CuCDBn]^{2+}$
Tyrosine	**2.54**	0.69	0.45
DOPA	**1.97**	0.08	0.33

From the c.d spectra and the results presented in Table 3.3 it is very clear that CuCDEn has the most favourable enantioselective properties towards tyrosine. The signal observed at 228 nm shows a much higher value of $\Delta\varepsilon$ for the D-diastereomeric complex compared to the L-diastereomeric complex. This indicates that the D-tyrosine enantiomer is included to a much greater extent than the L-tyrosine enantiomer. This obvious difference in inclusion cannot be seen using $[CuCDPn]^{n+}$ and $[CuCDBn]^{n+}$. The $\Delta(\Delta\varepsilon)$ values obtained in these two cases are approaching zero which suggests a similar level of inclusion of both enantiomers and no discrimination between them. Therefore of the three amino-CDs used in this work only $[CuCDEn]^{n+}$ is an effective chiral discriminator for tyrosine.

Bonomo *et al.* investigated the inclusion complexes of $[CuCDEn]^{n+}$ with D and L-phenylalanine which is structurally similar to tyrosine.[10] These workers reported bands in the c.d. spectra for these complexes at 236 nm and 286 nm which compare to the values obtained here for tyrosine (228 nm and 270 nm). They calculated a $\Delta(\Delta\varepsilon)$ value of 0.39 which is lower than that calculated for tyrosine here indicating CDEn is more stereoselective towards tyrosine than phenylalanine. However in this work the $\Delta(\Delta\varepsilon)$ values were calculated from bands in the UV region whereas Bonomo *et al.* calculated them from bands in the visible region.

In a separate study Bonomo *et al.* investigated the inclusion complexes of tyrosine with a bifunctionalised CD.[13] These workers reported a c.d. spectrum of the ternary complex of [Cu(A,BCDNH$_2$)] with D,L-tyrosine with bands at ~ 230 nm and 270-275 nm. This mirrors almost exactly the equivalent spectrum of tyrosine with CDEn recorded in this work.

Maccarrone *et al.* also used c.d. spectroscopy to study the inclusion complexes of various CuCDAm derivatives including CDEn with amino acids such as tyrosine.[14] However they found that the difference between the enantiomers in terms of $\Delta\varepsilon$ was not detectable. This result is surprising given the $\Delta(\Delta\varepsilon)$ recorded in this work (2.54). Again this could be attributed to these values being calculated from the visible region of the spectra *versus* the UV region here.

For DOPA, $[CuCDEn]^{n+}$ is again the most effective enantioselector. A $\Delta(\Delta\varepsilon)$ value of 1.97 was recorded which is slightly lower than the value for tyrosine. Again the D-enantiomer shows preferential inclusion over the L-isomer. This decrease in $\Delta(\Delta\varepsilon)$ may be surprising as the only difference between tyrosine and DOPA is the presence of an extra hydroxyl group on the aromatic side-chain. However it is possible that because of this extra polar group the non-polar CD cavity is repelling the side-chain of DOPA, thus leading to a decreased depth of inclusion. Again $[CuCDPn]^{n+}$ and $[CuCDBn]^{n+}$ show virtually no selection properties for DOPA.

3.5 Conclusion of Circular Dichroism Study

The circular dichroic spectra of the complexes studied suggest host-guest formation between the metallo-cyclodextrins and tyrosine and DOPA, with the formation of diastereomeric ternary complexes. Differences in intensity of the bands in these spectra suggest that the metallo-cyclodextrins are preferentially including one isomer and therefore can possibly be used for enantiomeric separation.

From the results obtained in this study, it can be shown that $[CuCDEn]^{n+}$ is the most enantioselective material for both tyrosine and DOPA. This enantioselection of $[CuCDEn]^{n+}$ results from the preferential inclusion of the D-enantiomer over the L-enantiomer within the CD cavity. It is therefore proposed that $[CuCDEn]^{n+}$ is acting as a multi-site enantioselector, utilising both the inclusion properties of the CD cavity and the coordinating ability of the Cu(II) ion. Cu(II) will have a tetragonally-distorted octahedral structure due to its d^9 configuration and therefore structural restrictions imposed by coordination of the guest to the copper(II) ion inhibit inclusion in the case of the L-enantiomer. A possible structure is given below in Figure 3.6. However the stoichiometry of the complexes must be determined to support any proposed structures.

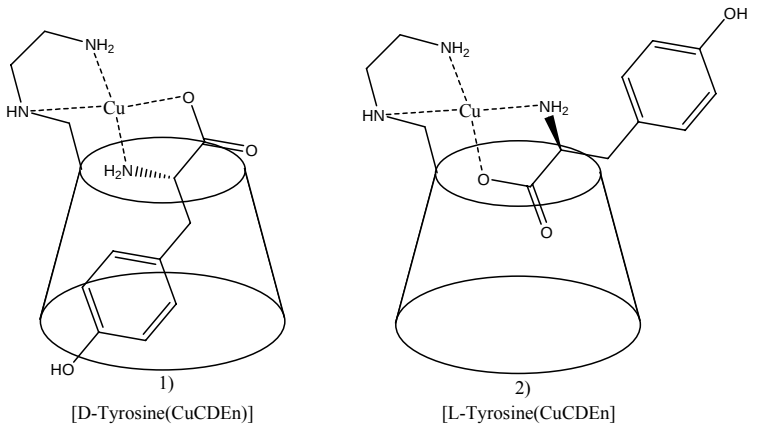

Figure 3.6 Proposed structures of the diastereoisomers of 1) [Cu(CDEn)(D-tyrosine)]$^{n+}$ and 2) [Cu(CDEn)(L-tyrosine)]$^{n+}$ showing enantioselective orientation

In the case of $[CuCDPn]^{n+}$ enantioselection may not be possible due to the structure of the 1,3-diaminopropane moiety. The longer alkane chain may be flexible enough to allow interaction of the aromatic units of both enantiomers with the cavity. For $[CuCDBn]^{n+}$ it is proposed that the length of the alkane chain prevents the 1,4-diaminobutane moiety acting as a bidentate ligand, which again may facilitate inclusion of both enantiomers in the cavity. Therefore these results suggest that one CuCDAm derivative is not a one stop shop for enantioselection.

3.6 References

[1] J.M. Bowen, T.A. Crone, V.L. Head, H.A. McMorrow, R.K. Kennedy and N. Purdie: *J. Forensic Sci.* **26**, (1981) 664

[2] J.M. Bowen, T.A. Crone, A.O. Hermann and N. Purdie: *Anal. Chem.* **52**(14), 2436 (1980); T.A. Crone and N. Purdie: *Anal. Chem.* **53**, (1981) 17

[3] J.M. Bowen and N. Purdie: *Anal. Chem.* **53**, (1981) 2237

[4] J.M. Bowen, T.A. Crone, R.K. Kennedy and N. Purdie: *Anal. Chem.* **54**, (1982) 66

[5] C. Donzé, E. Rizzarelli and G. Vecchio: *Supramolecular Chemistry* **10**, (1998) 33

[6] G. Impellizzeri, G. Pappelardo, F. D'Alessandro, E. Rizzarelli, M. Saviano, R. Iacovino, E. Benedetti, and C. Pedone: *Eur. J. Org. Chem.* 2065 (2000).

[7] M. Cotta Ramusino, M. Bartolomei and B. Gallinella: *J. Inclusion Phenom. Macrocyclic Chem.* **32**, (1998) 485

[8] M. Tarnai, Á. Buvári-Barcza and L. Barcza: *J. Inclusion Phenom. Macrocyclic Chem.* **34**, (1999) 311

[9] J.J. Czarnecki and D.W. Margerum: *Inorg. Chem.* **16**, (1977) 1997

[10] R.P. Bonomo, V. Cucinotta, F. D'Allessandro, G. Impellizzeri, G. Maccarrone and E. Rizzarelli: J. Inclusion *Phenom. Mol. Recog. Chem.* **15**, (1993) 167

[11] R. Corradini, A. Dossena, G. Impellizzeri, G. Maccarrone, R. Marchelli, E. Rizzarelli, G. Sartor and G. Vecchio: *J. Am. Chem. Soc.* **116**, (1994) 10267

[12] A. Rodger and B. Norden *Circular Dichroism and Linear Dichroism*, Oxford Chemistry Masters, Oxford University Press (1997), p. 6.

[13] R.P. Bonomo, T. Campagna and G. Vecchio, *Proc. Perspect. Inorg. Chem.* Bressanone (1993)

[14] G. Maccarone, E. Rizzarelli and G. Vecchio: Chiral Recognition by Functionalised Cyclodextrin Metal Complexes. In L. Fabbrizzi and A. Poggi (eds.), *Transition Metals in Supramolecular Chemistry,* Kluwer Academic Publishers, (1994), pp. 351-367.

4. Stoichiometry of Binary and Ternary Complexes

4.1 Introduction

As discussed previously in Chapter 2 enantioresolution by metallo-CDAm derivatives is dependent in the first instance on their ability to form ternary complexes with guest molecules, where the L and D isomers form diastereoisomeric complexes. To fully understand the types of complexes formed in these experiments, their stoichiometry must be assessed.

Various methods for the determination of the stoichiometry of complexes of CDs have been explored including microcalorimetry,[1] NMR spectroscopy[2] and surface tension measurement.[3] However Wiczk *et al.* describe electronic and fluorescence spectroscopic methods which are the most widely used.[4] In this work electronic spectroscopy was utilised.

Statistical evaluation of the data collected can be achieved using either a non-linear least-squares fitting method (Benesi-Hildebrand)[5] or the continuous variation technique (Job's Plot).[6] Reports by G. Pistolis and A. Malliaris[7] and O. Exner[8] suggest that the Benesi-Hildebrand method is not reliable for the determination of the stoichiometry and equilibrium constants of reactions involving weak complex formation. G. Pistolis *et al*. surmise that the method is incapable of differentiating between 1:1 and 2:1 stoichiometries.[7] As these are the most likely stoichiometries of our derivatives this method was not considered fit for purpose. The Job's plot has been used successfully by groups investigating CD complex formation and was therefore selected as the preferred method in this work.[9,10]

4.2 Theory

Inclusion complex formation can be described by the equilibrium,

$$hH + gG \rightleftharpoons C \qquad \textbf{Equation 4.1}$$

where H is the host molecule, G is the guest and C is the inclusion complex. The Job's method of continuous variation to calculate the stoichiometric quantities h and g involves measuring an observable property that is proportional to the concentration of product (*e.g.* UV-Vis absorbance) in a series of solutions of constant total molarity, with varying host to guest ratio. It is best to measure this absorbance at a wavelength where the product absorbs and not the reactants. If this is not possible it is feasible to mathematically adjust for the absorption of the reactants

Experimentally a series of solutions is prepared each containing the same total number of moles of H and G but a different ratio. If it is assumed that the total number of moles of H and G is 1 and the number of moles of H in a given solution is x then the number of moles of G is 1-x.

Therefore,

$$[H] + [G] = 1$$

$$[H] = x$$

$$[G] = 1 - x$$

$$\frac{[G]}{[H]} = r = 1 - \frac{x}{x}$$

If x < H then H is the yield limiting reagent (YLR) and [C] = x/H. A plot of [C] *versus* x for a series of solutions is linear with a positive slope.

If x > H then G is the YLR and [C] = 1-x/G. A plot of [C] *versus* x for a series of solutions is linear with a negative slope.

The maximum amount of complex is produced at the value of x where the two lines intersect.

Figure 4.1 shows a stylised example of a Job's Plot showing a 1:1 complexation predominant at equilibrium. Here the maximum point of inflection of the curve is at x = 0.5. If the predominant complexation was 1:2 then x = 0.33 would be the maximum.

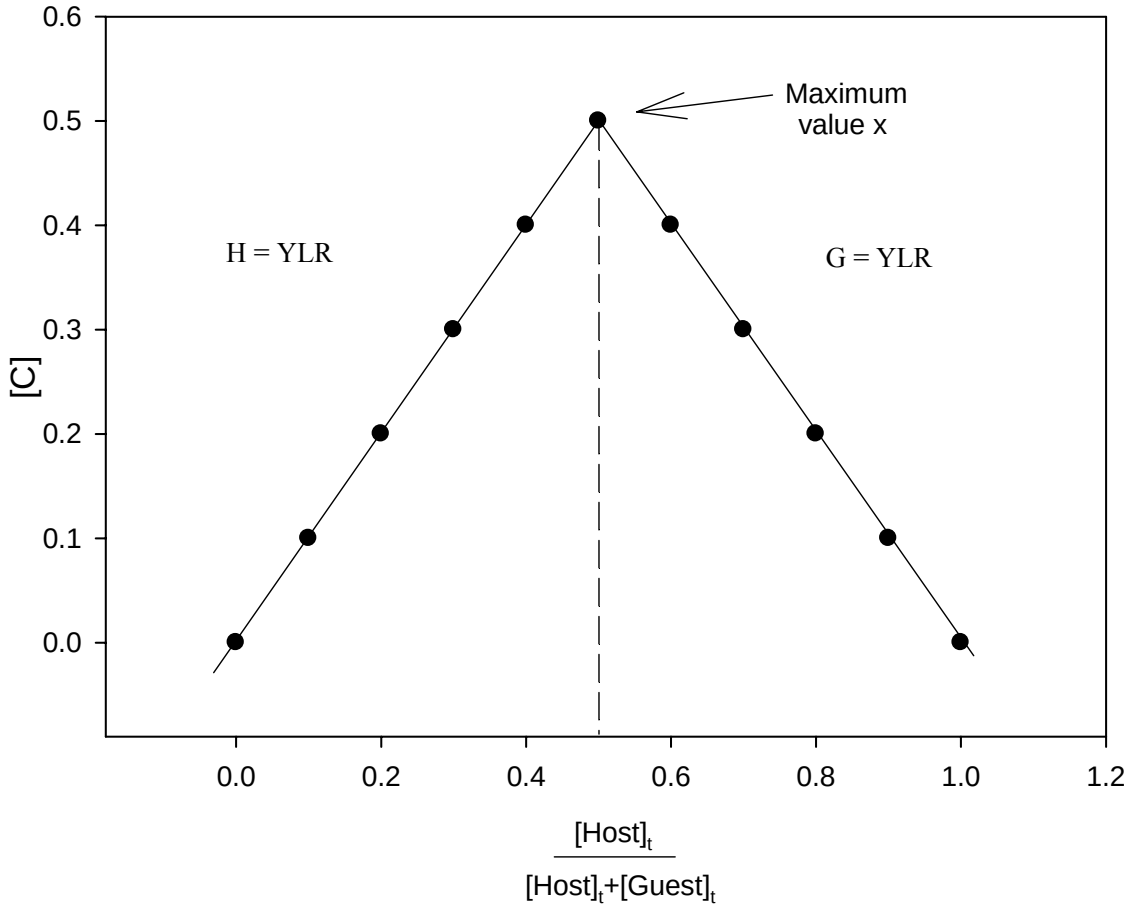

Figure 4.1 Example of a Job's plot showing 1:1 stoichiometry[11]

4.3 Experimental

Electronic spectra were measured at room temperature using a Perkin Elmer Lambda 900 UV/Vis/NIR Spectrometer. Parameters used in this work were: Slit Width: 0.1 nm, Accumulation: 1. Spectra were taken using quartz cells of 10 mm path length. Solutions used for recording the electronic spectra were as follows:

- Host:Guest studies of DOPA and carbidopa were performed using stock solutions of CuCDEn (0.002 mol dm^{-3}) and DOPA or carbidopa (0.002 mol dm^{-3}) dissolved in ammonium acetate buffer at pH 6.8.
- Due to its poor solubility, tyrosine was used in a lower concentration (0.001 mol dm^{-3}). The concentration of CuCDEn was adjusted accordingly.

For the Job's plots, absorbance data was recorded at 650, 670 and 450 nm for CDEn, DOPA and carbidopa respectively. New bands occur at theses wavelengths on formation of complexes with Cu(II) for these ligands. However no new band was observed on reaction of Cu(II) or CuCDEn with tyrosine. In this case a wavelength should be chosen where either the host or guest has no contribution to the absorption. 250 nm was chosen as tyrosine shows very little absorbance at this wavelength. Any unwanted contribution to the overall absorbance can be subtracted mathematically.

4.4 Results

4.4.1 Binary Complex of Cu and CDEn

Figures 4.2 and 4.3 show the spectra and Job's plot for the spectral titration of Cu(II) with CDEn using the continuous variation method. The concentrations of the solutions used and the absorbance data obtained are given in Table 8.2 in Appendix 8.2.

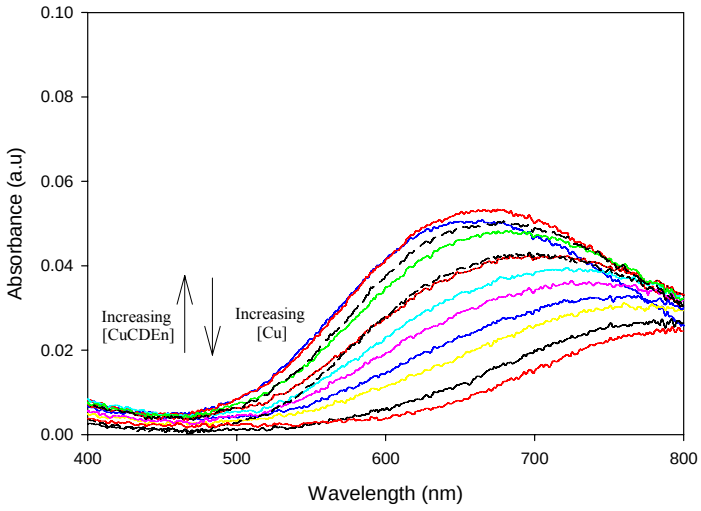

Figure 4.2 Spectral titration of Cu(II) with CDEn

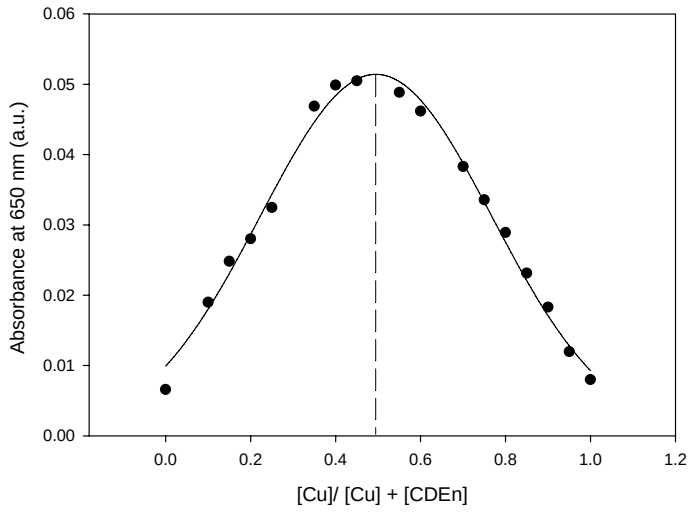

Figure 4.3 Job's plot from spectral titration of Cu(II) with CDEn

Figure 4.2 highlights the hypsochromic shift occurring gradually as the Cu^{2+} ion coordinates to the amino groups of the CDEn molecule (as discussed in Chapter 2). The absorbance values at 650 nm were plotted against [Cu] / [Cu] + [CDEn] and results are shown in Figure 4.3. Theoretically the Job's Plot should show two intersecting straight lines. However this is an idealised result and the curve shown above is more realistic. A best fit curve was fitted using Sigma Plot 11 ® and the maximum point extrapolated to the x axis gives a value of 0.53 which indicates a ratio of 1:1 for Cu:CDEn stoichiometry Bonomo *et al.* calculated the same stoichiometry in 1993 using a potentiometric method.[12] This is encouraging as potentiometric techniques are experimentally more complicated than spectral titrations. Matsui *et al.* also fitted UV absorbance data to a Job's Plot calculating a 1:2 Cu:CDEn complex.[9] The difference in results can be attributed to the difference in pH at which the experiments were carried out. Matsui *et al.* obtained results at a pH of 10.5 and at this pH both amino groups on CDEn (pKa_1 5.56, pKa_2 8.92[13]) will be deprotonated which may facilitate 1:2 complex formation. The results reported here and by Bonomo *et al.* were obtained at pH 6.8 and pH 7 respectively.

4.4.2 Binary Complexes of Cu and D- and L-Tyrosine

Figure 4.4 shows the spectra obtained from the titration of Cu(II) and D- and L-tyrosine respectively, along with the corresponding Job's plots obtained using the continuous variation method. The concentrations of the solutions used and the absorbance data are given in Table 8.3 and Table 8.4 in Appendix 8.2.

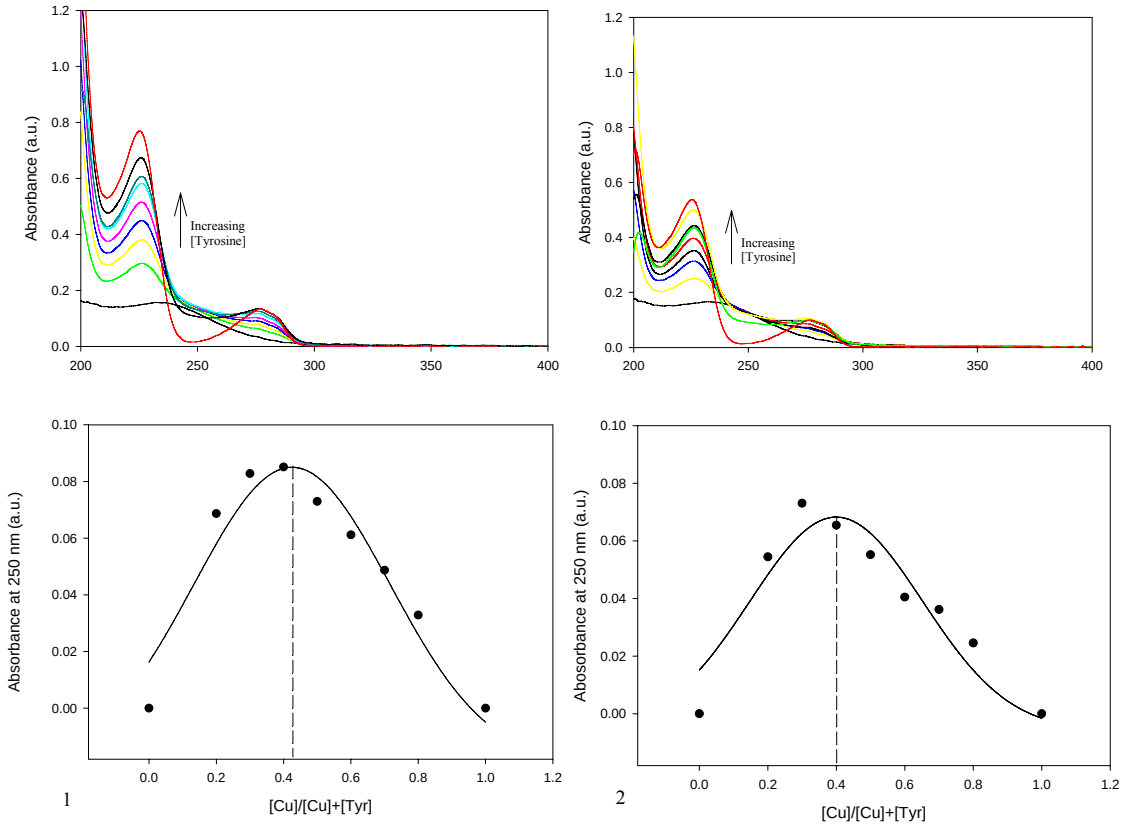

Figure 4.4 Spectral titration and Job's plots of Cu(II) with 1) D-tyrosine and 2) L-tyrosine

The Job's plots obtained from titration of Cu(II) with D-tyrosine and L-tyrosine both show inflection points at ~ 0.4. As shown in the case of CuCDEn above a value of 0.5 indicates a 1:1 complex. A value of 0.33 would indicate a 1:2 complex. As the inflection points lie between these values it is reasonable to suggest the presence of both 1:1 and 1:2 Cu:tyrosine complexes in equilibrium. Coordination of the copper ion to tyrosine is likely to occur at the electron donating amino nitrogen and carboxylic

oxygen. 1:1 and 1:2 complexes of Cu:tyrosine are well known and are used as low molecular weight analogs of superoxide dismutase.[14] 1:2 complexes are formed by copper(II) bridging two tyrosine molecules giving a *bis*-amino acid complex $[Cu(II)(Tyr)_2]^{2+}$.[15,16]

4.4.3 Ternary Complexes of D- and L-Tyrosine and CuCDEn

Figure 4.5 shows the spectra obtained from the titration of CuCDEn with D- and L-tyrosine along with the corresponding Job's plots obtained using the continuous variation method. The concentrations of the solutions used and the absorbance data obtained are given in Table 8.5 and 8.6 in Appendix 8.2.

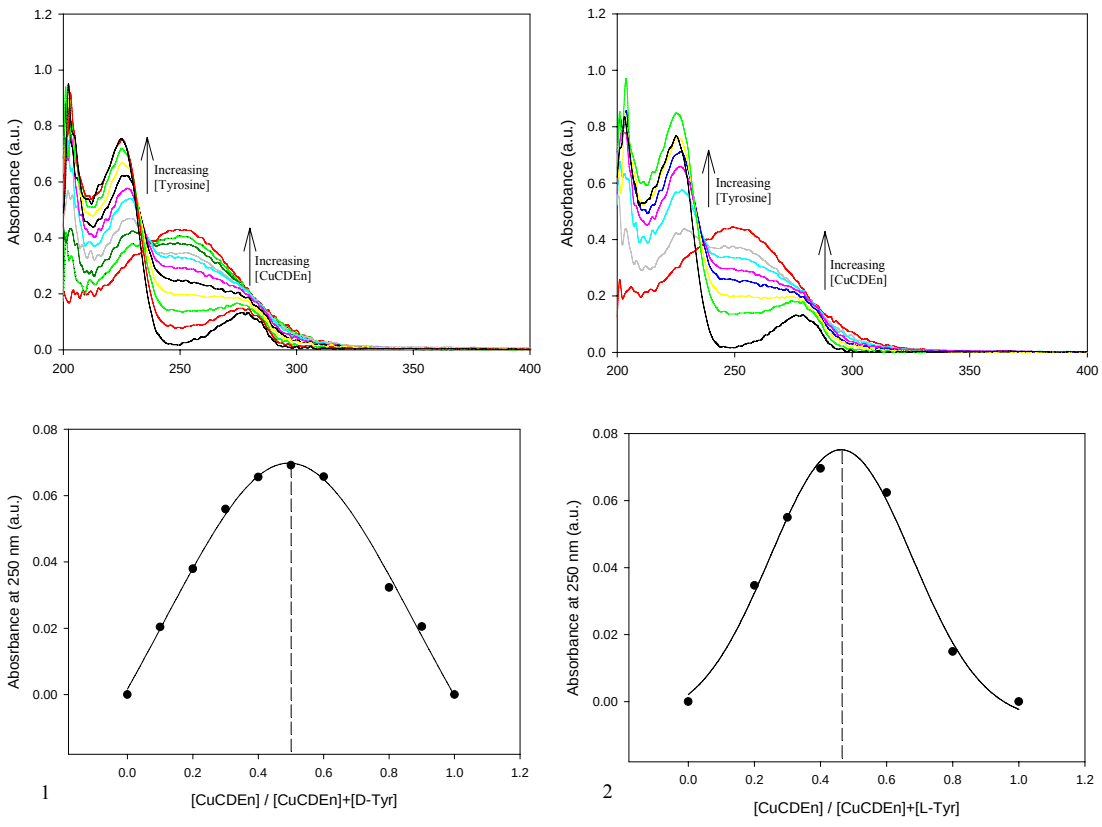

Figure 4.5 Spectral titration and Job's plots of CuCDEn with 1) D-tyrosine and 2) L-tyrosine

The Job's plots presented in Figure 4.5 show inflection points at 0.5 and 0.47 for the spectral titration of CuCDEn with D- and L-tyrosine respectively. These results suggest

the formation of 1:1 complexes of [CuCDEn(Tyr)] which agrees with the proposals of Bonomo *et al.* for similar complexes of CuCDEn with alanine, phenylalanine and tryptophan.

4.4.4 Binary Complexes of Cu and D- and L-DOPA

For enantioseparation to be successful the guest species must interact with both CDEn and the Cu(II) ion. Electronic spectroscopy studies of the ternary complexes of $[CuCDEn(DOPA)]^{n+}$ showed a sequential shift to lower wavelengths in λ_{max} of the d-d transition of copper as it coordinated to CDEn and then to DOPA. To verify this interaction the stoichiometry of Cu:DOPA was investigated. Figure 4.6 shows the spectra obtained for the titration of Cu(II) and D- and L-DOPA along with the corresponding Job's plots obtained using the continuous variation method. The concentrations of the solutions used and the absorbance data are given in Table 8.7 and Table 8.8 in Appendix 8.2.

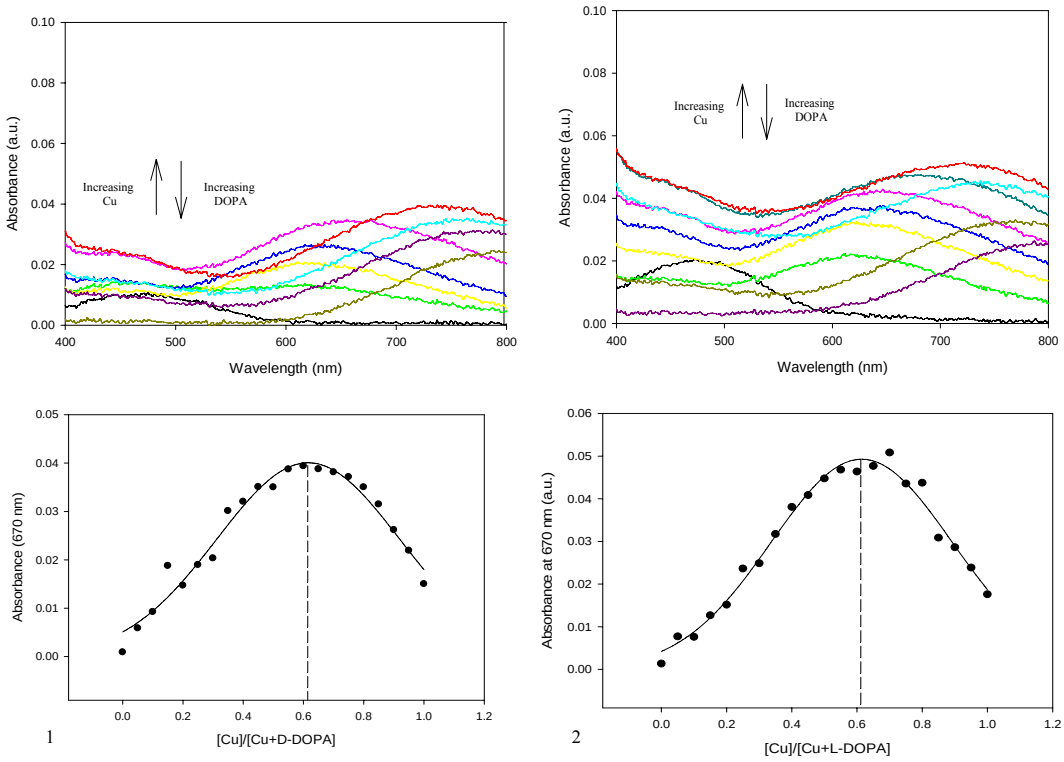

Figure 4.6 Spectral titration and Job's plots of Cu with 1) D-DOPA and 2) L-DOPA

The Job's plots obtained from titration of Cu(II) with D-DOPA and L-DOPA both show an inflection point at ~ 0.60. As shown in the case of CuCDEn above, a value of 0.5 indicates a 1:1 stoichiometry, but a value of 0.66 would represent a 2:1 complex. As the extrapolated value lies between these ratios, it is reasonable to suggest that both 1:1 and 2:1 ratios of Cu:DOPA are present in equilibrium.

DOPA is potentially a tetradentate ligand with four donor atoms including the amino nitrogen, the carboxylic oxygen and the two *ortho* phenolic hydroxy groups.[17] The coordination of catechols such as DOPA, by metal ions was studied by J. E. Gorton and R. F. Jameson in the late 60s where they investigated the complexes of Cu and DOPA by potentiometric measurements.[18] They found that when there was an excess of ligand present both 1:1 and 1:2 amino acid-like and pyrocatechol-like complexes formed *i.e.* coordination *via* N, O and catechol hydroxyl groups respectively.

4.4.5 Ternary Complexes of D- and L-DOPA with CuCDEn

Figures 4.7 shows the UV spectra of the continuous variation method for the D and L-[DOPACuCDEn]$^{+}$ ternary complexes along with the resultant Job's Plots. The concentrations of the solutions used and the absorbance data are given in Table 8.9 and Table 8.10 in Appendix 8.2.

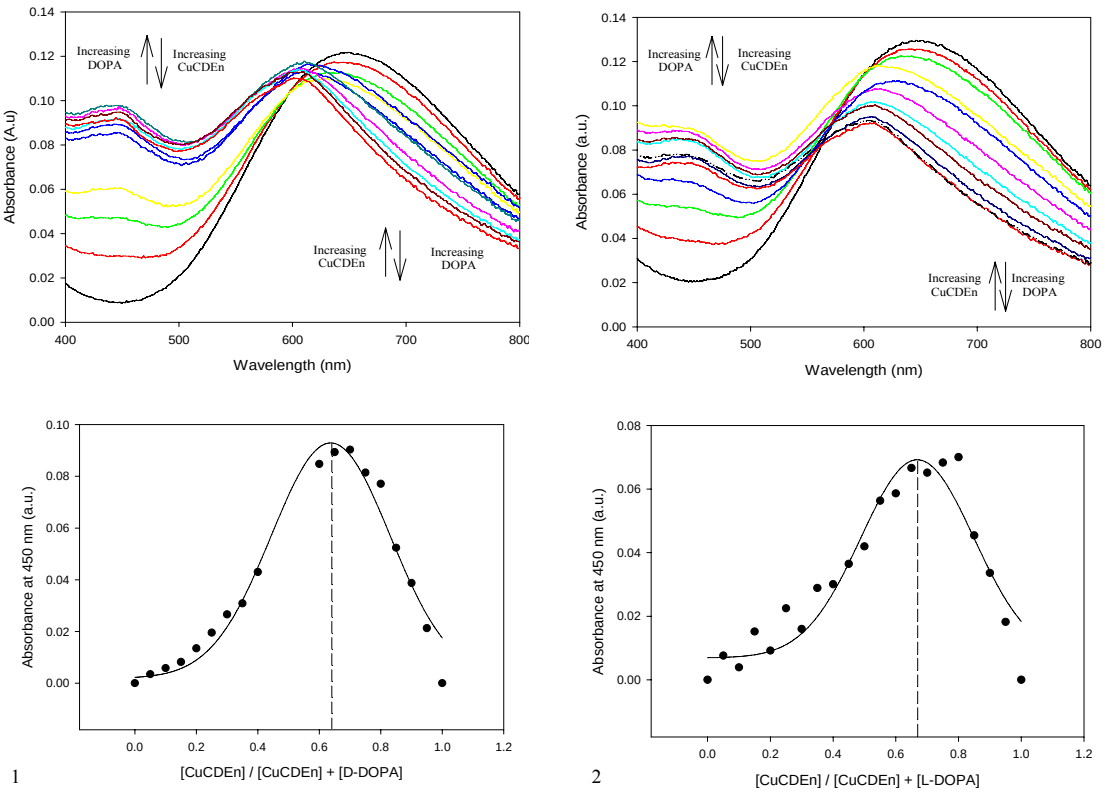

Figure 4.7 Spectral titration and Job's plots of CuCDEn with 1) D-DOPA and 2) L-DOPA

Both Job's plots for the spectral titration of CuCDEn and the enantiomers of DOPA indicate complexes in a ratio of 2:1 host-guest.

Bonomo *et al.* studied the thermodynamic properties of CuCDEn with some amino acids, namely alanine, phenylalanine and tryptophan.[12] To the best of the authors' knowledge no stoichiometric study exists in the literature for the complexes of CuCDEn with DOPA. However as DOPA contains an amino acid-like functional group and is structurally similar to phenylalanine (differing only by the presence of two hydroxyl groups on the *ortho* phenolic ring) comparisons can be made. Bonomo showed that the ternary complexes of all three amino acids exist as a $[Cu(CDEn)(AaO^-)]^+$ species with a 1:1 host guest ratio.

Therefore the results of this study suggest that the presence of the hydroxyl groups on the ortho phenolic ring of DOPA which gives the ligand its tetradentate character has resulted in the formation of a [(Cu(CDEn)$_2$)DOPA] complex.

4.4.6 Binary Complex of Cu and L-Carbidopa

Figure 4.6 shows the spectra obtained for the titration of Cu(II) and L-carbidopa along with the corresponding Job's plot obtained using the continuous variation method. The concentrations of the solutions used and the absorbance data are given in Table 8.11 in Appendix 8.2.

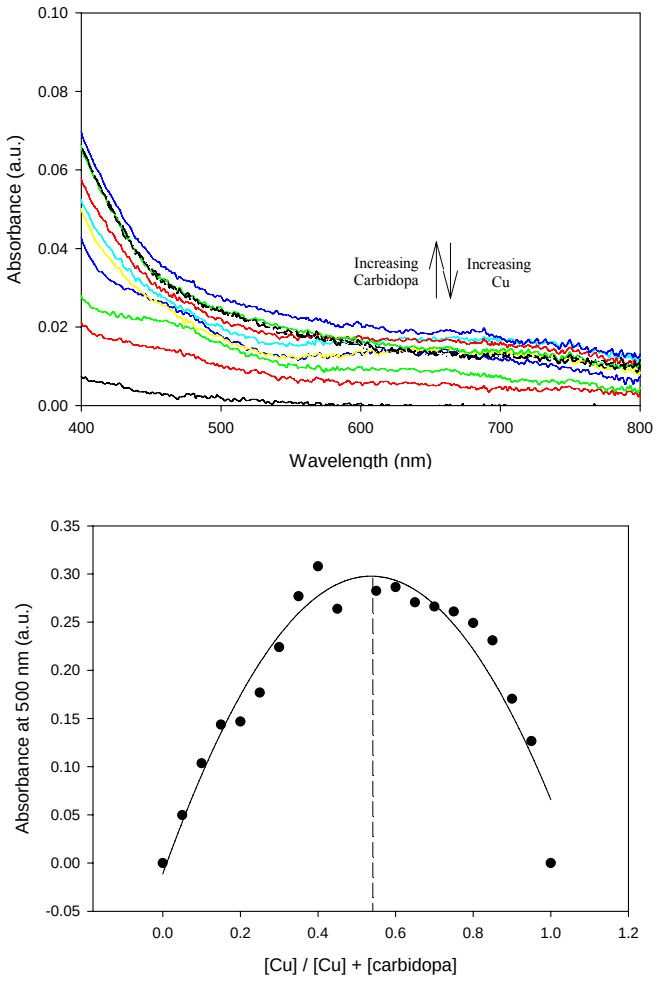

Figure 4.8 Spectral titration and Job's plot of Cu with L-carbidopa

The Job's plot representing the complex of carbidopa and copper is shown above with an inflection point of 0.54. As stated before a value of x = 0.55 would indicate a 1:1 complex. The curve in the plot above is quite broad with a maximum only achieved with curve fitting. However the value obtained does suggest a 1:1 Cu:carbidopa complex. Carbidopa has many structural similarities to DOPA with O, O and N, O coordination available to the copper ion. There is also the possibility for N, N coordination with copper.

4.4.7 Ternary Complex of L-Carbidopa and CuCDEn

Figure 4.9 shows the UV spectrum and Job's plot for the coordination of carbidopa to CuCDEn. The concentrations of the solutions used and the absorbance data are given in Table 8.12 in Appendix 8.2.

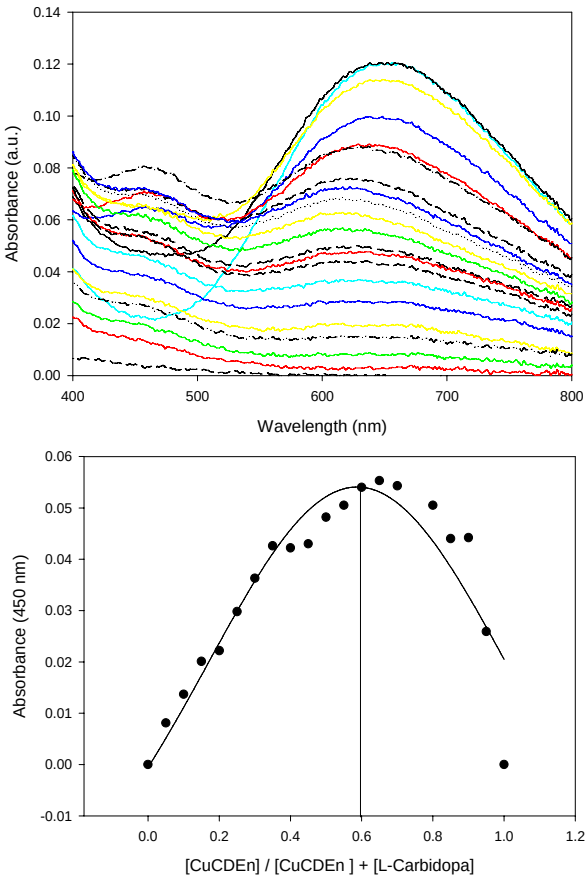

Figure 4.9 Spectral titration and Job's plot of CuCDEn with L-carbidopa

The Job's plot from the spectral titration of CuCDEn with L-carbidopa shows a maximum at ~ 0.6, which indicates that both 1:1 and 2:1 complexes are present in equilibrium. As mentioned previously carbidopa has potentially five donor atoms and therefore it is possible that complexes with 1:1 and 2:1 stoichiometry may form.

4.5 Conclusion of Stoichiometry Study

Table 4.1 details the stoichiometries of the binary complexes obtained in this study and based on these results proposed structures are shown in Figure 4.10.

Table 4.1 Stoichiometry results for the binary complexes of Cu(II) with CDEn, tyrosine, DOPA and carbidopa at pH 6.8

Metal	*Ligand*	*Stoichiometry*
Cu(II)	CDEn	1:1
Cu(II)	D-tyrosine	1:1 and 1:2
Cu(II)	L-tyrosine	1:1 and 1:2
Cu(II)	D-DOPA	1:1 and 2:1
Cu(II)	L-DOPA	1:1 and 2:1
Cu(II)	L-carbidopa	1:1

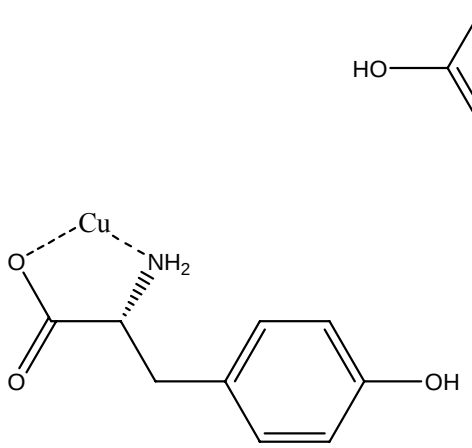

1:1 Cu(II) tyrosine complex

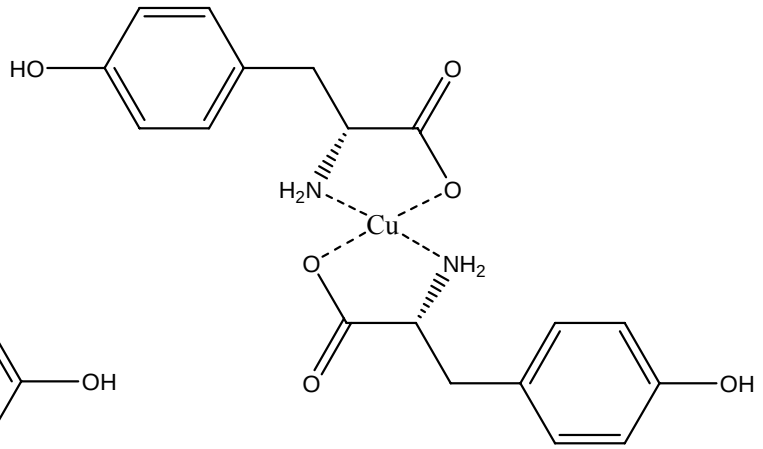

1:2 Cu(II) tyrosine complex

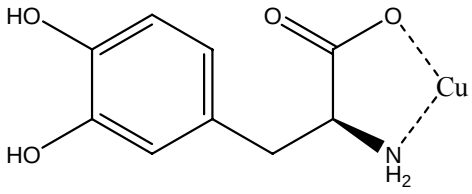

1:1 Cu(II) DOPA

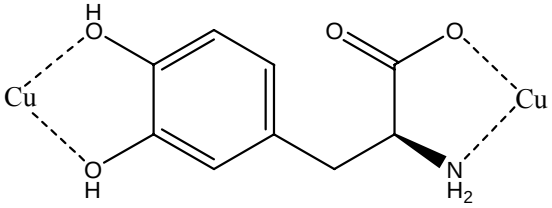

2:1 Cu(II) DOPA

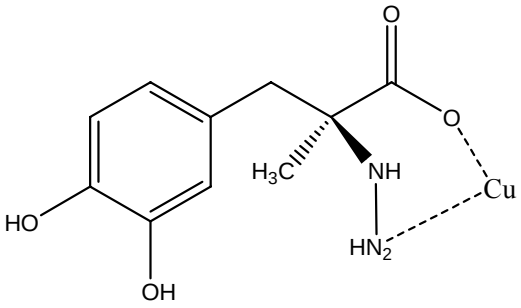

1:1 Cu(II) carbidopa

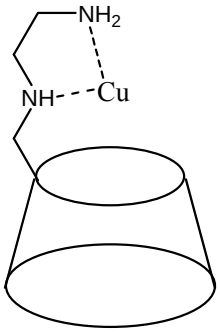

1:1 Cu(II) CDEn

Figure 4.10 Proposed structures of the Cu(II) complexes of tyrosine, DOPA , carbidopa and CDEn based on stoichiometry results (charges and water are omitted for clarity)

Support for these proposed structures can be obtained from the spectra presented earlier. On addition of $[Cu(H_2O)_6]^{2+}$ to solutions of CDEn, tyrosine, DOPA and carbidopa there is a hypsochromic shift in the d-d transition. This indicates coordination of the Cu(II) to a stronger ligand than water in each case. As nitrogen is present in all of the ligands studied and is a stronger donor than oxygen it is reasonable to assume that it is

involved in coordination to Cu(II) in each case. The results of the Job's plot for CuCDEn indicates a 1:1 complex of Cu:CDEn which compares favourably to work previously carried out by Bonomo *et al.*[12]

Table 4.2 summarises the results of the stoichiometric study for the ternary complexes and based on these results proposed structures for the diastereomeric complexes of tyrosine are given in Figure 4.11.

Table 4.2 Stoichiometry results for the ternary complexes of CuCDEn with tyrosine, DOPA and carbidopa at pH 6.8

Host	*Guest*	*Stoichiometry*
CuCDEn	D-tyrosine	1:1
CuCDEn	L-tyrosine	1:1
CuCDEn	D-DOPA	2:1
CuCDEn	L-DOPA	2:1
CuCDEn	L-carbidopa	1:1 and 2:1

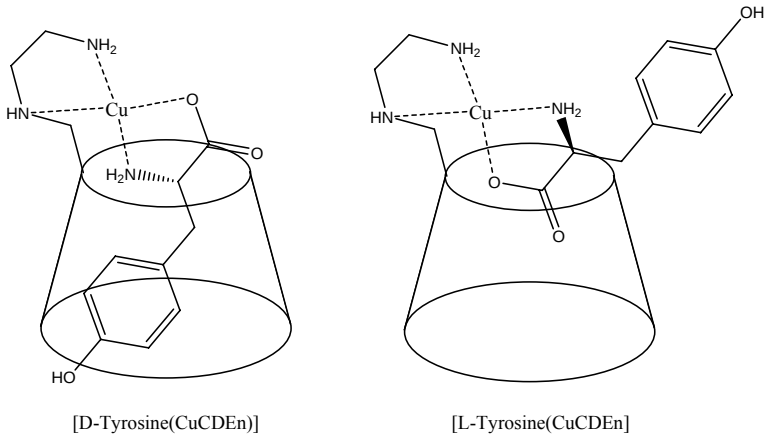

[D-Tyrosine(CuCDEn)] [L-Tyrosine(CuCDEn]

Figure 4.11 Proposed structures of the diastereoisomers of 1) [D-tyrosine(CuCDEn)] and 2) [L-tyrosine$(CuCDEn)_2$] (charges and water omitted for clarity)

Support for these structures can be obtained from electronic spectroscopy which indicated coordination to the metal centre via the nitrogen of the amine group and

oxygen of the carboxyl group of tyrosine. Circular dichroism also indicated a difference in inclusion between the two enantiomers, with D-tyrosine showing deeper inclusion into the CD cavity. Further support for this proposal can be obtained from Maccarrone *et al.* who proposed similar structures for the diastereoisomeric ternary complexes of tryptophan and CuCDEn.[19]

The results of the stoichiometric study carried out here suggests the formation of a 2:1 CuCDEn:DOPA ternary complex and therefore the structures shown in Figure 4.12 are proposed.

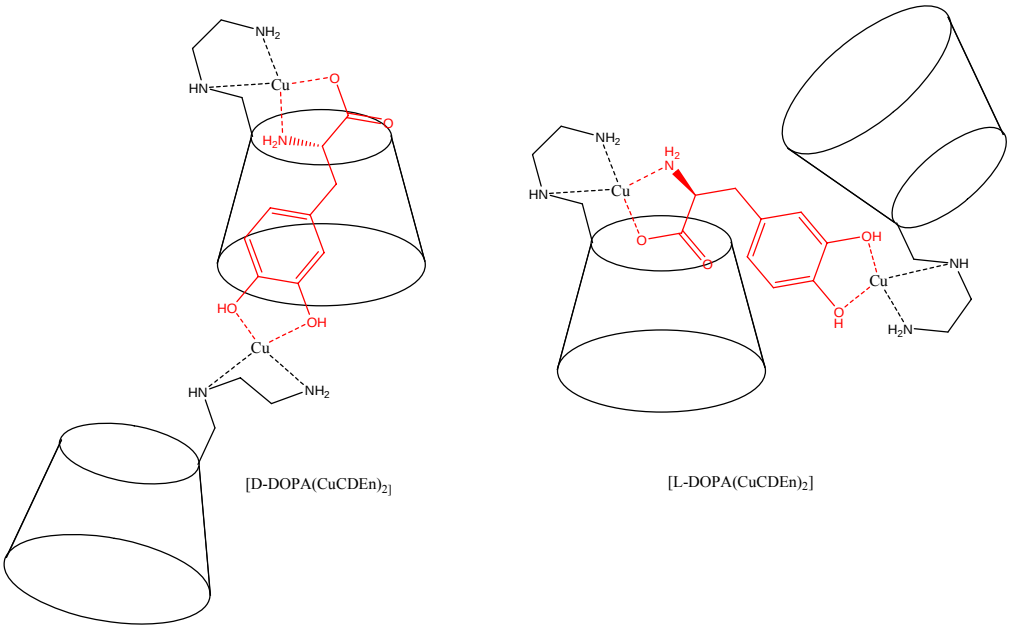

Figure 4.12 Proposed structures of the diastereoisomers of 1) [D-DOPA(CuCDEn)] and 2) [L-DOPA(CuCDEn)$_2$] (charges and water are omitted for clarity)

As before these proposals are supported by the results presented earlier. For DOPA a hypsochromic shift in the absorption spectrum for the ternary complex with CuCDEn *versus* the binary complex indicated further coordination of DOPA to the metal centre. Again c.d. spectroscopy shows differential inclusion between the two enantiomers with results indicating D-DOPA is included more fully than L-DOPA.

Electronic spectroscopy also suggested coordination of L-carbidopa to CuCDEn *via* the carboxyl and amino groups. The stoichiometric study suggested the existence of both 1:1 and 2:1 CuCDEn:L-carbidopa ternary complexes in solution. Due to the lack of a commercially available sample of D-carbidopa a circular dichroic experiment could not be carried out and therefore it is not possible to compare inclusion of the enantiomers in the CD cavity. However since the structures of DOPA and carbidopa are similar it is possible that the ternary complexes also have similar structures and therefore proposed structures for the carbidopa complexes are shown in Figure 4.13.

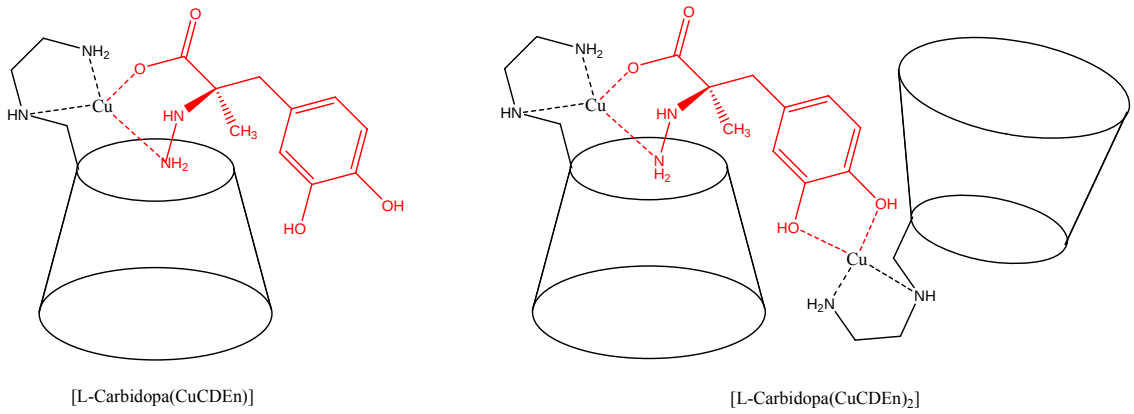

Figure 4.13 Proposed structures of the diastereoisomers of 1) [L-carbidopa(CuCDEn)] and 2) [L-carbidopa(CuCDEn)$_2$] (charges and water are omitted for clarity)

In conclusion it should be noted that the results above using the Job's method assumes that there is only one reaction at equilibrium. This may not always be the case. There may be many competing metal-ligand reactions taking place. A more rigours study therefore needs to be carried out using speciation and potentiometric studies.

4.6 References

[1] G. Castronuovo, V. Elia, D. Fessas, A. Giodano, F. Velleca: *Carbohydr. Res*. **272**, (1995) 31

[2] S.E Brown, J.H. Coates, S.F. Lincoln, D.R. coghlan, C.J. Eaton: *J. Chem. Faraday Trans*. **87**, (1991) 2699

[3] R. Lu, J. Hao, H. Wang, L. Tong: *J. Colloid Interface Sci*. **192**, (1997) 37

[4] W. Wiczk, J. Mrozek, N. Szabelski, J. Karolczak, K. Guzow, J. Malicka: *Chem. Phys. Lett.* **341**, (2001) 161

[5] H.A. Benesi, J.H. Hilderbrand: *J. Am. Chem. Soc*. **71**, (1949) 2703

[6] P. Job: *Annali di Chimica Applicata*. **9**, (1928) 113

[7] G. Pistolis, A. Malliaris: *Chem. Phys. Lett*, **303**, (1999) 334

[8] O. Exner, *Chemometr Intell Lab.* **39**, (1997) 85

[9] Y. Matsui, T. Yokoi, K. Mochida: *Chem Lett*, (1976) 1037

[10] K.L. Park, K.H. Kim, S.H. Jung, H.M. Lim, C.H. Hong, J.S. Kang: *J. Pharmaceut. Biomed. Anal.* **27**, (2002) 569

[11] K. Hirose: *J. Incl. Phenom Macro.*, **39**, (2001) 193

[12] R.P. Bonomo, V Cucinotta, F. D'Allessandro, G. Impellizzeri, G. Maccarrone, E. Rizzarelli: *J. Inc. Phenom. and Mol. Recog.* **15**, (1993) 167

[13] A. Giuffrida, C. León, V. Garcia-Canas, V. Cucinotta and A. Cifuentes: *Electrophoresis,* **30**, (2009) 1734

[14] I.I. Karuzina, G.I. Bachmanova, M.V. Izotov, A.n. Osipov and A.I. Varenitsa: *Biokihimiia,* **46**, (1981) 1754

[15] C. Richter, A. Azzi, U. Wesser and A. Weidel: *J. Biol. Chem.,.* **252**(14), (1977) 5061

[16] C.K. Siu, Y. Ke, Y. Guo, A.C. Hopkinson and K.W.M. Siu: *Phys. Chem. Chem. Phys.*, **10**, (2008) 5908

[17] H. Sigel: *Metal Ions in Biological Systems: Volume 9: Amino Acids and Derivatives as Ambivalent Ligands.* Marcell Dekker Inc. 1979

[18] J.E. Gorton, R.F. Jameson: *J. Chem. Soc. A. Inorg. Phys. Theor.* (1968) 2615

[19] G. Maccarone, E. Rizzarelli and G. Vecchio: Chiral Recognition by Functionalised Cyclodextrin Metal

Complexes. In L. Fabbrizzi and A. Poggi (eds.), *Transition Metals in Supramolecular Chemistry,* Kluwer Academic Publishers, (1994), p. 351-367

5. Separation of Enantiomers by Capillary Electrophoresis

5.1 Introduction

Electrophoresis is the movement of electrically charged particles or molecules in a conductive medium (usually aqueous) under the influence of an electric field.[1] Capillary electrophoresis (CE) describes a family of electrophoretic techniques that employ the use of a narrow tube or capillary. The system is a very simple concept but an extremely powerful technique that facilitates the separation of a wide variety of compounds. Initially CE as a technique was not very popular due to limitations with detection systems. However modern day CE instruments have overcome these initial problems and CE is now a versatile technique that offers high speed, high sensitivity and low limit of detection. Analytical chemistry has seen a major increase in the study of the separation of enantiomers and the number of papers published in this area, using CE has exponentially increased in recent years.[2]

Just as HPLC has different modes, such as reversed phase and ion exchange, CE also has distinct modes of operation. The most common CE modes used are:

- Capillary zone electrophoresis

Capillary zone electrophoresis (CZE) is the simplest form of CE and separates analytes based on their mass to charge ratio. The separation relies mostly on pH-controlled dissociation of acids or protonation of basic groups on the analyte.

- Electrokinetic chromatography

Electrokinetic chromatography (EKC) is a family of electrophoresis techniques named after electrokinetic processes including, electroosmosis, electrophoresis and chromatography. An example of EKC is cyclodextrin mediated-EKC (CD-EKC).

Separation occurs due to the differential interaction of enantiomers with CDs present in the background electrolyte (BGE) or buffer allowing for enantiomeric separation.

- Micellar electrokinetic chromatography

Micellar electrokinetic chromatography (MEKC) is another mode of EKC in which surfactants are added to the BGE to form micelles. Separation is based on the differential partition of analytes between the micelle and solvent. MEKC is very useful for separating mixtures containing both ionic and neutral species.

- Capillary gel electrophoresis

Capillary gel electrophoresis (CGE) is an evolution of traditional gel electrophoresis. It incorporates a polymer into the capillary to create a molecular sieve. This allows analytes with similar mass to charge ratios to be separated by size. The technique has been employed for the analysis of proteins and DNA sequencing and genotyping.

- Capillary isoelectric focusing

Capillary isoelectric focusing (CIEF) allows the separation of amphoteric molecules such as proteins by electrophoresis in a pH gradient generated between the anode and cathode. The analyte will migrate to a point in the capillary where its net charge is zero. Once the sample has been focused into a band it is pushed past the detector using pressure.

- Capillary isotachophoresis

Like isoelectric focusing, capillary isotachophoresis (CITP) relies on zero electroosmotic flow. The capillary is filled with a leading electrolyte that has a higher mobility than any of the sample components to be determined. Then the sample is

injected. A terminating electrolyte occupies the opposite reservoir, and the ionic mobility of that electrolyte is lower than any of the sample components. Separation will occur in the gap between the leading and terminating electrolytes based on the individual mobilities of the analytes. Both anions and cations can be determined, though not in the same run.

- Non-aqueous capillary electrophoresis

Non-aqueous capillary electrophoresis (NACE) separates analytes in a medium composed of organic solvents. The viscosity and dielectric constants of organic solvents affect the analyte mobility and also the electroosmotic flow allowing separation.

As with HPLC there are two methods in CE for the separation of enantiomers, indirect and direct separation. Indirect separation in CE closely mirrors that of HPLC, with the use of chiral derivatisation agents before separation to form diastereomeric derivatives that differ in their physical and chemical behaviour. Thorsen, Engstrom and Josefsson reported the use of (+) and (-)-1-(9-anthryl)-2-propyl chloroformate as a chiral derivatising agent for the separation of amino acids and small peptides in 1997.[3] Kleidernigg and Lindner reported the use of (1R,2R)-N-((2-isothiocyanato)cyclohexyl)-6-methoxy-4-quinolinylamide) as a fluorescence tag for the separation of amino acids and chiral amines.[4]

Cyclodextrins are the most frequently used chiral selectors in CE and they allow for the direct separation of enantiomers. Snopek *et al.* reported the first application of CDs for the separation of enantiomers using capillary isotachophoresis (CITP) in 1988.[5] Guttman *et al.*[6] used *β*-CD incorporated in capillary gel electrophoresis (CGE) and Fanali[7] published the first paper dealing with the use of CDs in capillary zone

electrophoresis (CZE). However it is CD-EKC and a related mode Chiral Ligand Exchange CE (CLECE) in particular that applies to this work and will be discussed in greater detail later. Before this it is important to understand the mechanism of separation in CE.

5.1.1 Separation Mechanism

The separation mechanism in capillary electrophoresis is based on electrophoretic mobility and electroosmotic flow. Electrophoretic mobility (μ) is the movement of charged species in a fluid due to an applied electric field and is defined according to the equation,

$$\mu = \frac{q}{6\pi r\eta}$$

Equation 5.1

where μ is the ion velocity, q is the charge, r is Stokes Radius of the ion and η is the viscosity of the solution. Therefore charged solute molecules are separated due to differences in their charge or electrophoretic mobilities and will migrate towards the electrode of opposing charge. Without the presence of a background electrolyte (BGE), negatively charged anions would migrate to the anode and into the source vial. However the BGE, because of its electroosmotic flow (EOF) carries them along to the detector.

The EOF of the BGE is the motion of BGE through the capillary caused by the application of an electric field. Generally the direction of the EOF is towards the cathode so that the BGE will flow from the source to the destination vial. Electroosmotic flow has a relatively flat profile when compared to a laminar flow in HPLC. This is due to the frictional forces solutes experience in both techniques. In CE, frictional drag causes the EOF at the wall of the capillary to flow at a slightly lower rate

than through the rest of the capillary. This reduction in flow is quite small as the area near the wall of the capillary is very small. This flat or electrodynamic flow profile offers many advantages such as all solute molecules experience the same velocity regardless of position in the capillary cross-section and samples elute as narrow bands giving narrow peaks. This is in contrast to solutes in HPLC moving through columns under the influence of a pumping system. Solutes at the centre of the column move at a faster rate than those nearer the column wall. This uneven flow profile, shown below in Figure 5.1, leads to a higher degree of band broadening and relatively broad peaks in HPLC.[1]

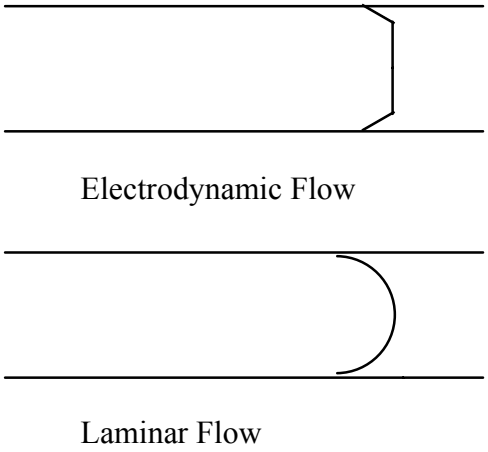

Figure 5.1 Electrodynamic and laminar flow profiles

Most surfaces possess a negative charge which results from the ionisation of the surface or the adsorption of ionic species. In fused silica capillaries both processes occur and this results in the inside wall being extremely negatively charged. As the walls of the capillary are negatively charged, a layer of cations builds up near the surface to maintain the charge balance. This creates a double layer of ions near the surface and a potential difference known as the zeta potential.

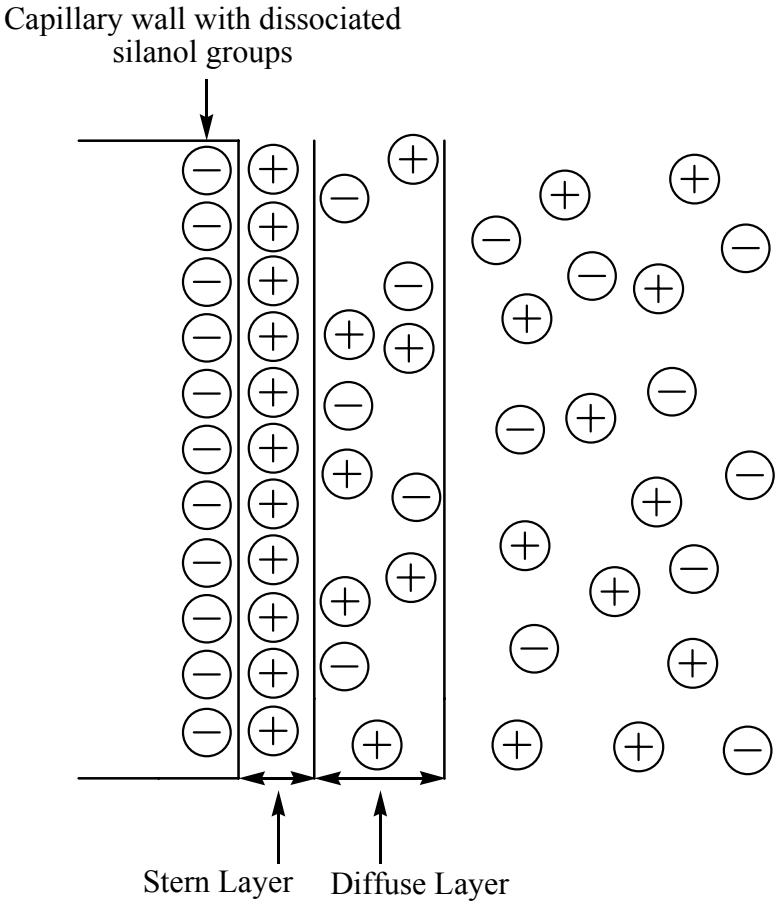

Figure 5.2 Schematic representation of the electric double layer

Figure 5.2 gives a representation known as the Stern model of the electric double layer, showing that the double layer is made up of two sections. The first part has the approximate width of one ion, which is almost fixed to the surface of the capillary. The second part as the name suggests is diffuse and extends into the liquid. When an electric field is applied, the cations in the mobile diffuse layer are pulled towards the negatively charged cathode. As these cations are solvated they "drag" the bulk BGE solution with them, causing electroosmotic flow towards the cathode. Therefore positively charged analytes will also migrate towards the cathode. Negatively charged analytes will migrate towards the cathode, despite being attracted towards the anode because the EOF of the BGE is greater than the electrophoretic mobility of the anions. Neutral molecules are not influenced by electrophoretic mobilities as they carry no charge and therefore they

move through the capillary at the same rate as the EOF. Figure 5.3 shows the order of migration in CE and Figure 5.4 shows an idealised electropherogram.

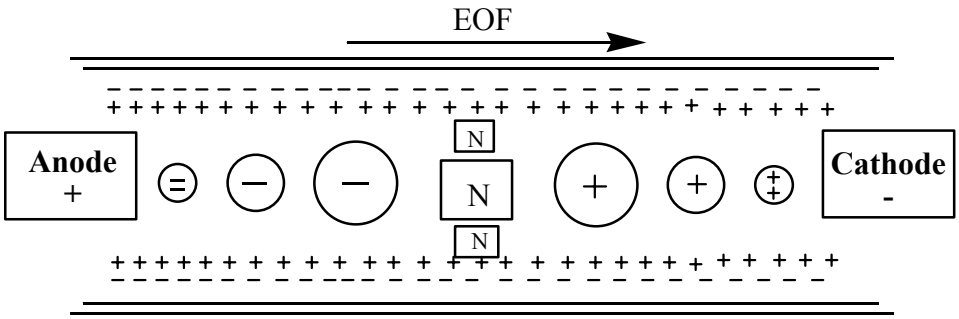

Figure 5.3 Order of migration in CE

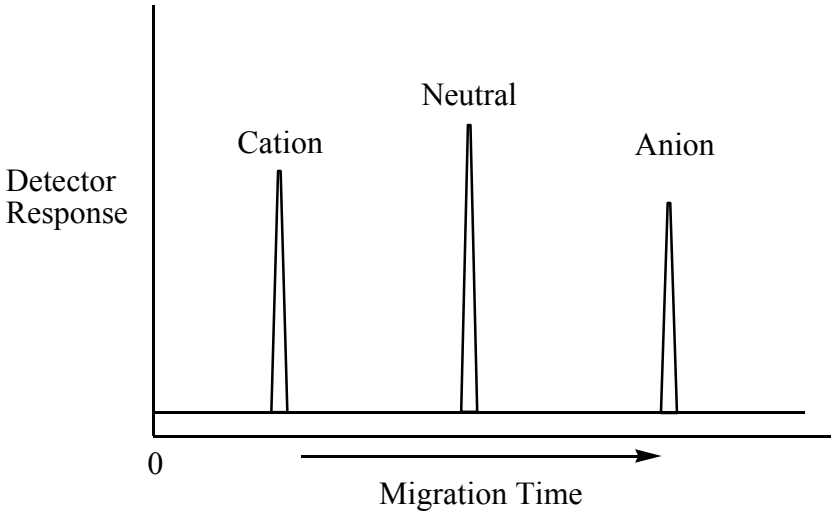

Figure 5.4 Idealised electropherogram in normal polarity mode

5.1.2 Capillary Electrophoresis Instrumentation

The main components of a CE system are:

- Sample vial
- Capillary (typically fused silica externally coated with a polyimide layer)
- High-voltage power supply (0 to +/-30kV)

- Detector
- Source and destination vials
- Data handling system

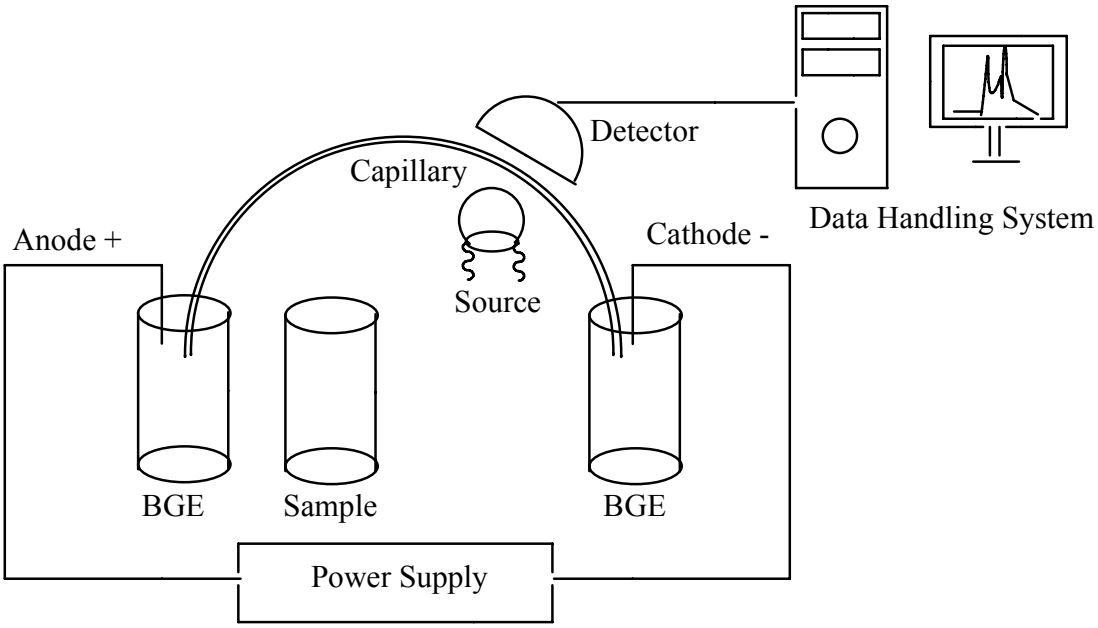

Figure 5.5 Capillary electrophoresis system schematic

5.1.3 Sample Introduction

Capillary electrophoresis is a microchemical method, as the capillaries used typically have a total volume of nanolitres to microlitres, which therefore requires a very precise and accurate sample introduction method.

Various sample introduction methods exist for capillary electrophoresis including, hydrostatic, electrokinetic and hydrodynamic. A hydrostatic injection relies on a pressure difference induced by raising the sample end reservoir above the detection end reservoir. This difference in pressure forces the analyte into the capillary. To end the injection process the capillary is removed from the sample vial and placed in a BGE

reservoir. To calculate the volume of analyte introduced into a capillary (V_{inject}) using this injection method, the following equation is employed.[8]

$$V_{inject} = \frac{\rho g r^4 \Delta h t_{inject}}{8 \eta L}$$ **Equation 5.2**

where ρ is the BGE density, g the gravitational force constant, Δh the difference in height between the two reservoirs, η is the BGE viscosity, t_{inject} the injection time, r the radius of the capillary and L the length of the capillary.[9]

Electrokinetic injections are generally simpler to perform than either the hydrostatic or hydrodynamic methods and they rely on the principles of electrophoretic and electroosmotic movement. The capillary tip is dipped into the sample vial, a potential is applied for a few seconds and the capillary is then placed in a BGE vial. As this technique is driven by the electroosmotic flow (EOF) and electrophoretic mobility of the analyte, analytes with the highest electrophoretic mobility will be preferentially introduced over those with lower mobilities.[10] The following equation is used to estimate the electrokinetic injection volume, V_{inject}[8]

$$V_{inject} = \frac{E_{inject}}{E_{seperate}} \times \frac{t_{inject}}{t_{retention}} \times V_{capillary}$$ **Equation 5.3**

where E_{inject} is the injection potential, $E_{separate}$ the separation potential, t_{inject} the time of injection, $t_{retention}$ is the retention time of the analyte and $V_{capillary}$ is the volume of the capillary.

There are several techniques that may be employed in hydrodynamic injection, such as pressure injection. Pressure injections can be achieved by placing the inlet of the capillary into a sample vial and applying a pressure to the vial. The volume of sample injected (V_{inject}) can be calculated using the Poiseuille equation,

$$V_{inject} = \frac{\Delta P r^4 \pi t}{8 \eta L}$$ **Equation 5.4**

where ΔP is the pressure across the capillary, r is the radius of the capillary, t is the time the pressure is applied, η is the viscosity of the sample and L is the total capillary length.

5.1.4 Detection

Detection in CE is very similar to that of HPLC, in that separated samples elute from the capillary in solution and the most widely used detection systems are UV-Vis absorption, fluorescence, laser-induced fluorescence and mass spectrometry. UV-Vis absorption detection was used in this work and a schematic representation of the diode array system is given in Figure 5.6.

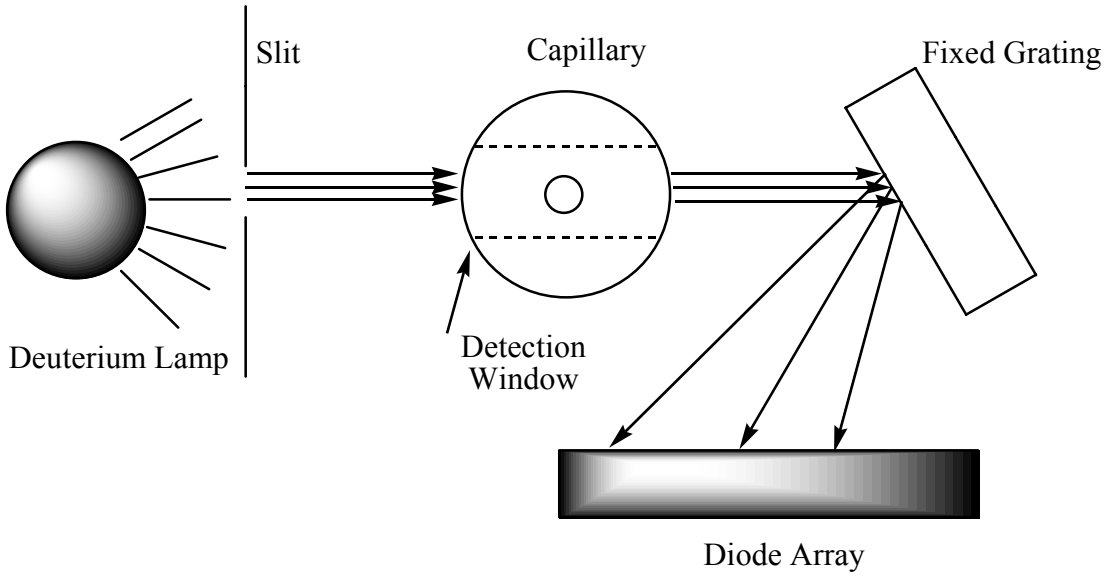

Figure 5.6 UV-Vis absorption with a diode array detector in CE

White light of all UV-Vis wavelengths is generated by a deuterium lamp and passes through a window in the protective covering of the capillary and onto a grating that

diffracts the light into different wavelengths. The light then falls onto an array typically containing 200-500 diodes. Like a HPLC diode array detector wavelengths are selected by electronically sampling signals from the appropriate diodes. This allows for quantitative (electropherograms) and qualitive data, as well as peak purity and peak identification through stored libraries to be obtained. One attractive feature of UV-Vis absorption detection is that it is a non-destructive method, allowing for further analysis of the sample solution by other detectors placed downstream on the capillary.

5.1.5 Chiral Ligand Exchange Capillary electrophoresis

Chiral Ligand Exchange CE (CLECE) is related to Electrokinetic Chromatography (EKC). EKC separation is based on both electrophoretic migration and chromatographic separation and results from the partitioning of the analyte within *pseudo* phases with different effective mobilities. Many types of molecules can be used as *pseudo* phases or phase additives with micelles, crown ethers and cyclodextrins being the most popular. The ability to include guest molecules and their inherent chirality make cyclodextrins an excellent choice as chiral mobile phase additives (CMP). Anionic sulfated cyclodextrins are useful as CMP additives due to interactions with cationic analytes. With metallo-cyclodextrins adding the coordination properties of a metal centre to the inclusion ability of the cavity gives a multi-modal chiral selector enhancing the enantioselective properties. This is analogous to enzyme systems which often contain metal centres.

The exploitation of ligand exchange in liquid chromatography dates back to the early 1960s, when Helfferich achieved separation by binding a metal ion to a cationic exchanger, resulting in the first ion exchange columns.[11] However it was not until 1985 when a ligand exchange process was first used in capillary electrophoresis. Grassman *et al.* used a BGE containing a copper(II) ion bound to two histidine molecules to separate the racemates of some α-amino acids.[12] It took 18 more years for the first paper to be

published on the use of metallo-CDs and CE in a chiral ligand exchange separation. In 2003 Cucinotta *et al.* synthesised an imidazole-bound histamine CD derivative and used it to separate the enantiomers of tryptophan in the presence of copper(II) ions.[13]

Cucinotta *et al.* detail the following criteria which must be fulfilled for a CLECE separation to be successful: [14]

- The analyte and metallo-CD must form a ternary complex in solution.
- The rate of ternary complex formation must be fast.
- There must be a structural difference in the ternary complexes of the two enantiomeric analytes.
- The ternary complex and free analyte must have different electrophoretic mobilities.

The results of the electronic spectroscopy and circular dichroism studies presented earlier have suggested that the first three of these criteria have been met by the metallo-CDs in this work. UV-Vis spectroscopy showed coordination of copper(II) to CDEn by a hypsochromic shift in the d-d transition band. A further shift in λ_{max} indicates subsequent coordination of tyrosine, DOPA and carbidopa to this binary system, creating ternary complexes. The rate of ternary complex formation is high as the colour change occurred immediately on mixing the solutions. Differences in the depth of inclusion of each enantiomeric pair of analytes was seen using circular dichroism spectroscopy.

For the ternary complexes and free analytes to have different electrophoretic mobility, they must carry different charges. It is possible to predict the average net charge of the analytes under investigation at a particular pH using the dissociation constants of the various functional groups (pKa values). As an amino acid tyrosine contains both an amino and a carboxyl group, making it both an acid and a base. Usually the structure

shows both the acidic and basic groups within the same molecule but these groups react with each other to form a dipolar ion known as a zwitterion which has no net charge. This is shown for the simplest amino acid, alanine in Figure 5.7.

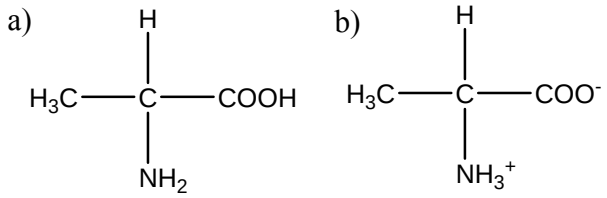

Figure 5.7 Structure of alanine in the a) unionised form and b) zwitterionic form

Therefore in aqueous solution amino acids can act as proton donors or proton acceptors. All amino acids are weak polyprotic acids due to the –COOH and $-NH_3^+$ groups and DOPA and carbidopa behave in a similar manner. The Henderson-Hasselbalch equation (Equation 5.5) can be used to determine the ratio of the concentrations of an undissociated acid (RCOOH) and its conjugate base ($RCOO^-$) at a particular pH.

If the dissociation equilibrium is written as;

$$RCOOH + H_2O \rightleftharpoons RCOO^- + H_3O^+$$

then the Henderson-Hasselbalch equation is;

$$pH = pKa + log\left(\frac{[RCOO^-]}{[RCOOH]}\right)$$ **Equation 5.5**

Rearranging gives;

$$pH - pKa = log\left(\frac{[RCOO^-]}{[RCOOH]}\right)$$ **Equation 5.6**

Taking tyrosine as an example and using the pKa of the carboxyl group (2.20), substitution into equation 5.6 at the pH of the experiments (6.8) gives;

$$6.8 - 2.2 = log\left(\frac{[RCOO^-]}{[RCOOH]}\right) = 4.6$$

$$\frac{[RCOO^-]}{[RCOOH]} = 39{,}811$$

Therefore at pH 6.8, the carboxylic acid group of tyrosine is effectively ionised and in the form of $RCOO^-$.

Using the pKa of the RNH_3^+ group (9.11) and given the equilibrium;

$$RNH_3^+ + H_2O \rightleftharpoons RNH_2 + H_3O^+$$

then

$$\frac{\log[RNH_2]}{[RNH_3^+]} = -2.31$$

$$\frac{[RNH_2]}{[RNH_3^+]} = 0.0049 \quad \frac{\sim 0}{1} \sim 0$$

Therefore at pH 6.8 the amino group of tyrosine is present as RNH_3^+. Similarly the side chain of tyrosine at pH 6.8 is present as ROH. Combining these calculations shows that at pH 6.8, tyrosine is present in the zwitterionic form.

The net charge on an amino acid can also be estimated from the isoelectric point (pI) which is the pH at which most of the molecules in solution have a net charge of zero. pI can be found from the titration curve of the amino acid. The acid dissociation equilibria of tyrosine and a theoretical titration curve are given in Figures 5.8 and 5.9 respectively.

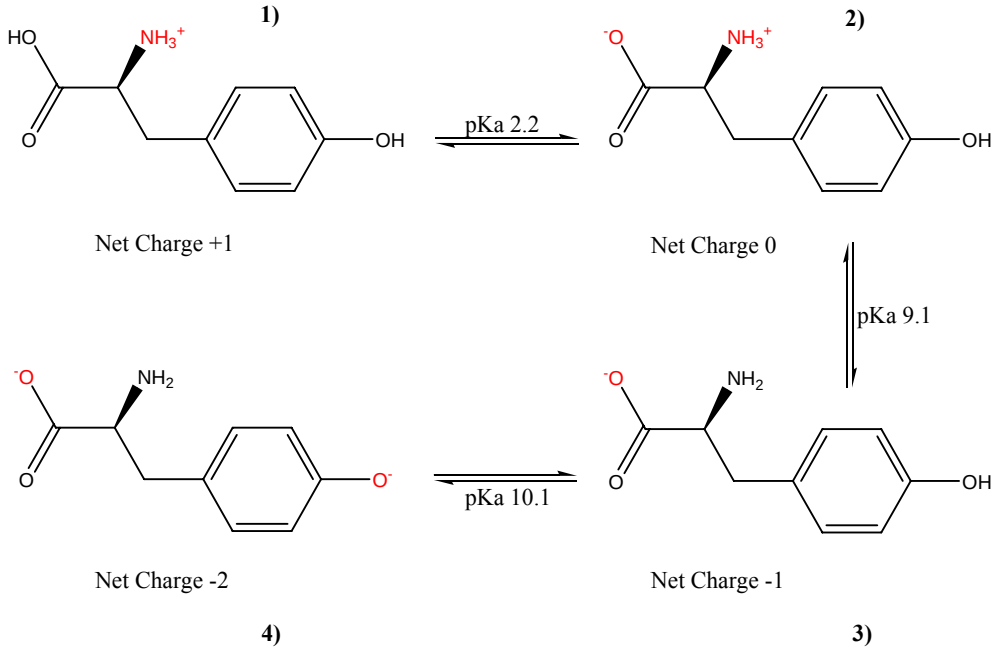

Figure 5.8 Acid dissociation equilibria for tyrosine

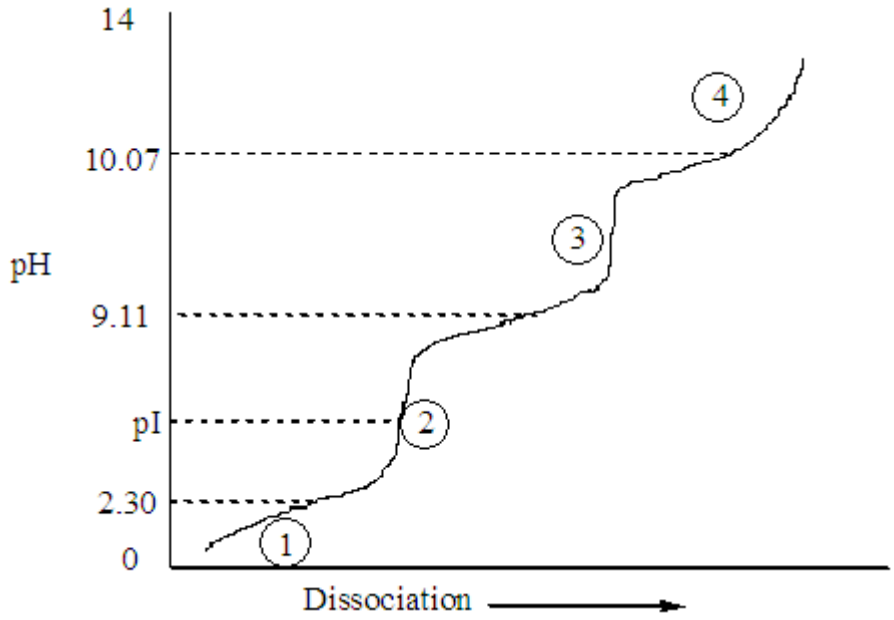

Figure 5.9 Theoretical titration curve for tyrosine

Structure two above shows tyrosine with a net zero charge and therefore from the titration curve the isoelectric point (pI) is halfway between the pKa values for the carboxyl and amino group.

$$pI = \frac{1}{2}(2.2 + 9.11) = 5.65$$

Since the pH of the experiments in this work (6.8) is ~ 1 log unit above the pI, only a very small amount of the $-NH_3^+$ group has dissociated and the majority of the molecules are present as the zwitterion.

The acid dissociation equilibria for DOPA and carbidopa are given in Figures 5.10 and 5.11.

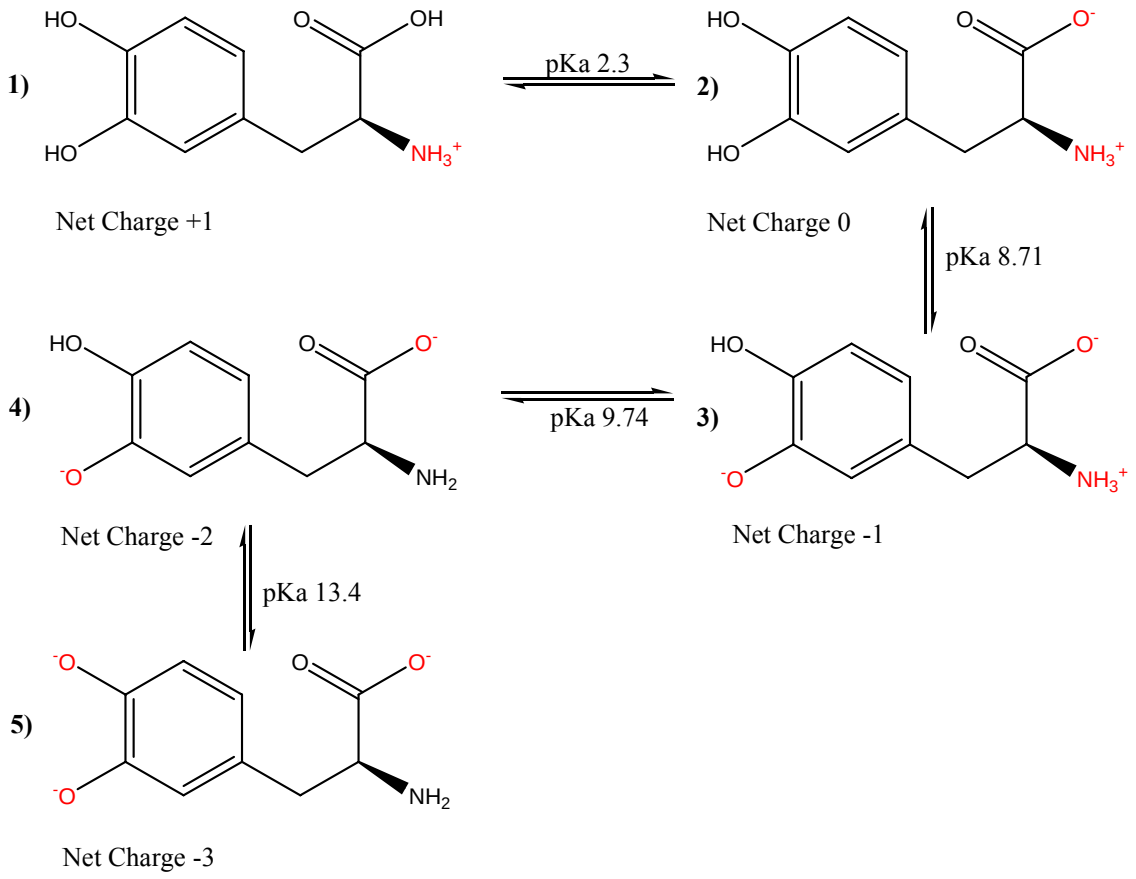

Figure 5.10 Acid dissociation equlibria for DOPA

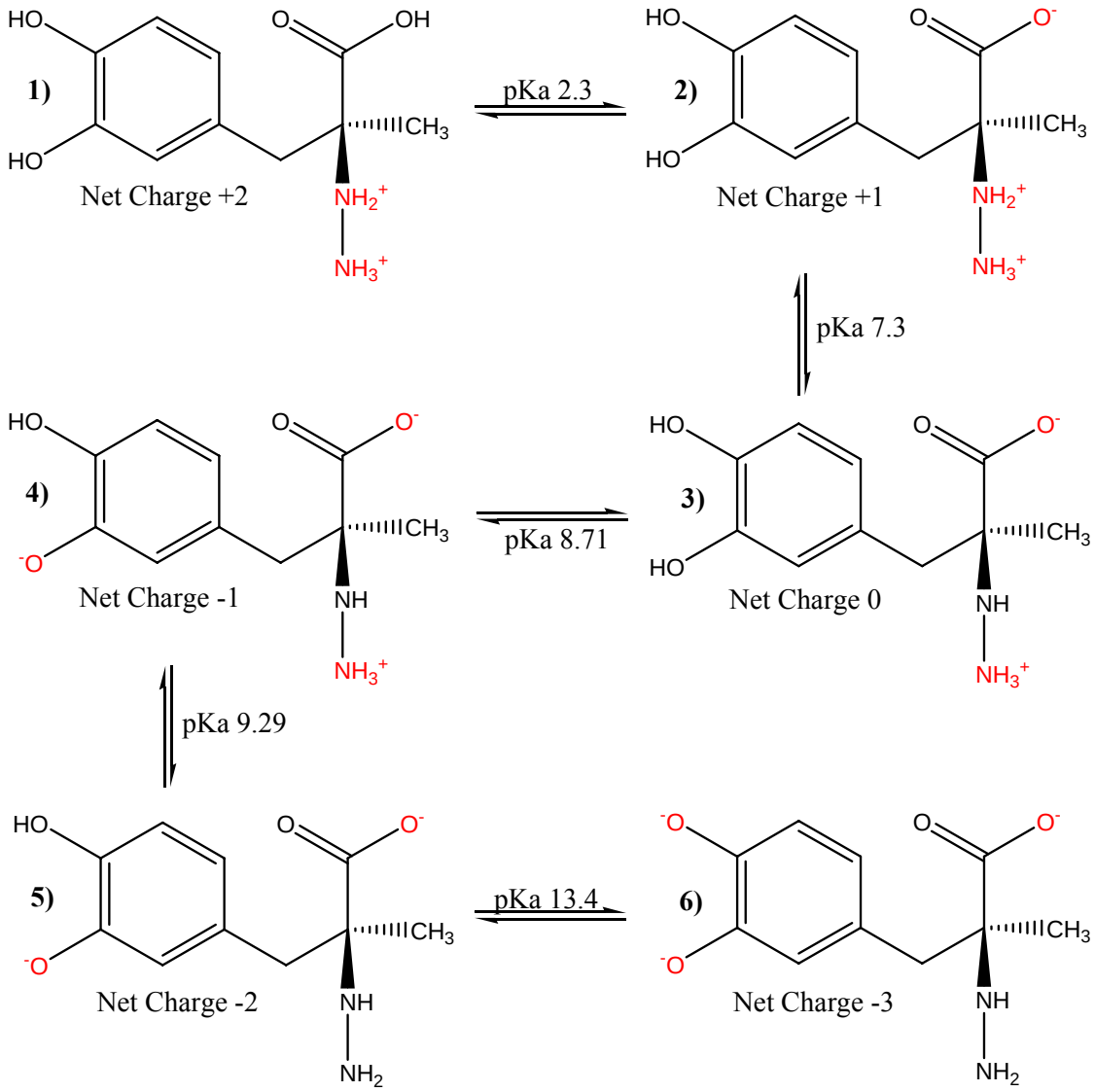

Figure 5.11 Acid dissociation equilibria for carbidopa

From the above equilibria, the pI of DOPA can be calculated as 5.50 (1/2(2.3+8.71)) and the pI of carbidopa as 8.01 (1/2(7.3+8.71)). The pH of 6.8 in this work is only ~ 1 log unit above the pI of DOPA. Therefore only a small fraction of the –OH groups has dissociated and most of the DOPA molecules are zwitterionic. For carbidopa the pH is ~ 1 log unit below the pI and therefore only a small fraction of the –NH group is protonated. Again most of the carbidopa molecules are zwitterionic. Bonomo *et al.* have studied the coordination properties of CDEn towards Cu^{2+} and have shown that at the pH used in this work the most stable species is $[Cu(CDEn)]^{2+}$.[15]

Combining the results of these calculations with the results obtained in the electronic spectroscopy, c.d. spectroscopy and stoichiometry studies leads to the structures of the ternary complexes shown in Figure 5.12.

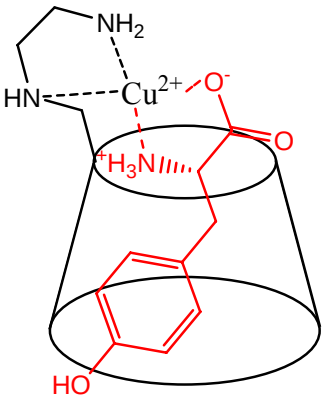

[D-tyrosine(CuCDEn)]$^{2+}$

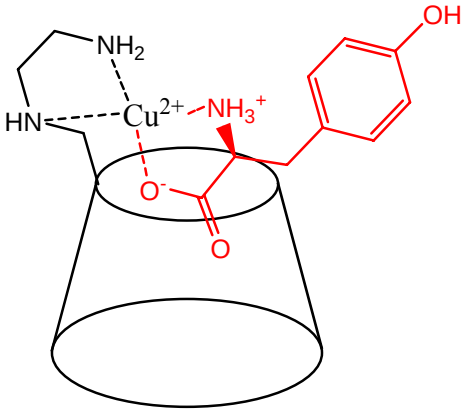

[L-tyrosine(CuCDEn]$^{2+}$

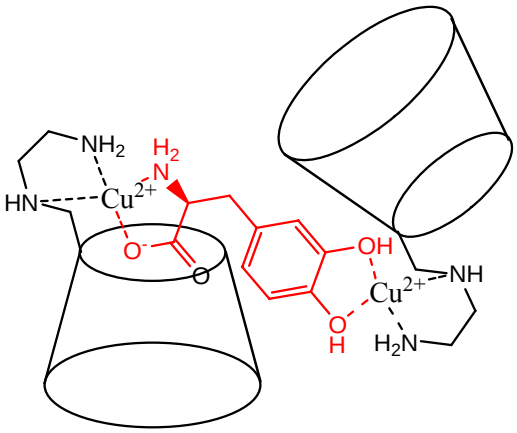

[L-DOPA(CuCDEn)$_2$]$^{4+}$

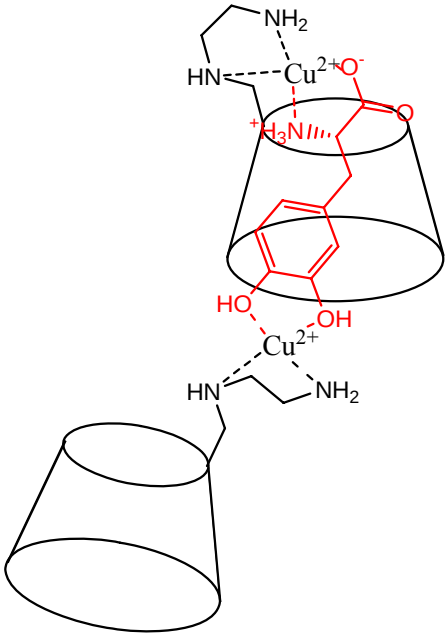

[D-DOPA(CuCDEn)$_2$]$^{4+}$

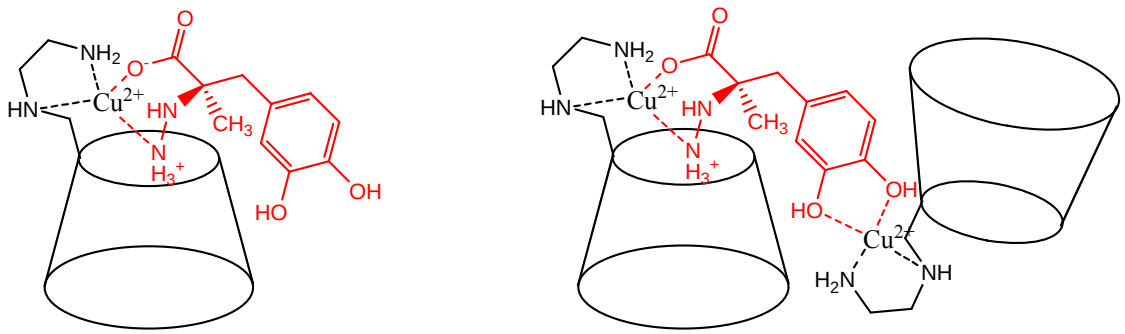

Figure 5.12 Structures at pH 6.8 of the proposed ternary complexes

Comparing the structures of the analytes and their ternary complexes shows that they have different charges which should result in different electrophoretic mobilities. Therefore all the criteria for separation by CLECE to be theoretically possible have been met for CuCDEn and all three guest analytes.

5.1.6 Separation of DOPA and Carbidopa

There are few CE based methods available in the literature for the separation of the components of anti-Parkinson's medications. Fanali *et al*. described the use of CZE for the separation of L-DOPA, carbidopa and benserazide.[16] Using various BGE it was discovered that L-DOPA and benserazide could be separated between pH 2.5-7.0. L-DOPA and carbidopa could only be separated at pH 8.5. However a mixture of the three analytes was not resolved even when BGE additives such as CDs, sodium dodecyl sulphate, organic modifiers and polyvinyl propylene were utilised. As anti-Parkinson's medicines only contain L-DOPA and either carbidopa or benserazide, a scenario whereby all three analytes would need to be separated is unlikely to arise. However it is important to note that this is another example of how one universal method for separating chiral or structurally similar analytes does not exist. Saraç *et al.* screened various cyclodextrin derivatives for the separation of D,L-DOPA and D,L-carbidopa.[17]

Baseline separation of the enantiomers of DOPA was achieved using the single isomer heptakis(2,3-diacetyl-6-sulfato)-*β*-cyclodextrin (HDAS-*β*-CD) and sulfobutyl ether-β-cyclodextrin (SBE-β-CD) at a pH of 2.5. The resolution and peak widths using SBE-*β*-CD were found to be poor and resulted in poor sensitivity. D,L-Carbidopa was baseline separated using the anionic CD derivatives sulfobutyl ether-*β*-cyclodextrin (SBE-*β*-CD) and carboxymethyl-*β*-cyclodextrin (CM-*β*-CD) at pH 2.5. CM-*β*-CD resolved both analytes with good peak shape with resolution values of 7.88. However SBE-*β*-CD was discounted for this separation due to low enantioselectivity. The sensitivity of the methods was shown to be sufficient to meet current guidelines by being able to detect 0.2% unwanted D-enantiomer in L-enantiomer samples. The simultaneous separation of all four analytes by CE using one chiral selector was not carried out. Instead two different selectors were favoured for each separation. This is another example of how there is no universal selector currently available for regulatory compliance testing. The choice of a suitable selector is entirely sample specific.

Ha *et al.* also investigated the separation of L-DOPA and L-carbidopa by CZE using various neutral and charged cyclodextrins.[18] It was discovered that neutral cyclodextrins (namely *α*-CD, *β*-CD, *γ*-CD, methyl-*β*-CD and hydroxypropyl-*β*-CD) had no effect on the chiral separation. Chiral resolution was successfully achieved using charged highly sulfated *β*-cyclodextrin and sulfated *β*-cyclodextrin as chiral selectors, in normal and reversed polarity mode. Ha *et al.* found that using normal polarity mode in this study led to excessive run times of over 50 mins and poor sensitivity. For this reason a reversed polarity method was developed and the run times were reduced to ~ 10 mins. It was possible to detect 0.1% of the D impurities in L-carbidopa and L-DOPA. The International Conference on Harmonization of Technical Requirements for Registration

of Pharmaceuticals for Human Use recommends an impurity level of 0.2 %, twice the level detectable in the method described above.[18]

5.1.7 Experimental

Analysis was performed on a Beckman P/ACE MDQ Method Development System (Fullerton, CA, USA) equipped with diode array detector (DAD) and controlled by 32 Karat Software. The system performance was evaluated regularly using Beckman's own performance test mix P/ACE MDQ Test Mix B with Run Buffer A. Separation was performed on an uncoated fused-silica capillary (50 cm total length, 37.5 cm effective length) at 12-25 kV. Capillary temperature was 20 ^{o}C and sample tray temperature 15 ^{o}C. All solutions were prepared in HPLC grade water. A BGE at pH 6.8 was prepared by dissolving ammonium acetate in water to give a 0.002 M solution. Although ammonium acetate is not a true buffer, it has been shown to be useful as the BGE for CE experiments involving metallo-cyclodextrins as chiral selectors.[19] Problems have been encountered when using true buffer solutions (such as NH_3/NH_4^+) and metallo-cyclodextrins due to competing coordination of the metal ion to components of the buffer system. A BGE at pH 2.5 was prepared by mixing 0.55 cm^3 of 1 M sodium dihydrogen phosphate with 1.454 cm^3 of 1 M *ortho*-phosphoric acid in water to give a 0.02 M solution. Stock solutions of CDEn and $CuSO_4.5H_2O$ of 0.1 M and DOPA and carbidopa of 0.001 M were prepared in HPLC grade water.

The capillary was conditioned using the following parameters;

Daily Rinse:

- 0.1 mol dm^{-3} HCl (10 mins)
- HPLC Grade H_2O (5 mins)
- 0.1 mol dm^{-3} NaOH (15 mins)
- 0.02 mol dm^{-3}BGE (15 mins)

Pre-run:

- 0.1 mol dm^{-3} NaOH (3 mins)
- BGE (5 mins)

Values for the effective mobility μ (corrected for EOF) and resolution (R_s) were calculated using the following formulae,

$$\mu_{(Analyte)} = \frac{L * l}{\Delta V * t * 60}$$

Equation 5.7

$$\mu_{(EOF)} = \frac{L * l}{\Delta V * t_{EOF} * 60}$$

Equation 5.8

$$\mu_{(Effective)} = \mu_{(Analyte)} - \mu_{(EOF)}$$

Equation 5.9

where L = total capillary length (cm) and l = effective capillary length (cm) as determined by the manufacturer. ΔV = applied voltage (kV), t = migration time of analyte (mins.) and t_{EOF} = migration time of neutral marker (mins.).

$$R_s = 2\frac{t2 - t1}{w1 + w2}$$

Equation 5.10

where t1 and t2 refer to the migration time of the first analyte to elute and second analyte to elute respectively and w1 and w2 are the peak widths of these analytes (mins.)

5.2 Results and Discussion

5.2.1 Instrument Test

A test mix separation was performed on each new capillary to verify the instrument was operating correctly. This was carried out using Beckman Test Mix B and Run Buffer A as sample and BGE respectively. The electropherogram was then compared to the example separation given in the CE user guide (Figure 5.13).

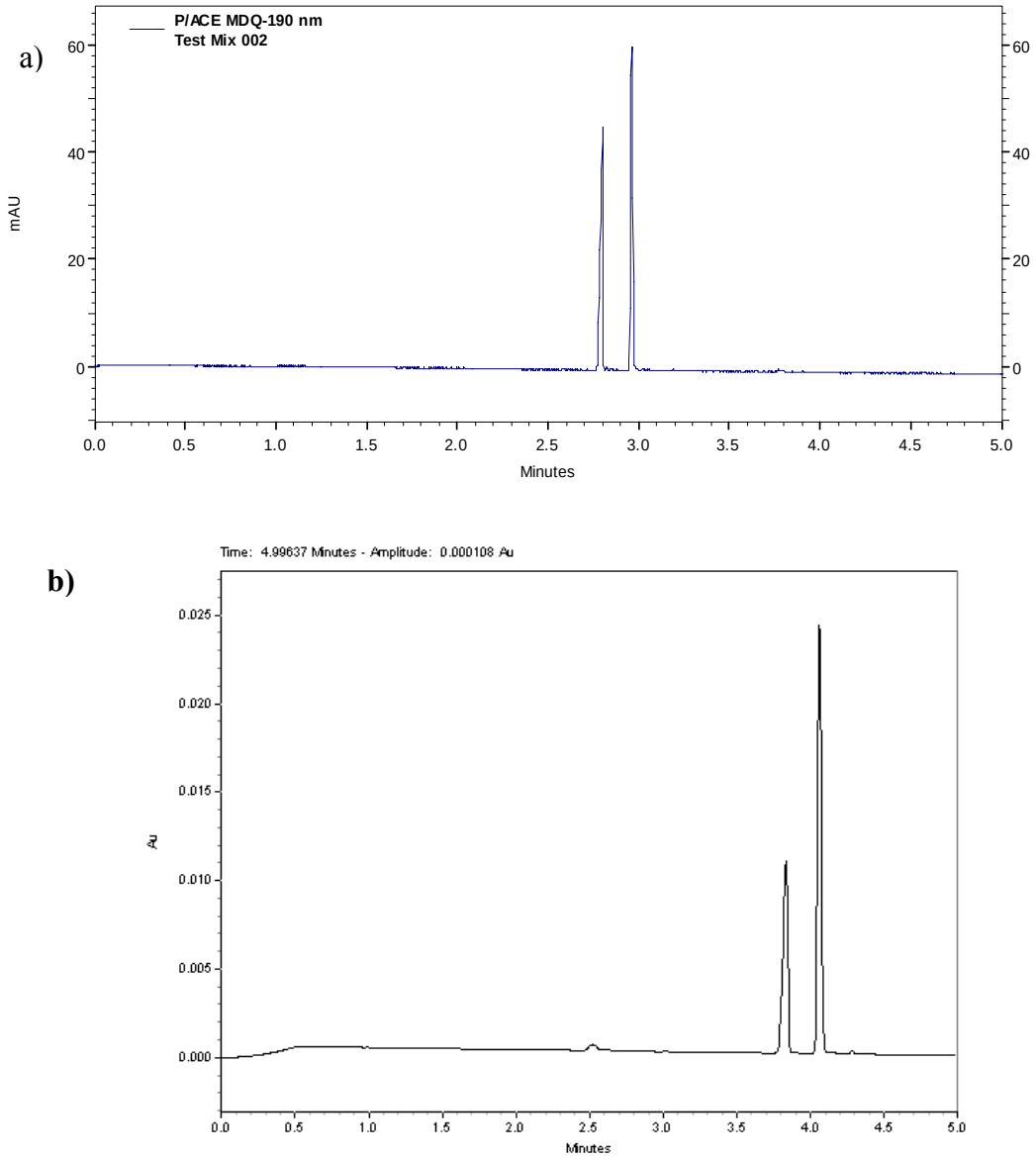

Figure 5.13 a) Electropherogram of Test Mix B. BGE was Run Buffer A and b) Electropherogram of Test Mix B supplied by Beckman P/ACE MDQ user guide

The electropherograms compare very favourably and differ only in the migration times of the two peaks, due to the use of a shorter capillary in the system employed in this work (50 cm used by Beckman *versus* 37.5 cm effective length in this study).

5.2.2 Separation of L-DOPA and L-Carbidopa

To ensure there are no unwanted signals arising from the BGE an electropherogram of the BGE at pH 6.8 was recorded and is presented in Figure 5.14. From this it can be seen that injecting ammonium acetate as a sample results in a stable baseline with a stable current.

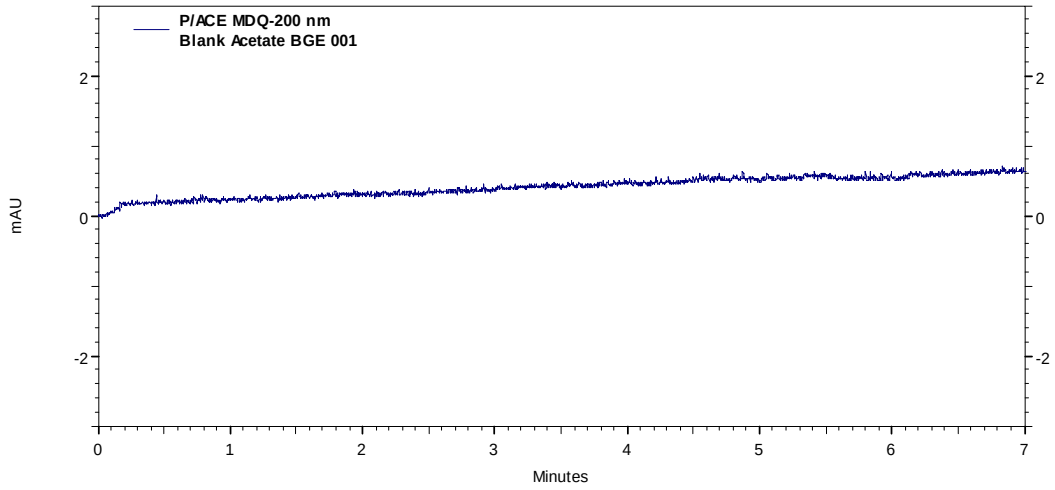

Figure 5.14 Electropherogram of system baseline using BGE at pH 6.8 0.02 M ammonium acetate as sample

The velocity of migration of an analyte in capillary electrophoresis will depend upon the electroosmotic flow (EOF) which is measured using a neutral marker, in this case acetone. Normally 6-8 µL of acetone is added to each sample solution and its migration time compared to the migration times of the analyte peaks. It should be noted however, that when performing a separation using CuCD derivatives the EOF must be measured in a separate experiment, to avoid precipitates of non-soluble copper salts blocking the capillary. The electropherogram of acetone in BGE at pH 6.8 is given in Figure 5.15 and shows a negative peak for acetone at 5.4 min.

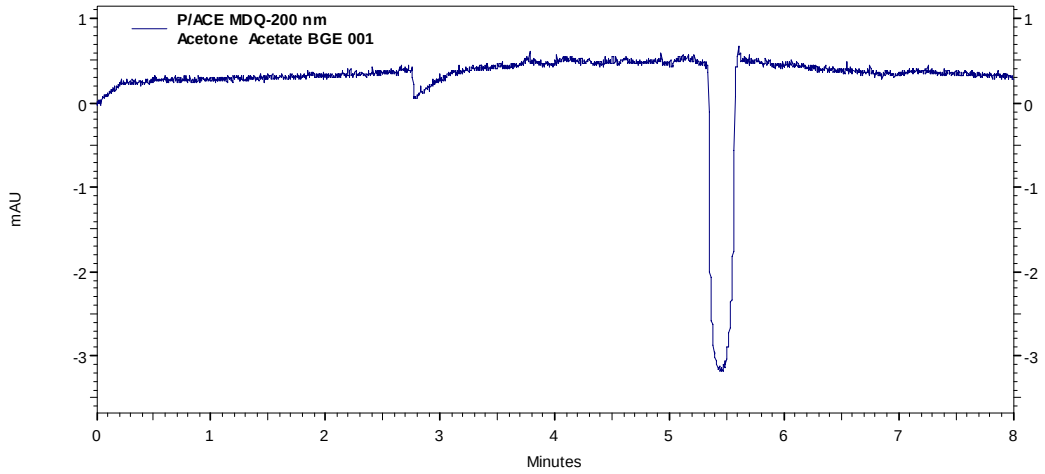

Figure 5.15 Electropherogram of acetone (EOF Marker) in BGE at pH 6.8

Any analyte with a net positive charge will migrate before acetone and an analyte with a net negative charge will migrate after acetone. The electropherograms of L-DOPA, L-carbidopa and a mixture of the two in the presence of the neutral marker acetone were therefore recorded and are presented in Figure 5.16 a, b and c respectively.

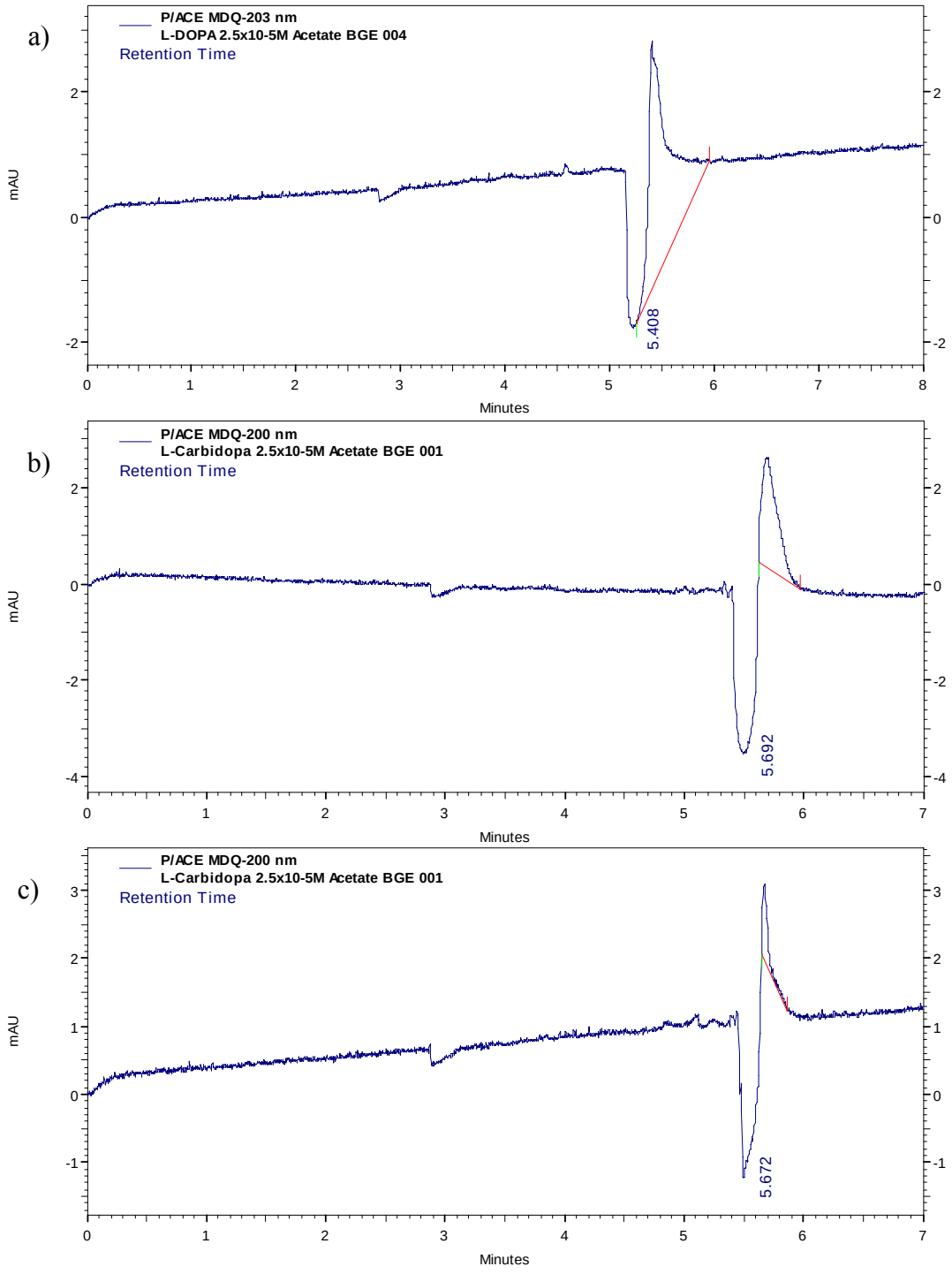

Figure 5.16 Electropherograms of acetone and a) L-DOPA b) L-carbidopa and c) L-DOPA + L-carbidopa all at $2.5x10^{-5}$ M with BGE at pH 6.8

In the electropherogram shown in Figure 5.16a a signal can be seen co-migrating with the negative signal for acetone which is assigned to L-DOPA. Co-migration occurs at pH 6.8 as L-DOPA is in the zwitterionic form with a net charge of zero and therefore it

co-migrates with the neutral marker. L-Carbidopa shows a similar response (Figure 5.16b). For the mixture of L-DOPA and L-carbidopa a signal can again be seen co-migrating with the neutral marker indicating a neutral charge on the analytes but more importantly there is no evidence of separation (Figure 5.16c).

The mobilities of both analytes were corrected by subtracting the mobility of the EOF (μ_{EOF}) from the analyte mobilities ($\mu_{analyte}$) to give their effective mobilities ($\mu_{effective}$) as described in the experimental section. Table 5.1 details the effective mobilities of L-DOPA and L-carbidopa.

Table 5.1 Calculated mobilities corrected for EOF

Analyte	*Analyte Mobility* ($\mu_{analyte}$)	*Mobility of EOF* (μ_{EOF})	*Effective Mobility* ($\mu_{effective}$)
L-DOPA	0.482	0.501	-0.019
L-Carbidopa	0.474	0.458	-0.016

This result indicates that CE separation of the two analytes at this pH did not occur due to their similar effective mobilities and so a chiral selector is required. CuCDEn was therefore added to the same BGE to enhance the separation of the analytes. Work previously carried out by our group on chiral separations of tyrosine used concentration values of CDEn in the range of 1.2-48 mM.[20] The concentration ratio of copper to CDEn was kept constant at 1.2:1 CDEn:Cu in order to limit the amount of free copper in the system and to ensure the formation of the binary CuCDEn complex.[13,19,21,22]

Figure 5.17 below shows an electropherogram obtained using these conditions and a mixture of L-DOPA and L-carbidopa as analyte.

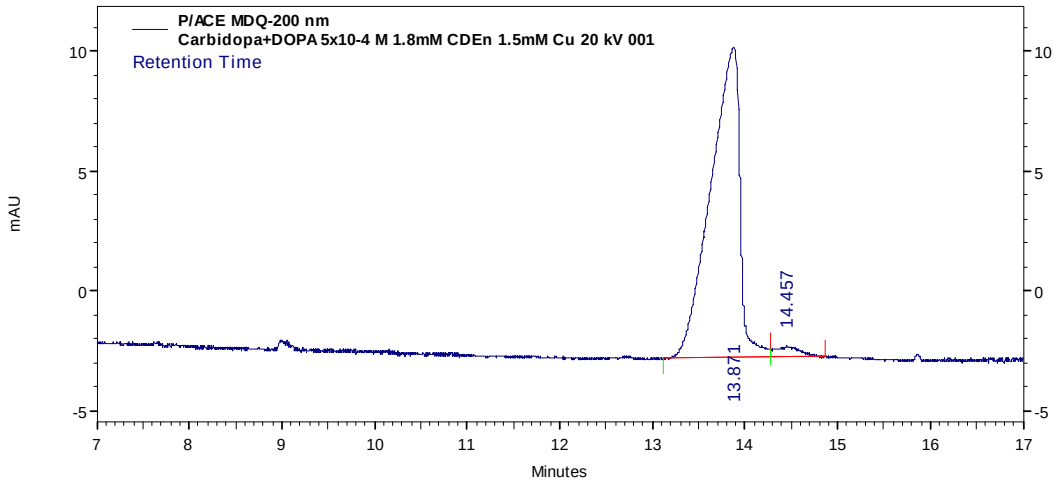

Figure 5.17 Electropherogram of L-DOPA + L-carbidopa both at $2.5x10^{-4}$ M with 1.8 mM CDEn 1.5 mM Cu added to BGE (pH 6.8, +20 kV)

As can be seen from the above electropherogram no separation of the isomers has occurred. Various experimental conditions were changed such as CuCDEn concentration, ammonium acetate concentration and voltage. However successful separation of L-DOPA and L-carbidopa was not achieved using CuCDEn as a selector. pH can also influence separation. Ha *et al.* achieved successful separation of these analytes using various cyclodextrin derivatives at a pH of 2.5.[18] Saraç *et al.* also used pH 2.5.[17] However when using CuCDEn the pH range is limited to 6-8. Above this pH range insoluble copper hydroxides can form and below this range copper does not coordinate to CDEn. Therefore CuCDEn may be a poor choice of chiral selector due to the limited pH range. It was therefore decided to use CDEn alone as a chiral selector at pH 2.5. Figure 5.18 (a + b) shows the electropherograms obtained using CDEn at concentrations of 1 and 2 mM respectively.

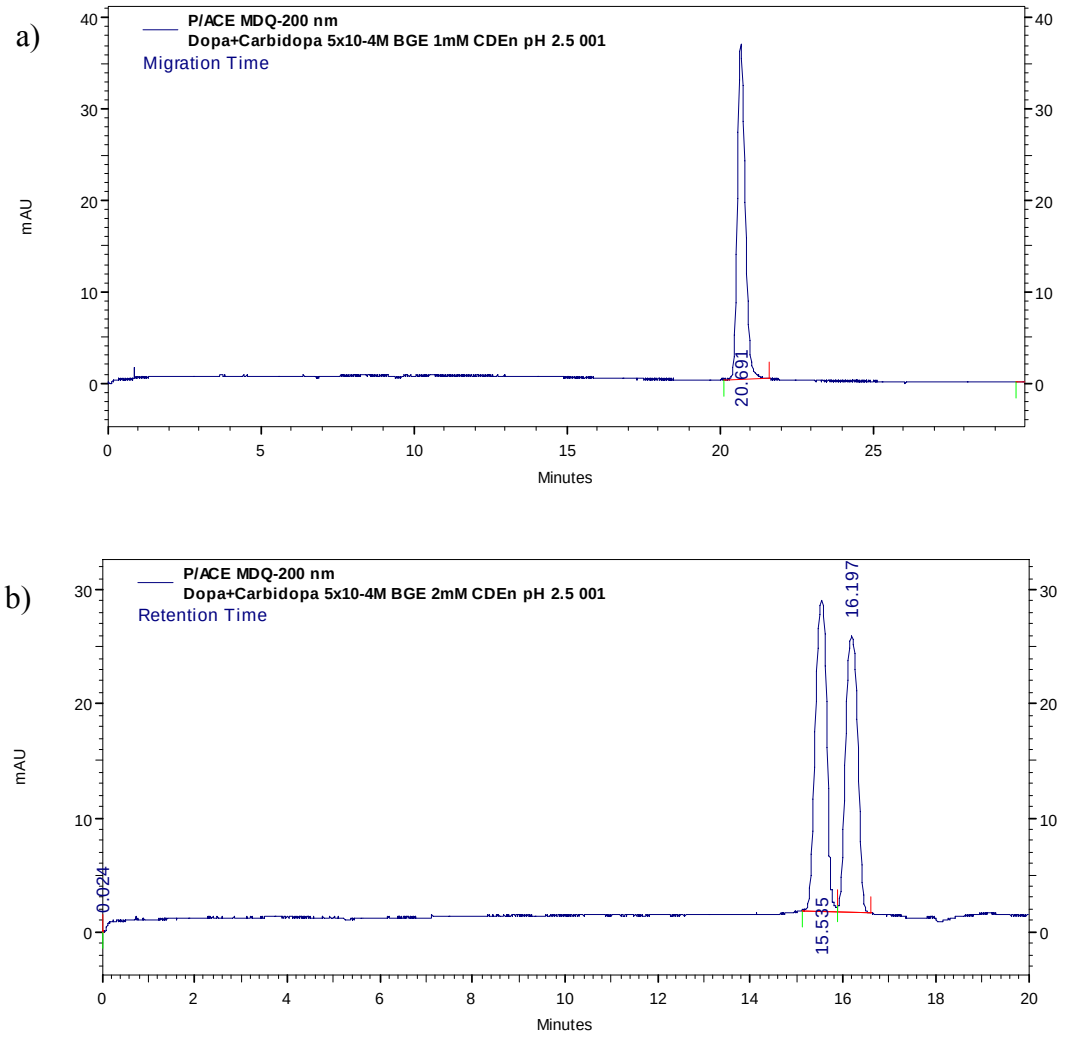

Figure 5.18 Electropherogram of a) L-carbidopa + L-DOPA (both $5x10^{-4}$ M) with 1mM CDEn in BGE and b) L-carbidopa + L-DOPA (both $5x10^{-4}$ M) with 2mM CDEn in BGE (pH 2.5, +20kV)

No separation of DOPA and carbidopa was achieved at the lower concentration. However baseline separation was achieved within ~ 16 mins. on increasing the CDEn concentration to 2 mM. Using Equation 5.11 the resolution was found to be $R_s = 2.36$. Ha *et al.* did not report R_s values for the separation of the isomers and Saraç *et al.* performed the separation of D,L-DOPA and D,L-carbidopa in separate experiments. Therefore direct comparison of resolution values is not possible and the only data that can be compared is the difference in migration time of the two analytes. In our work Δt is 0.66 mins. which compared well with Fanali *et al.* who show a value of 0.50 mins.

To determine the order of migration of the analytes the sample was spiked with excess L-DOPA and the electropherogram is presented in Figure 7.19.

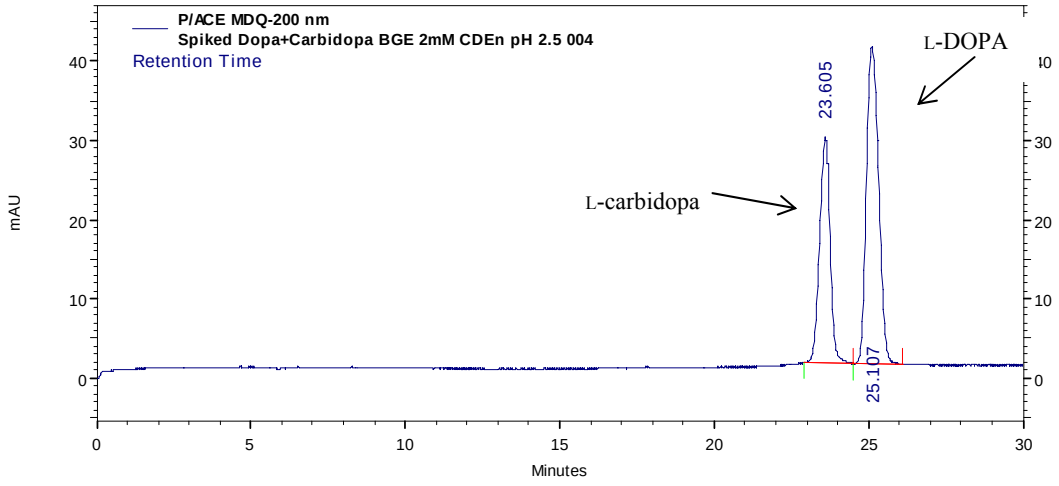

Figure 5.19 Electropherogram of L-carbidopa ($5x10^{-4}$ M) + L-DOPA ($8.3x10^{-4}$ M) with 1mM CDEn (pH 2.5 +25 kV)

From the above electropherogram the order of migration was found with L-carbidopa migrating before L-DOPA.

The same experiment was carried out using CE in reverse polarity mode. In this mode the positions of the anode and cathode are reversed with the anode placed at the detector end of the capillary. The capillary length between injection and detection is now shorter which can lead to reduced analysis time. Figure 5.20 compares the effect of normal and reversed polarity mode on effective capillary length. It should be noted that in reversed polarity mode the voltage used in order to decrease migration times must be decreased due to the shorter capillary length.

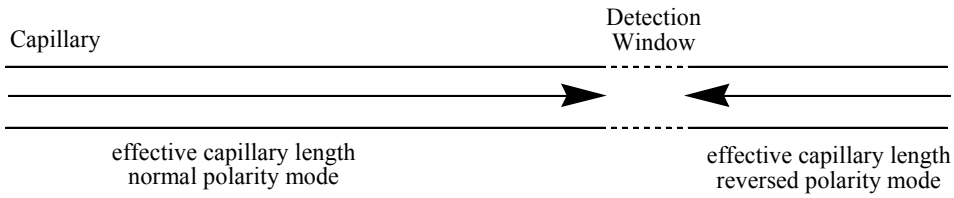

Figure 5.20 Difference in effective capillary length in normal and reversed polarity modes

Figure 5.21 shows the electropherograms DOPA and carbidopa in reversed polarity mode.

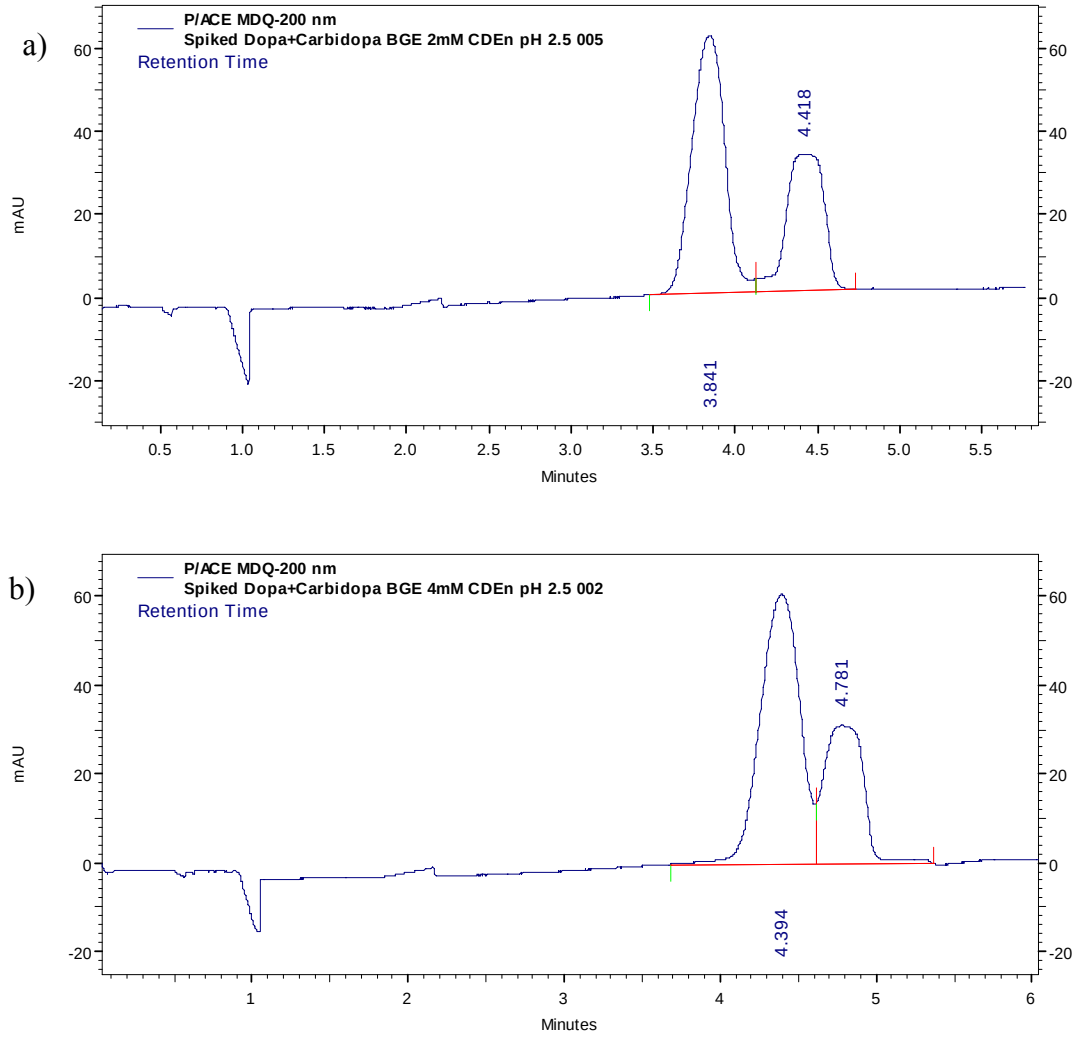

Figure 5.21 Electropherogram of L-carbidopa ($5x10^{-4}$ M) + L-DOPA ($8.3x10^{-4}$ M) with a) 2mM CDEn in BGE and b) 4 mM CDEn in BGE (pH 2.5, -12kV)

Comparing the electropherograms in Figure 5.21 shows that changing to reversed polarity mode reduced the migration times from ~ 16 minutes to 5 minutes. However the peak shape broadened but baseline separation still occurred (Figure 5.21a). It can also be seen that the order of migration changed so that DOPA migrated faster than carbidopa. Baseline separation was not achieved using 4 mM CDEn. Therefore the

optimum conditions were determined to be 2 mM CDEn in BGE at pH 2.5 in normal polarity mode and under these conditions the resolution was found to be 2.36.

5.2.3 Separation of D- and L-DOPA

In an attempt to separate the enantiomers of DOPA, the optimum parameters found for the successful separation of L-DOPA and L-carbidopa were applied. Figure 5.22 shows the electropherograms obtained when using CDEn as the chiral selector in the BGE at pH 2.5 and normal polarity mode.

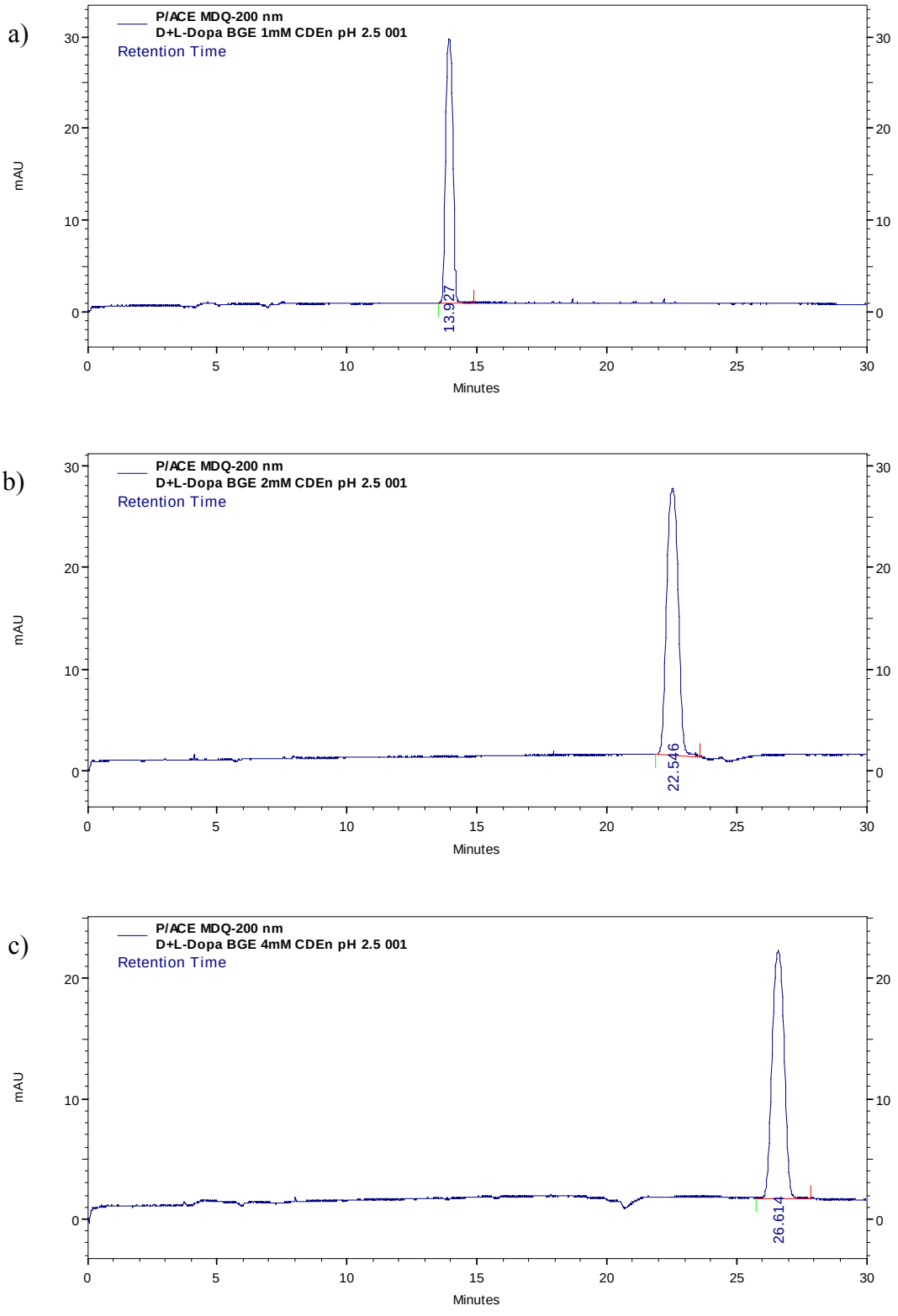

Figure 5.22 Electropherogram of D,L-DOPA (both $5x10^{-5}$ M) with a) 1 mM b) 2 mM and c) 4 mM CDEn in BGE at pH 2.5 (+20 kV)

From the electropherograms above it can be seen that there was no separation of D,L-DOPA using CDEn in BGE at pH 2.5 and CE in forward polarity mode. Increasing the concentration of CDEn to facilitate the separation caused an increase in migration time (~ 25 minutes using 4 mM CDEn). Therefore electropherograms were recorded (Figure 5.23) at higher concentrations of CDEn in reversed polarity mode in an attempt to achieve separation.

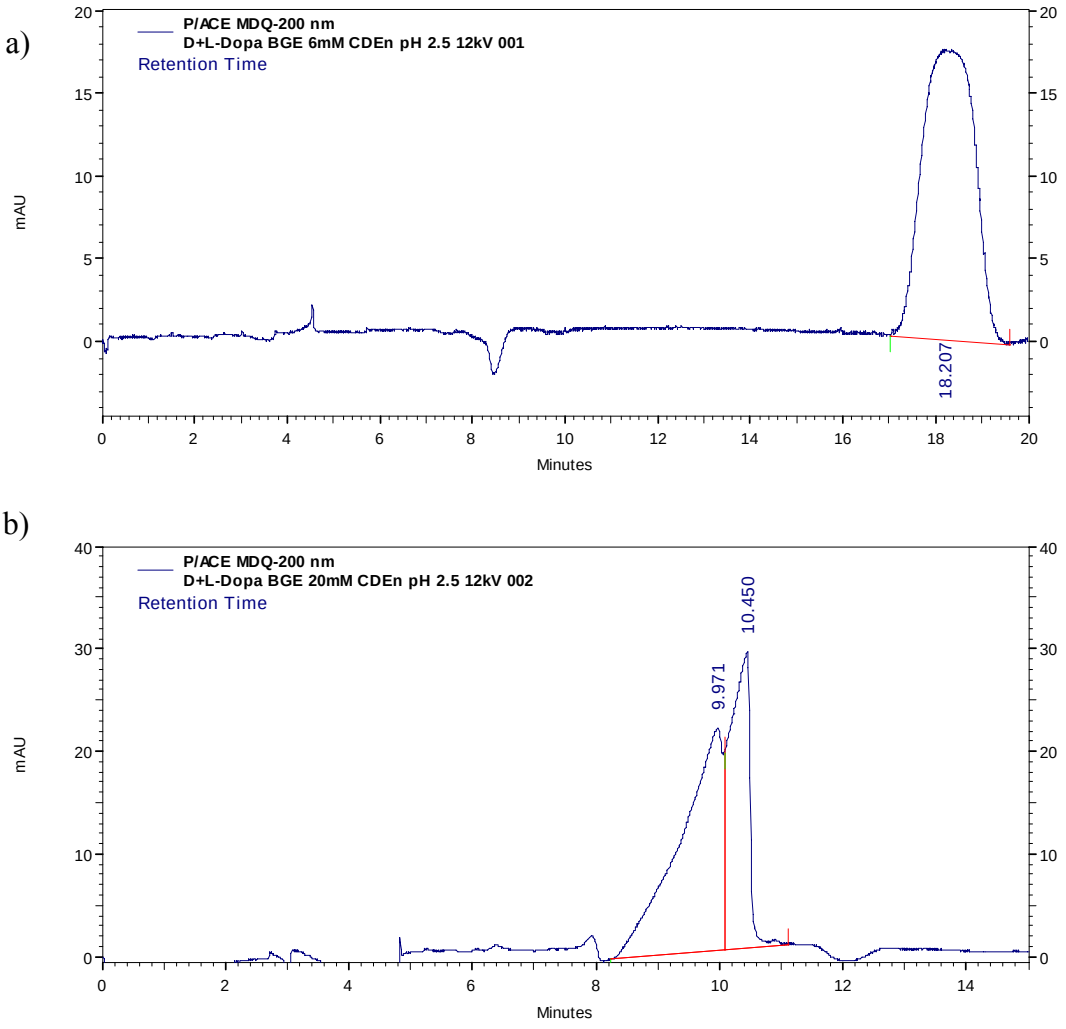

Figure 5.23 Electropherogram of D,L-DOPA (both $5x10^{-5}$ M) using a) 6 mM b) 20 mM CDEn in BGE at pH 2.5 (-12 kV)

Figure 5.23a gives an electropherogram showing the reduced retention time of the analytes in reversed polarity mode. Partial separation was obtained using 20 mM CDEn

in the BGE at pH 2.5 and -12 kV (Figure 5.23b). Two peaks are evident in this electropherogram at 9.97 and 10.45 mins however they are not baseline separated. Further increases in the concentration of CDEn did not improve separation.

The results obtained above agree with earlier suggestions that the amino-cyclodextrin derivatives may be guest specific as chiral selectors in CE. With this in mind sulfated-*β*-cyclodextrin (SCD) was chosen as an alternative chiral selector to CDEn since anionic chiral selectors such as SCDs are useful for separating cationic analytes due to strong electrostatic interactions. In SCDs the hydroxyl groups are substituted by SO_3^- groups and the SCD used in this work had a degree of substitution of 7-11 substitutions per molecule.

Figure 5.24 shows the electropherogram of D,L-DOPA separated using normal polarity mode and 0.2 % (w/v) SCD in the BGE (pH 2.5) using +25 kV. Two well defined peaks are visible in the electropherogram (L-DOPA migrating first) with a resolution value of 3.62.

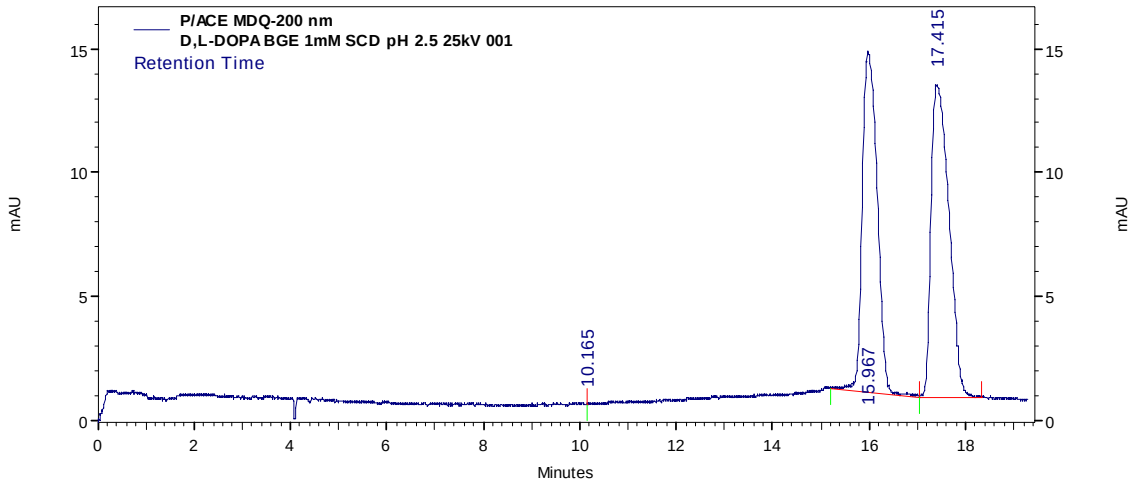

Figure 5.24 Electropherogram of D,L-DOPA (excess L-DOPA) with 0.2 % (w/v) SCD in BGE (pH 2.5, +25 kV)

5.3 Conclusion of Capillary Electrophoresis Study

The separation of L-carbidopa from L-DOPA, the components of many anti-Parkinson's medications is a complex analytical problem due to the analytes having similar chemical structures. At pH 6.8 it was found that in CE their effective mobilities were very similar which did not allow for their separation when using ammonium acetate as a BGE. To enhance the separation CuCDEn was added to the BGE as a chiral selector. Despite changing the concentration of the chiral selector and BGE and changing the voltage, separation was not observed.

Other workers have shown that at a more acidic pH of 2.5 the difference between the effective mobilities of carbidopa and DOPA is greater.[16,17,18] However the binary complex CuCDEn does not form at this pH. Therefore CDEn alone was used as the selector. Separation of L-DOPA and L-carbidopa was achieved using 2 mM CDEn in the BGE at a pH of 2.5 and gave retention times of ~ 16 mins in normal polarity mode. The resolution was calculated to be 2.36 with DOPA migrating as the second peak. Lower migration times (~ 5 mins) were achieved by reversing the polarity.

Chiral separation of D,L-DOPA was attempted and no separation was achieved in normal polarity mode. However there was some evidence of initial separation using 20 mM CDEn in the BGE at pH 2.5 in reversed polarity mode, but no baseline separation was recorded. An alternative method was proposed using sulfated cyclodextrins (SCDs). Chiral resolution of D,L-DOPA was achieved in normal polarity mode using 0.2 % (w/v) SCD in the BGE at pH 2.5 with a resolution of 3.62.

In conclusion, the results obtained in this work suggest that the metallo-cyclodextrin derivatives are not versatile chiral selectors due to the fact that their use is limited by pH. These complexes are only stable within a pH range of 6.5-8. Amino-cyclodextrins are also not versatile selectors it is difficult to determine their exact mode of action but

since they are neutral molecules it is possible that they give a narrow separation window. Unlike the anionic sulfated derivatives they will not have strong interactions with cationic analytes. Therefore there will be little difference in the mobility of free and complexed analytes. Cucinotta *et al.* has suggested that the separation mechanism of charged cyclodextrin derivatives relies on the differences in the velocity of migration between the analyte and the analyte-CD complex. [23] Wren and Rowe suggest that for separation of enantiomers it is necessary to maximise the difference in the stability constants of the diastereomeric complexes with CD.[24] Therefore electrostatic interactions between charged CDs and charged analytes may not be the only factor influencing separation.

5.4 References

[1] D.R. Baker: *Capillary Electrophoresis*, Wiley, 1995.

[2] B. Chankvetadze: *Capillary Electrophoresis in Chiral Analysis*, Wiley, 1997, p. 353

[3] G. Thorsen, A. Engstrom, B. Josefsson: *J Chromatogr A*, **786**, (1997) 347

[4] O.P. Kleidernigg and W. Lindner: *J Chromatogr A.,* **795**, (1998) 251

[5] J. Snopek, I. Jelinek and E. Smolkova-Keulemansova: *J Chromatogr*, **438**, (1988) 211

[6] A. Guttman, A. Paulus, A.S. Cohen, N. Grinberg and B.L. Karger: *J Chromatogr.* **448**, (1988) 41

[7] S. Fanali: J *Chromatogr.* **474**, (1989) 441

[8] P. Camilleri, *Capillary Electrophoresis, Theory and Practice Second Edition,* CRC Press, (1998)

[9] D.J Rose and J. W. Jorgenson: *Anal. Chem.*, **60**, (1998) 642

[10] J.W. Jorgenson and K.D. Lukacs: *Science*, **222**, (1983) 266

[11] F. Helfferich, *Nature*, **189**, (1961) 1001

[12] E.Grassman, J.E. Kuo, R.N. Zare, *Science*, **230**, (1985) 813

[13] V. Cucinotta, A. Giuffrida, G. Grasso, G. Maccarrone and G. Vecchio, *Analyst*, **128,** (2003) 134

[14] A. Van Eeckhaut and Y. Michotte: *Chiral Separations by Capillary Electrophoresis, Colume 100*, CRC Press, (2009)

[15] R.P. Bonomo, V Cucinotta, F. D'Allessandro, G. Impellizzeri, G. Maccarrone, E. Rizzarelli: *J. Inc. Phenom. and Mol. Recog.* **15**, (1993) 167

[16] S. Finali, V. Pucci, C. Sabbioni and M.A. Raggi: *Electrophoresis,* **21,** (2000) 2432

[17] S. Saraç, B. Chankvetadze and G. Blaschke: *J. Chromatogr. A,* **875,** (2000) 379

[18] P.T.T. Ha, A.V. Schepdael, T. Hauta-aho, E. Roets and J. Hoogmartens: *Electrophoresis,* **23,** (2002) 3404

[19] V. Cucinotta, A. Giuffrida, G. Maccarrone, M. Messina and G. Vecchio: *Electrophoresis* , **27,** (2006) 1471

[20] C.F. Potter: *Metallo-cyclodextrin complexes for the separation of chiral materials, synthesis and characterisation.* PhD Thesis, http://arrow.dit.ie/sciendoc/18/

[21] V. Cucinotta, A. Giuffrida, D. La Mendola, G. Maccarrone, A. Puglisi, E. Rizzarelli and G. Vecchio: *J. Chromatogr. B.* **800,** (2004) 127

[22] V. Cucinotta, A. Giuffrid, G. Maccarrone, M. Messina, A. Puglisi, E. Rizzarellia and G. Vecchio *Dalton Trans.,* (2005) 2731

[23] V. Cucinotta, A. Contino, A. Giuffrida, G. Maccarrone and M. Messina: *J. Chromatogr. A.***1217,** (2010) 953

[24] S.A.C. Wren and R.C. Rowe, *J. Chromatogr*. 603, (1992) 235

6. Conclusion

In this work copper(II) complexes of aminoalkane derivatives of *β*-cyclodextrin (CDEn, CDPn and CDBn) were investigated to determine if they provide a more versatile solution than sulfated derivatives for the direct separation of enantiomers and analytes with similar chemical structures (DOPA, benserazide and carbidopa) using capillary electrophoresis. Tyrosine was used as a model compound.

Binary complexes of the amino-CD derivatives with copper(II) were formed in solution and were analysed using electronic absorption spectroscopy. Significant shifts in the position of λ_{max} for the d-d transition of copper(II) showed the successful coordination of Cu(II) to the amino group of the CDs. The results suggested that CDEn and CDPn behave as bidentate ligands and coordinate to the metal ion through the two nitrogen atoms of the diaminoalkane moiety. The shift in λ_{max} for CDBn was less pronounced indicating it acts as a monodentate ligand as a result of the longer aminoalkane chain. The complexation of these binary complexes with D,L-tyrosine, D,L-DOPA and L-carbidopa resulted in the formation of ternary complexes. Evidence of the formation of these complexes was demonstrated by further hypsochromic shifts in λ_{max} for the d-d transition of copper(II). It was also found that benserazide did not form a stable complex with any of the binary complexes.

To assess the enantioselective properties of the CuCDAm species both the binary and ternary complexes of tyrosine and DOPA were studied using circular dichroism spectroscopy. The study allowed the examination of the degree of inclusion of the guest moieties within the cyclodextrin cavity. It was proposed that due to structural restrictions imposed by both the CD cavity and the presence of the metal centre caused two configurations to form for the L and D ternary complexes and that these take the form of diastereoisomers one with the aromatic side-chain orientated away from the CD

cavity and one towards or in the cavity. The results suggested that $[CuCDEn]^{2+}$ was the most effective chiral selector of those studied for both guests.

The stoichiometry of all the complexes formed was studied using the Job's method of continuous variation. Table 6.1 summarises the results obtained.

Table 6.1 Results of the continuous variation study showing complex stoichiometries

Metal	*Ligand*	*Stoichiometry*
Cu(II)	CDEn	1:1
Cu(II)	D-tyrosine	1:1 and 1:2
Cu(II)	L-tyrosine	1:1 and 1:2
Cu(II)	D-DOPA	1:1 and 2:1
Cu(II)	L-DOPA	1:1 and 2:1
Cu(II)	L-carbidopa	1:1

Host	*Guest*	*Stoichiometry*
CuCDEn	D-tyrosine	1:1
CuCDEn	L-tyrosine	1:1
CuCDEn	D-DOPA	2:1
CuCDEn	L-DOPA	2:1
CuCDEn	L-carbidopa	1:1 and 2:1

Combining the results of the electronic absorption, circular dichroism and stoichiometry studies allows us to suggest the following ternary complex structures in Figure 6.1-6.3.

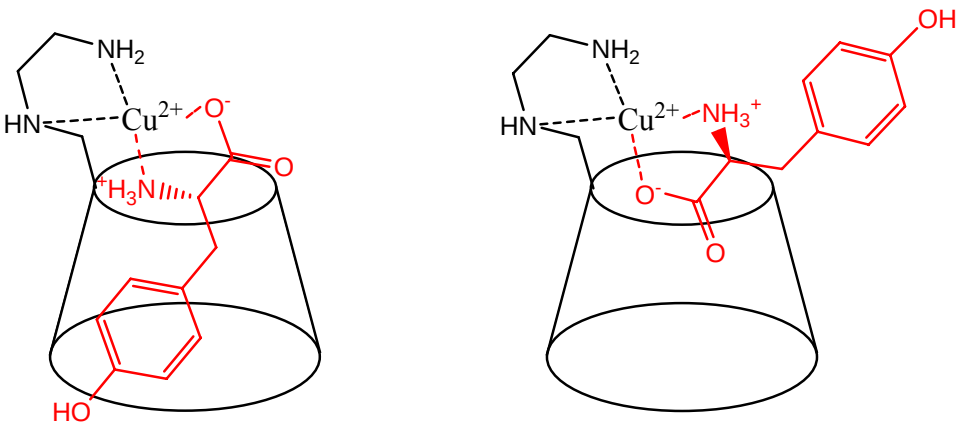

[D-tyrosine(CuCDEn)]$^{2+}$ [L-tyrosine(CuCDEn]$^{2+}$

Figure 6.1 Proposed structures of the ternary complexes of D,L-tyrosine with [CuCDEn]$^{2+}$ at pH 6.8

Support for these structures can be obtained from electronic spectroscopy which indicated coordination to the metal centre *via* the nitrogen of the amine group and oxygen of the carboxyl group of tyrosine. Circular dichroism also indicated a difference in inclusion between the two enantiomers, with D-tyrosine showing deeper inclusion into the CD cavity. The stoichiometric study showed 1:1 complexation for CuCDEn:tyrosine. Further support for the proposed structure can be obtained from Maccarrone *et al.* who proposed similar structures for the diastereoisomeric ternary complexes of tryptophan and CuCDEn.[1]

For DOPA a hypsochromic shift in the absorption spectrum for the ternary complex with CuCDEn *versus* the binary complex indicated further coordination of DOPA to the metal centre. Again c.d. spectroscopy shows differential inclusion between the two enantiomers with results indicating D-DOPA is included more fully than L-DOPA. The Job's plot indicated 2:1 complexation for CuCDEn:DOPA. These results led to the following proposed structures (Figure 6.2).

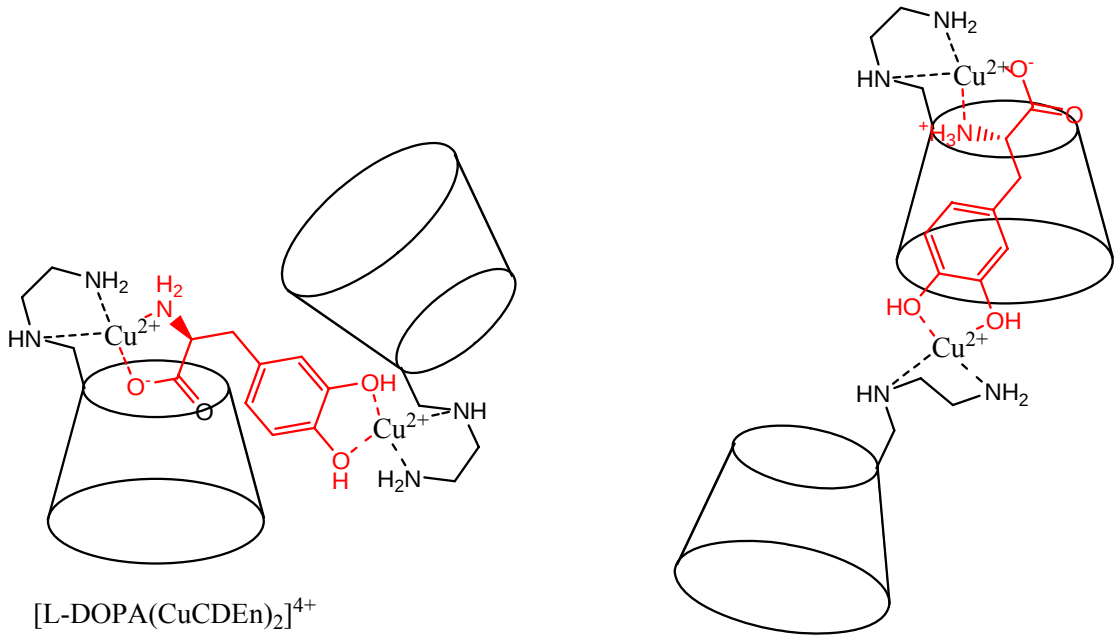

Figure 6.2 Proposed structures of the ternary complexes of D,L-DOPA with $[CuCDEn]^{2+}$ at pH 6.8

Electronic spectroscopy also suggested coordination of L-carbidopa to CuCDEn *via* the carboxyl and amino groups. The stoichiometric study suggested the existence of both 1:1 and 2:1 CuCDEn:L-carbidopa ternary complexes in solution. Due to the lack of a commercially available sample of D-carbidopa a circular dichroic experiment could not be carried out and therefore it is not possible to compare inclusion of the enantiomers in the CD cavity. However since the structures of DOPA and carbidopa are similar it is possible that the ternary complexes also have similar structures and therefore proposed structures for the carbidopa complexes are shown in Figure 6.3.

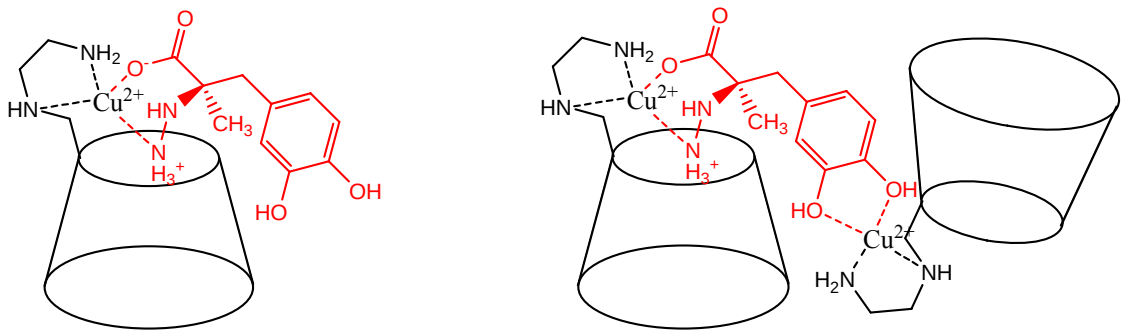

[L-carbidopa(CuCDEn)]$^{2+}$ [L-carbidopa(CuCDEn)$_2$]$^{4+}$

Figure 6.3 Proposed structures of the ternary complexes of L-carbidopa with [CuCDEn]$^{2+}$ at pH 6.8

The circular dichroism study suggested that CuCDEn may be the most effective chiral selector of those studied for the chiral separation for DOPA. In the capillary electrophoresis study CuCDEn was added to the BGE at pH 6.8 in an effort to resolve the enantiomers of DOPA and perform the separation of L-DOPA from L-carbidopa. The separation of L-carbidopa from L-DOPA is a complex analytical problem due to the analytes having similar chemical structures. At pH 6.8 it was found that their effective mobilities were very similar which did not allow for their separation when using ammonium acetate alone as a BGE. To enhance the separation CuCDEn was added to the BGE. Changes to various experimental conditions were explored such as CuCDEn concentration, ammonium acetate concentration and voltage. However successful separation of L-DOPA and L-carbidopa was not achieved.

Other workers have shown that at a more acidic pH of 2.5 the difference between the effective mobilities of carbidopa and DOPA is greater.[2,3,4] However the binary complex CuCDEn does not form at this pH. Therefore CDEn alone was used as the selector in the BGE at pH 2.5. Separation of L-DOPA and L-carbidopa was achieved using 2 mM CDEn and gave retention times of ~ 16 mins. The resolution was calculated to be 2.36 with DOPA migrating as the second peak. Lower migration times (~ 5 mins) were

achieved by reversing the polarity. To the best of the author's knowledge this represents the first time DOPA and carbidopa have been separated using CDEn.

Chiral separation of D,L-DOPA was attempted and no separation was achieved in normal polarity mode. However there was some evidence of initial separation using 20 mM CDEn in the BGE at pH 2.5 in reversed polarity mode, but no baseline separation was recorded. An alternative method was proposed using sulfated cyclodextrins (SCDs) as a chiral selector. Chiral resolution of D,L-DOPA was achieved using 0.2 % (w/v) SCD in the BGE at pH 2.5 with a resolution of 3.62 in normal polarity mode.

In conclusion, the results obtained in this work suggest that amino-cyclodextrin derivatives are guest selective for chiral separations in capillary electrophoresis and do not represent a universal method for separations required for regulatory compliance. Since separations were obtained using the anionic sulfated derivatives it is suggested that host molecules with a permanent charge are more useful and therefore inclusion is not the only factor needed for separation to be successful. Since the sulfated group is a coordinating ligand it would be interesting in future to investigate if metallo complexes of SCDs can be formed and to study their enantioselective ability.

6.1 References

[1] G. Maccarone, E. Rizzarelli and G. Vecchio: Chiral Recognition by Functionalised Cyclodextrin Metal Complexes. In L. Fabbrizzi and A. Poggi (eds.), *Transition Metals in Supramolecular Chemistry,* Kluwer Academic Publishers, (1994), p. 351-367

[2] S. Finali, V. Pucci, C. Sabbioni and M.A. Raggi: *Electrophoresis,* **21,** (2000) 2432

[3] S. Saraç, B. Chankvetadze and G. Blaschke: *J. Chromatogr. A,* **875,** (2000) 379

[4] P.T.T. Ha, A.V. Schepdael, T. Hauta-aho, E. Roets and J. Hoogmartens: *Electrophoresis,* **23,** (2002) 3404

7. Synthesis and Characterisation

7.1 Introduction

The following section details the materials and methods used in the synthesis and characterisation of 6-*O*-monotosyl-6-deoxy-*β*-cyclodextrin (CDTs), 6-deoxy-6-[1-(2-amino)ethylamino]-*β*-cyclodextrin (CDEn), 6-deoxy-6-[1-(3-amino)propylamino]-*β*-cyclodextrin (CDPn) and 6-deoxy-6-[1-(4-amino)butylamino]-*β*-cyclodextrin (CDBn).

Amino derivatives of CDs can be prepared by an indirect approach. A widely used intermediate is mono-6-deoxy-6-tosyl-*β*-cyclodextrin (CDTs). A common method for preparation of CDTs involves reaction of *β*-CD with excess *p*-toluenesulphonyl chloride, with recrystallisation from water.[1] Due to the importance of these sulphonates acting as intermediates for the further synthesis of other modified CDs, there exist many other methods of preparation.[2, 3, 4, 5] For instance CDTs can be prepared by the reaction of *β*-CD with *p*-toluenesulphonyl chloride in pyridine.[1] This route has the disadvantage that the product is obtained in poor yield and must be separated from multitosylated by-products by chromatography along with the inherent difficulties of using pyridine as a solvent. The synthesis used in this study is a slightly modified version of an aqueous-based method reported by Brady *et al.*[4]

Monoamine derivatives of CDs have been prepared by the treatment of the corresponding tosylate with ammonia.[1] Analogous reactions of primary and secondary amines have also been reported as a method for attaching amino groups at the C6 position of a CD.[6] These materials can then be exploited for further modification, since the amino groups are substantially more nucleophilic than the CD hydroxyl groups. Matsui *et al.* published a synthesis route for 6-deoxy-6-[1-(2-amino)ethylamino]-*β*-cyclodextrin (CDEn) in 1976.[9] A modified version of Matsui's synthesis was also

reported by Singh *et al*.[7] The diaminoalkane derivatives CDEn, CDPn and CDPn prepared here follow a modified synthesis of the route proposed by Singh *et al*.

7.2 Experimental

All materials were purchased from commercial sources and were used without further purification. *β*-Cyclodextrin was supplied kindly by Wacker Chemie UK. Percentage yields are given based on the hydrated material and melting points as a decomposition range. Decomposition ranges were recorded using an Electrothermal 9100 melting point apparatus. It should be noted that the decomposition ranges given here (m.p. (dec.)) are the temperature at which the sample started to change colour.

^{1}H and ^{13}C NMR spectra for *β*-CD and its derivatives were measured at 100 and 400 MHz respectively, using a Bruker Avance III 400 NMR spectrometer. Spectra were recorded at room temperature using DMSO (for *β*-CD and tosylated derivatives) and D_2O (for amino derivatives) as solvents. Spectra were referenced to the solvent peaks.

FTIR spectra were recorded at room temperature using a Perkin Elmer Spectrum GX FTIR Spectrometer. Spectra were obtained of solid samples as KBr disks. The spectra were measured over a range of 4000-370 cm^{-1} with a resolution of 4 cm^{-1}, an interval of 0.5 cm^{-1} and an accumulation of 16.

Raman spectra were recorded using a LabRAM HR System Raman Spectrometer. The Raman spectrometer is controlled using the software package Labspec 5. All Raman spectra of solid samples were collected at room temperature using the following parameters: Time: 30 s, Accumulation: 10, Grating: 1800 lines/mm, Slit: 900 μm, Laser: 785 nm, Objective: 10×, Filter: 100 %, Hole: 900 μm. After alignment of optics, the system was calibrated using silicon as a calibrant (520 nm). A spectral window of

200-4000 cm^{-1} was used. The laser beam was focused on the solid sample and the scattered radiation efficiently gathered by the objective of the microscope.

7.3 Results

All of the results obtained compare favourably with work previously carried out by this group and other workers.[1,4,7,8,9,10]

Synthesis of 6-*O*-monotosyl-6-Deoxy-*β*-cyclodextrin (CDTs)

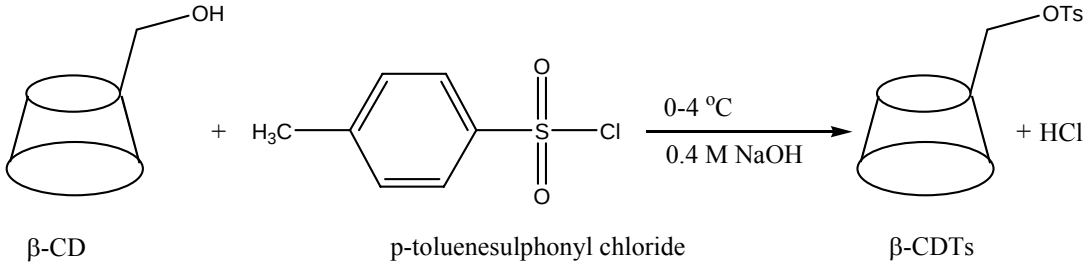

Scheme 7.1 Synthesis of 6-*O*-monotosyl-6-deoxy-*β*-cyclodextrin (CDTs)

β-cyclodextrin hydrate (10.01 g, 7.61 mmol) was dissolved in NaOH (100 cm^3 of 0.4 mol dm^{-3}). The solution was cooled in ice and *p*-toluenesulphonyl chloride (3 g, 15.79 mmol) was added. The mixture was stirred for 3 hours at 0 – 4 °C. The mixture was then filtered and the pH of the filtrate adjusted to 6.5 using HCl (1 mol dm^{-3}, 20 cm^3) and a precipitate formed. The filtrate was cooled at 4 °C for 24 hours. The product was removed by filtration, washed with acetone and recrystallised from water several times. The solid was recovered by filtration, washed with acetone and allowed to dry at 60 °C for 4 hours. It should be noted that rapid cooling to 60 °C of the mixture was employed during the recrystallisation to avoid significant hydrolysis.[4]

Yield: 4.89 g, 45% (based on hydrated material) **Literature Value:** 20-30 %[10]

m.p: 163 °C (dec.) **Literature Value:** 161-162 °C[10]

^{1}H NMR (DMSO) δ (ppm) 7.74 (H8) 7.42 (H9) 5.73 (OH2, OH3) 4.83 (H1) 4.46 (OH6) 4.32 ($H6_b$) 3.66 (H6) 3.60 (H3) 3.51 (H5) 3.32 (H4) 3.21 (H2) 2.43 (H11)

^{13}C NMR (DMSO) δ (ppm) 144.88 (C10) 132.64 (C7) 129.93 (C9) 127.61 (C8) 102.25 (C1') 101.94 (C1) 101.29 (C1'') 81.66 (C4') 81.50 (C4'') 81.15 (C4) 73.08 (C3) 72.70 (C2' or C3') 72.43 (C2) 72.07 (C5) 69.76 (C6') 68.95 (C5') 59.95 (C6) 59.91 (C6'') 21.24 (C11).

FTIR (cm^{-1}) 1647 (complexed water), 1364 (asymmetric SO_2-O stretch), 1159 (symmetric SO_2-O stretch), 837 and 814 (*para*-disubstituted benzene ring)*

Raman (cm^{-1}) 3061 (aromatic C-H stretch of alkyl benzene), 1597 (ring stretch of benzene derivatives), 1208 and 1178 (symmetric SO_2 stretch), 796 (ring vibration of *para*-disubstituted benzene), 669 (benzene ring in-plane deformations), 634 (benzene ring in-plane deformations)*

*New bands relative to β-CD

^{13}CNMR

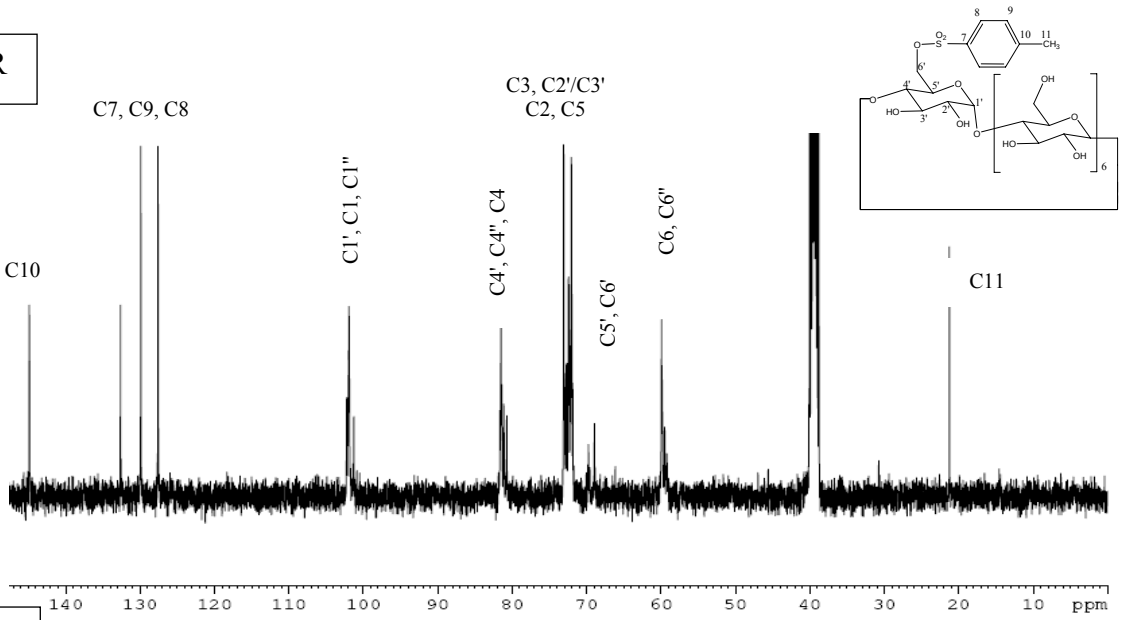

^{1}HNMR

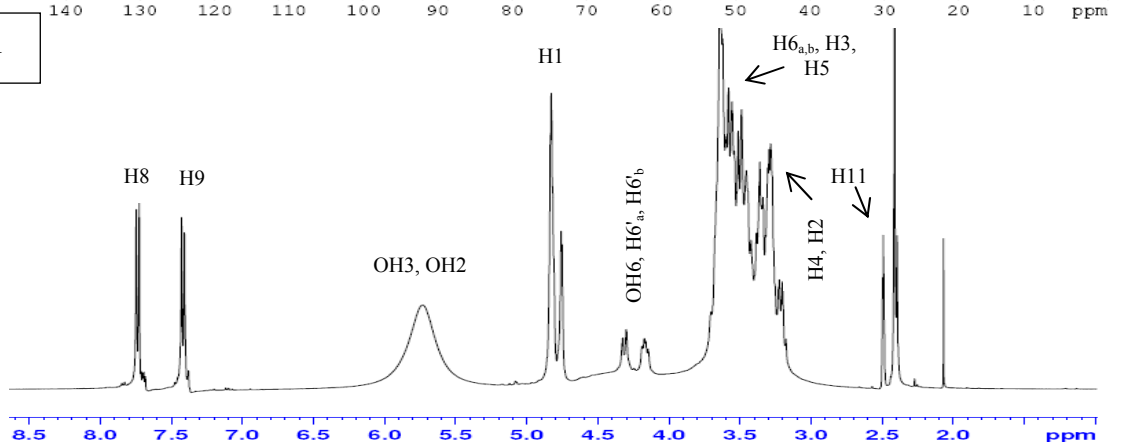

IR

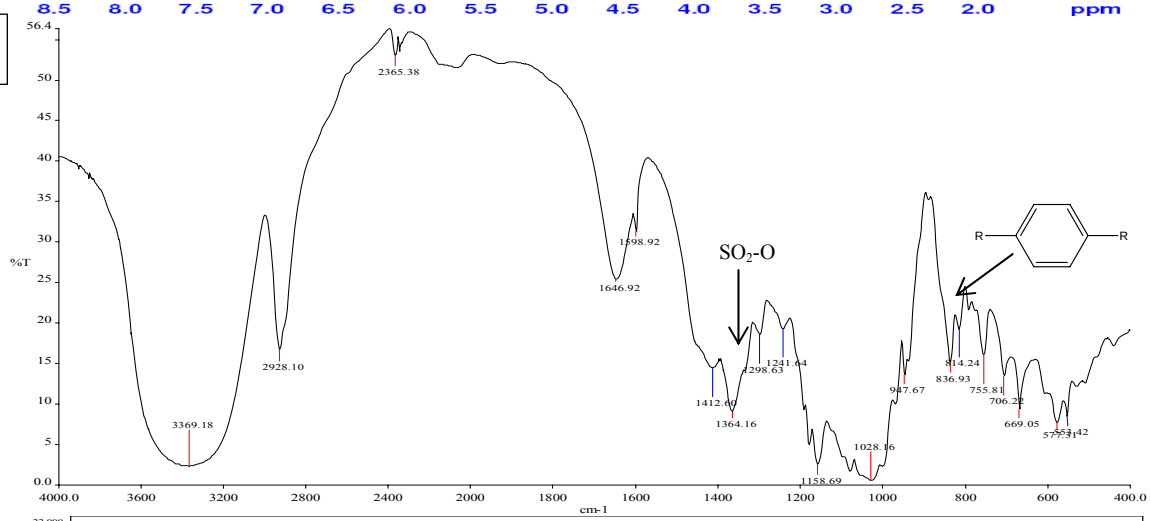

Raman

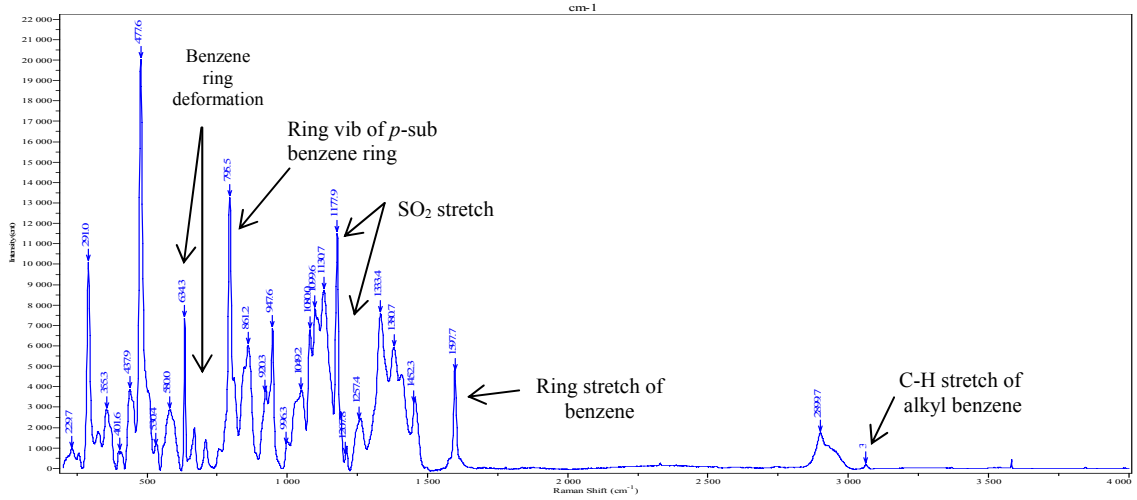

Synthesis of 6-deoxy-6-[1-(2-amino)ethylamino]-*β*-cyclodextrin (CDEn)

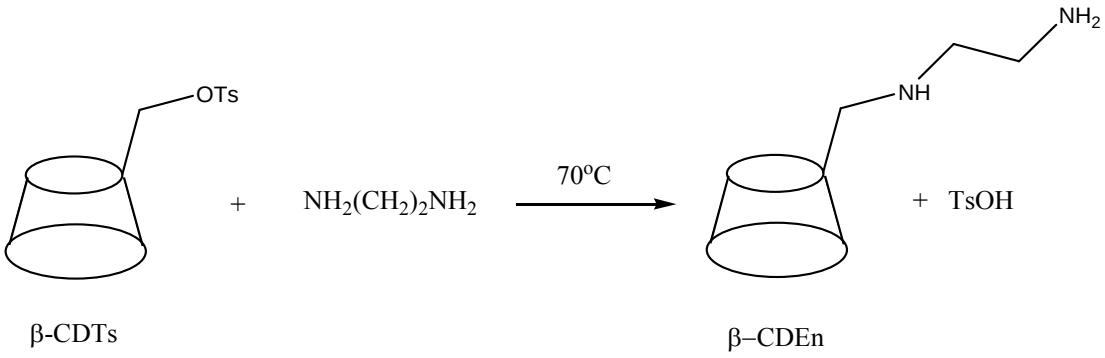

Scheme 7.2 Synthesis of 6-deoxy-6-[1-(2-amino)ethylamino]-*β*-cyclodextrin (CDEn)

6-*O*-monotosyl-6-deoxy-*β*-cyclodextrin (*β*-CDTs) (19.28 g, 13.45 mmol) was dissolved in 1,2 diaminoethane (70 cm^3, 1.05 mol) and refluxed under nitrogen for 24 hours at 70 °C. The mixture was then concentrated under vacuum and gave a pale yellow viscous oil. The oil was then dissolved in a minimum volume of water: methanol (3:1) mixture. The solution was then slowly added to cold acetone and a precipitate formed. The precipitate was recovered by filtration, washed with acetone and dried in air. The product was dissolved in a minimum volume of water (60 °C). A minimum volume of acetone was added to just initiate crystallization and the mixture was cooled to 4 °C. The product was recovered by filtration, washed with acetone and dried at 60 °C for 4 hours. To achieve a pure product the recrystallization step was repeated 3-4 times.

Yield: 14 g, 76.5 % (based on hydrated material) **Literature Value:** 37-60 %[10]

m.p: 250 °C (dec.) **Literature Value:** 268-271 °C[10]

^{1}H NMR (D_2O) δ (ppm): 5.09 ($H1_{\beta}$), 3.94 (H3), 3.84 ($H6_{a,b}$), 3.83 (H5), 3.62 (H2), 3.57 (H4), 3.45 (H4'), 3.04 ($H6'_{\alpha}$), 2.81 ($H6'_{\beta}$, H8), 2.71 (H7)

^{13}C NMR (D_2O) δ (ppm): 101.77 (C1), 101.49 (C1'), 83.42 (C4'), 81.03 (C4) 80.86 (C4''), 72.99 (C3), 72.93 (C2'/C3'), 71.95 (C2), 71.70 (C5), 70.33 (C5'), 60.15 (C6), 49.41 (C9), 49.08 (C6'), 39.33 (C8).

FTIR (cm^{-1}) 1622 (complexed water), 1586 (N-H bending vibrations), 1492 (C-H_2 scissoring mode of aminoalkane group), 818 (N-H wag)*

Raman (cm^{-1}) 3520 (N-H stretch)*

*These are new bands relative to β-CD

^{1}HNMR

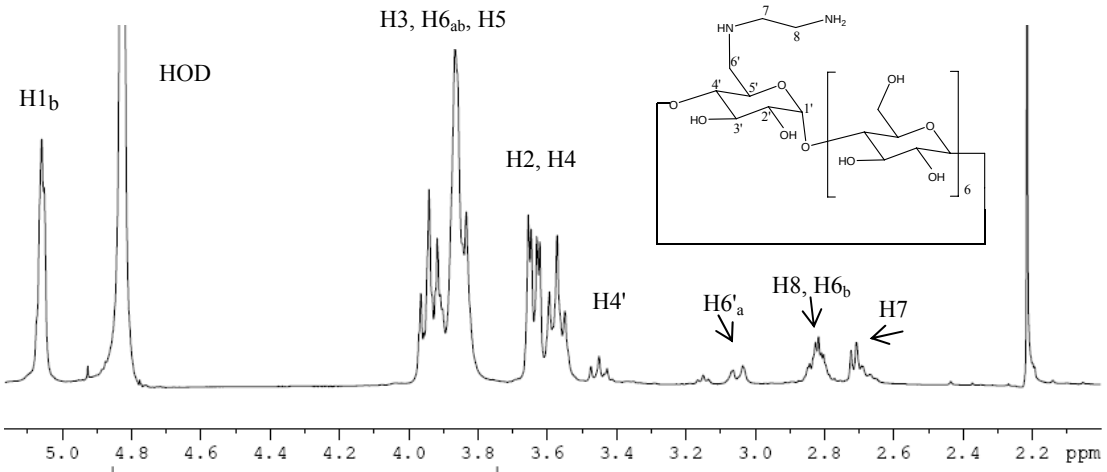

^{13}CNMR

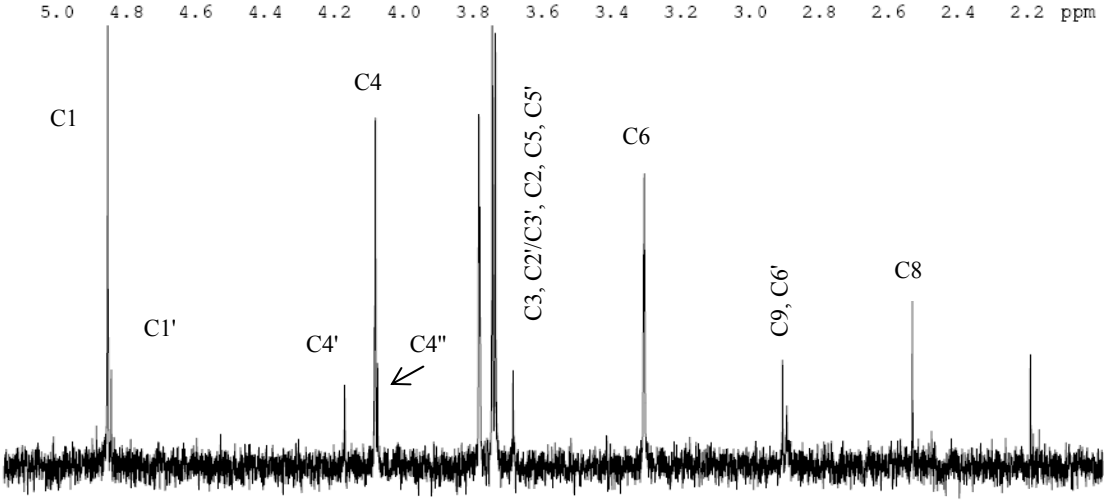

IR

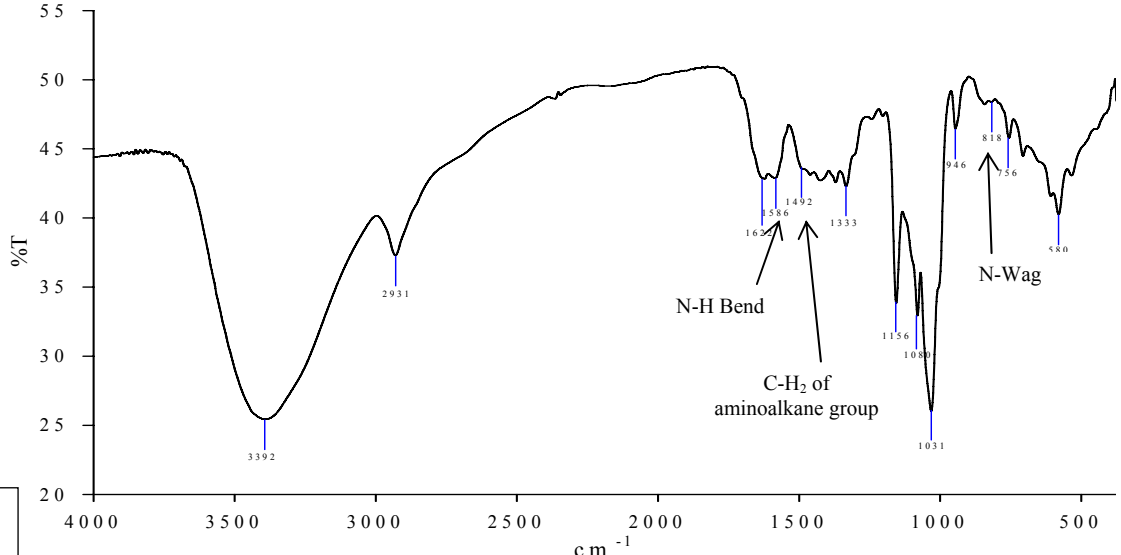

Raman

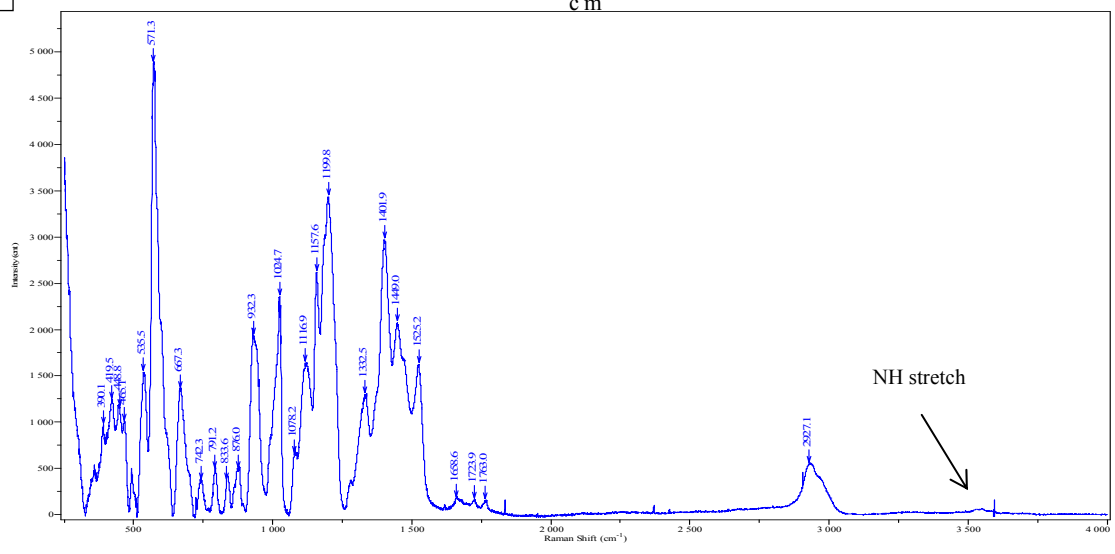

Synthesis of 6-Deoxy-6-[1-(3-amino)propylamino]-*β*-cyclodextrin (CDPn)

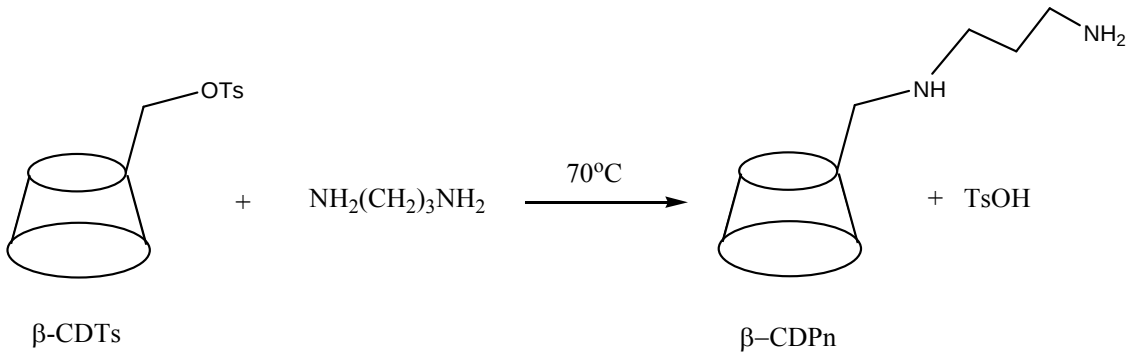

Scheme 7.3 Synthesis of 6-deoxy-6-[1-(3-amino)propylamino]-*β*-cyclodextrin (CDPn)

6-*O*-monotosyl-6-deoxy-*β*-cyclodextrin (*β*-CDTs) (3.97 g, 2.77 mmol) was dissolved in 1,3 diaminoethane (18 cm^3, 0.216 mol) and refluxed under nitrogen for 24 hours at 70 ^oC. The mixture was then concentrated under vacuum and gave a pale yellow viscous oil. The oil was then dissolved in a minimum volume of water: methanol (3:1) mixture. The solution was then slowly added to cold acetone and a precipitate formed. The precipitate was recovered by filtration, washed with acetone and dried in air. The product was dissolved in a minimum volume of water (60 °C). A minimum volume of acetone was added to just initiate crystallization and the mixture was cooled to 4 °C. The product was recovered by filtration, washed with acetone and dried at 60 °C for 4 hours. The recystallization step was repeated 3-4 times to achieve a pure product.

Yield: 2.54 g, 66 % (based on hydrated material) **Literature Value:** 93 %[10]

m.p: 260 ^oC (dec.) **Literature Value:** 268-271 ^oC[10]

^{1}H NMR (D_2O) δ (ppm): 5.04 ($H1_{\beta}$), 3.94 (H3), 3.84 ($H6_{a,b}$), 3.81 (H5), 3.61 (H2), 3.55 (H4), 3.4 (H4'), 3.01 ($H6'_{b}$), 2.80 ($H6'_{a}$, H9), 2.60 (H7), 1.71 (H8)

^{13}C NMR (D_2O) δ (ppm): 101.7 (C1), 101.4 (C1'), 83.5 (C4'), 81.0 (C4) 80.7 (C4''), 72.9 (C3), 72.9 (C2'/C3'), 71.9 (C2), 71.7 (C5), 70.2 (C5'), 60.1 (C6), 49.3 (C6'), 46.2 (C7), 38.1 (C9), 29.0 (C8)

FTIR (cm^{-1}) 1634 (complexed water), 1572 (N-H bending vibration), 1485, 1472 (C-H_2 scissoring mode of aminoalkane group), 818 (N-H wag)*

Raman (cm^{-1}) 3533 (N-H stretch)*

*These are new bands relative to β-CD

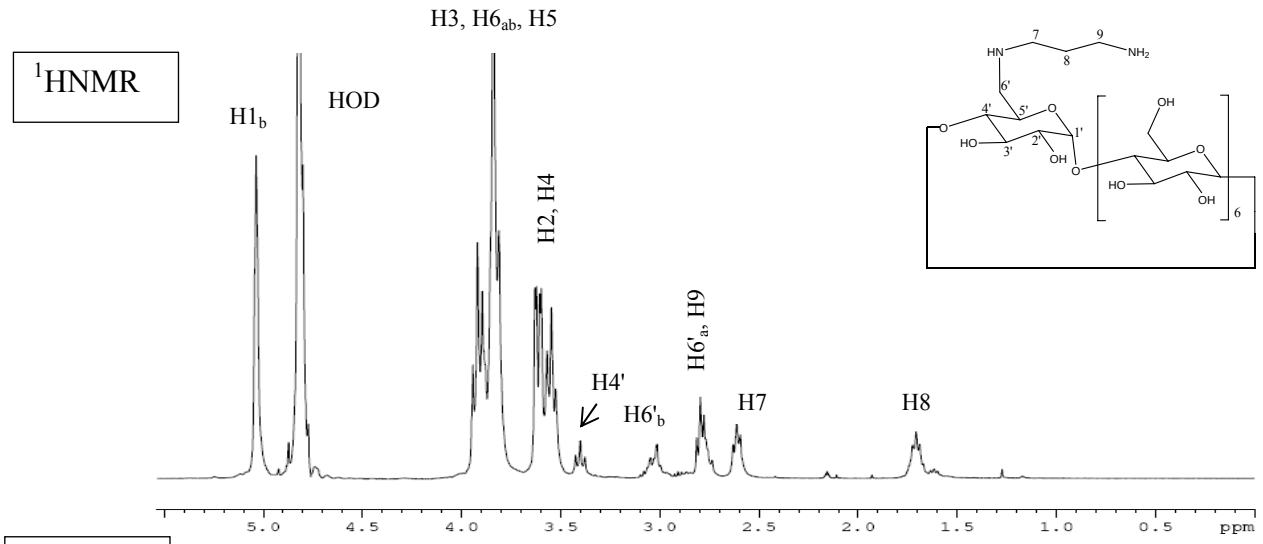
^{1}HNMR
H3, H6$_{ab}$, H5
H1$_b$
HOD
H2, H4
H4'
H6'$_b$
H6'$_a$, H9
H7
H8
HN
NH$_2$
HO
OH
5.0
4.5
4.0
3.5
3.0
2.5
2.0
1.5
1.0
0.5
ppm

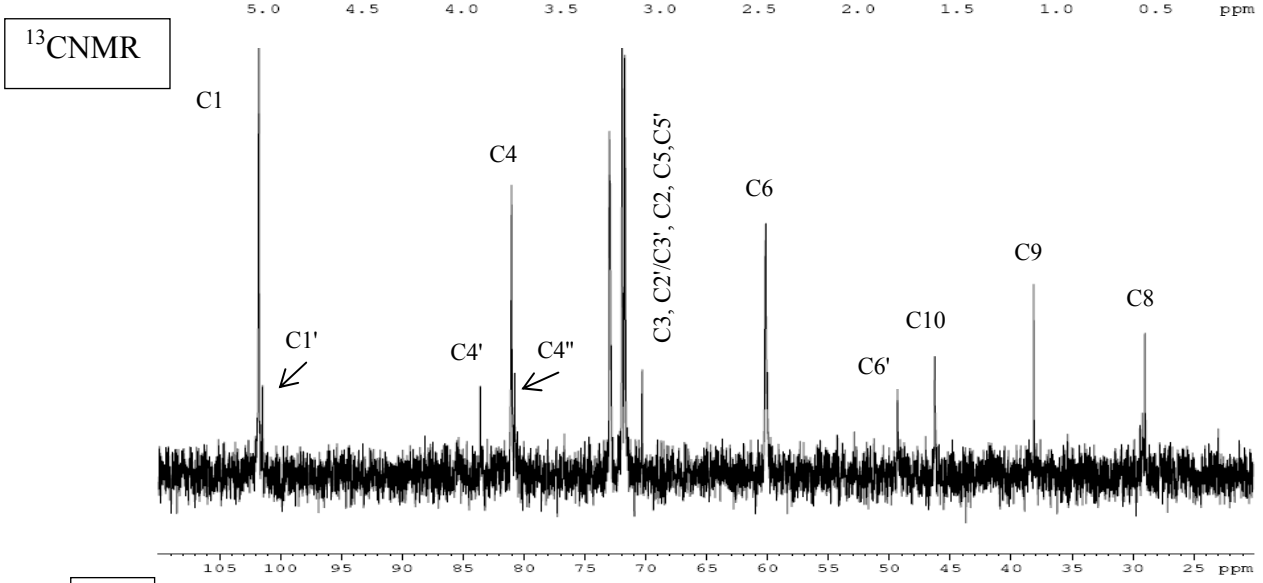
^{13}CNMR
C1
C1'
C4
C4'
C4"
C3, C2'/C3', C2, C5,C5'
C6
C6'
C10
C9
C8
105
100
95
90
85
80
75
70
65
60
55
50
45
40
35
30
25
ppm

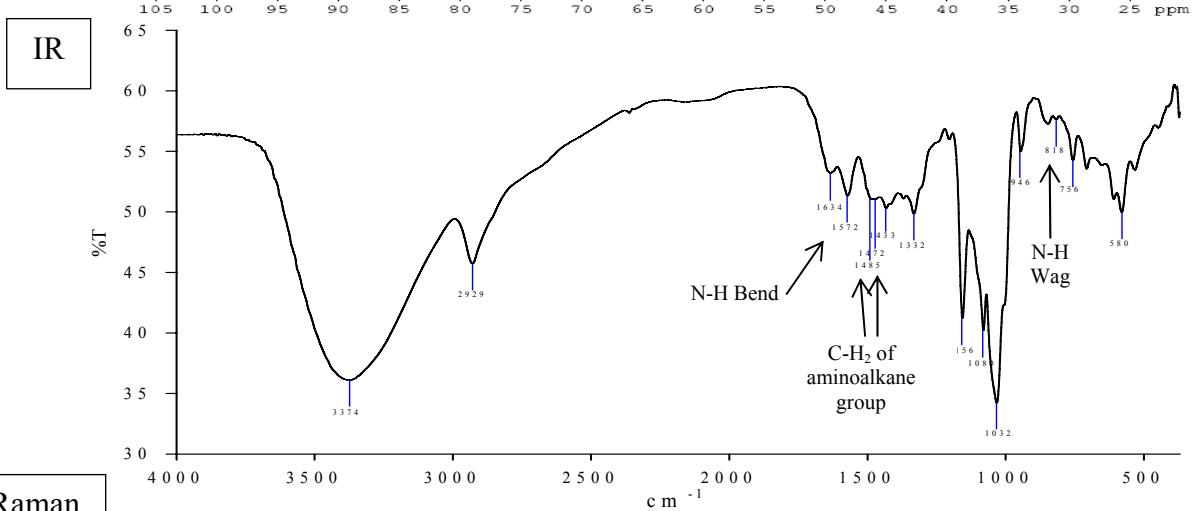
IR
%T
65
60
55
50
45
40
35
30
4000
3500
3000
2500
2000
1500
1000
500
c m $^{-1}$
3374
2929
1634
1572
1433
1332
1485
1156
1108
1032
946
818
756
580
N-H Bend
C-H$_2$ of aminoalkane group
N-H Wag

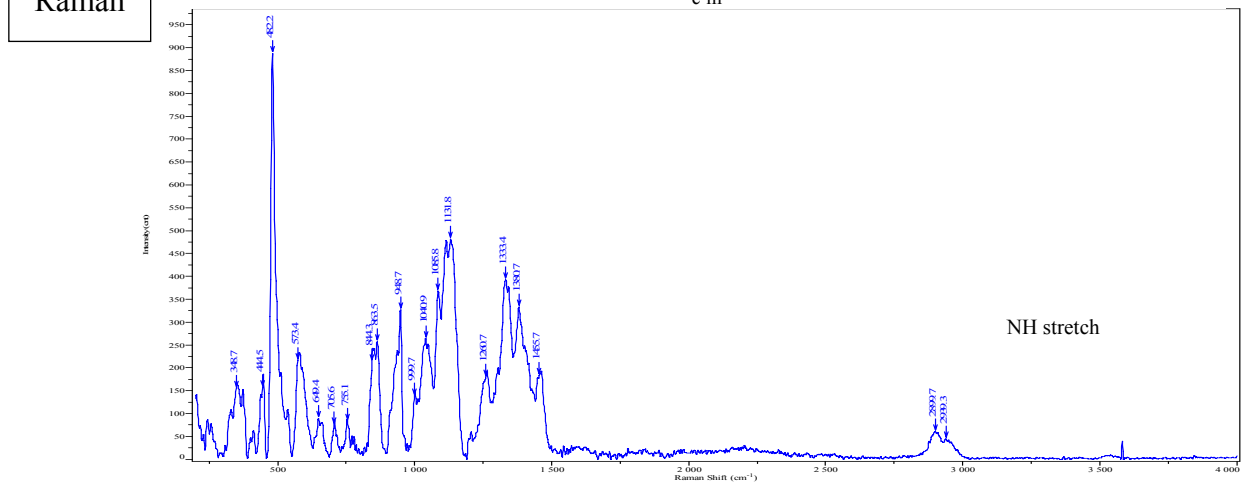
Raman
Intensity
422
3487
4445
574
649
705
795
843
935
987
1009
1058
1138
1207
1334
1387
1457
2893
2939
NH stretch
500
1 000
1 500
2 000
2 500
3 000
3 500
4 000
Raman Shift (cm^{-1})

Synthesis of 6-Deoxy-6-[1-(4-amino)butylamino]-*β*-cyclodextrin (CDBn)

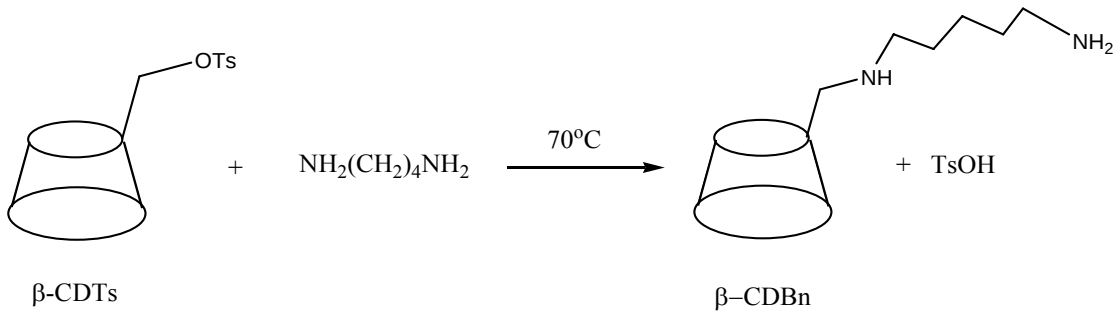

Scheme 7.4 Synthesis of 6-deoxy-6-[1-(4-amino)butylamino]-*β*-cyclodextrin (CDBn)

6-*O*-monotosyl-6-deoxy-*β*-cyclodextrin (*β*-CDTs) (4.00 g, 2.79 mmol) was dissolved in 1,4 diaminobutane (22 cm^3, 0.248 mol) and refluxed under nitrogen for 24 hours at 70 ^oC. The mixture was then concentrated under vacuum and gave a pale yellow viscous oil. The oil was then dissolved in a minimum volume of water: methanol (3:1) mixture. The solution was then slowly added to cold acetone and a precipitate formed. The precipitate was recovered by filtration, washed with acetone and dried in air. The product was dissolved in a minimum volume of water (60 °C). A minimum volume of acetone was added to just initiate crystallization and the mixture was cooled to 4 °C. The product was recovered by filtration, washed with acetone and dried at 60 °C for 4 hours. The recystallization step was repeated 3-4 times to achieve a pure product.

Yield: 2.8 g, 72 % (based on hydrated material) **Literature Value:** 71 %[10]

m.p: 260 ^oC (dec.) **Literature Value:** 260 ^oC[10]

^{1}H NMR (D_2O) δ (ppm): 5.04 ($H1_{\beta}$), 3.95 (H3), 3.92 ($H6_{a,b}$), 3.84 (H5), 3.60 (H2), 3.55 (H4), 3.40 (H4'), 3.02 ($H6'_{a}$), 2.81 ($H6'_{b}$, H10), 2.58 (H7), 1.54 (H8,H9)

^{13}C NMR (D_2O) δ (ppm): 101.75 (C1), 101.40 (C1') 83.43 (C4'), 81.01 (C4), 80.74(C4'') 72.98 (C3), 72.98 (C2'/C3'), 71.93 (C2), 71.93 (C5), 71.70 (C5'), 60.16 (C6), 49.29 (C7), 48.36 (C6'), 39.67 (C10), 26.62 (C9). 25.67 (C8)

FTIR (cm^{-1}) 1653 (complexed water), 1634 (N-H bending vibration), 1489, 1472 (C-H_2 scissoring mode of aminoalkane group), 816 (N-H wag)*

Raman (cm^{-1}) 3534 (N-H stretch)*

*These are new bands relative to β-CD

^{1}HNMR

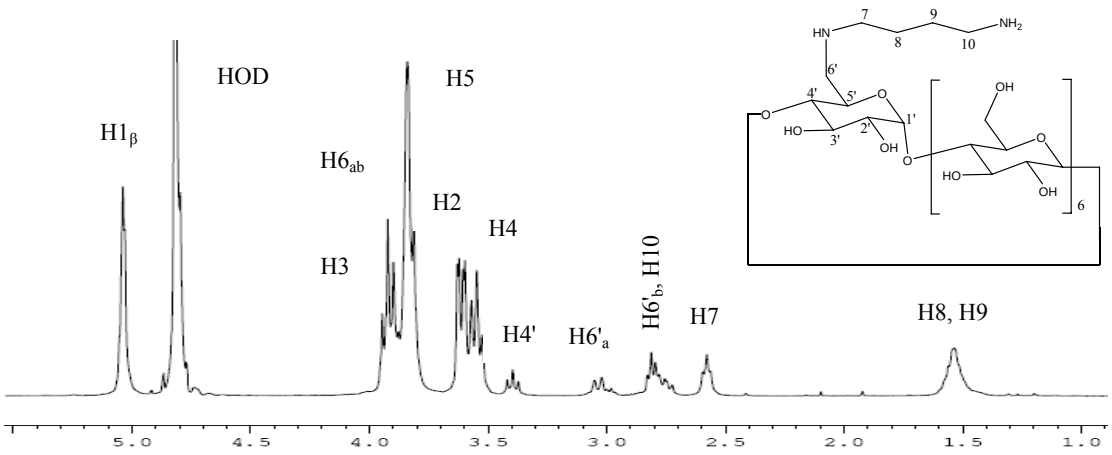

^{13}CNMR

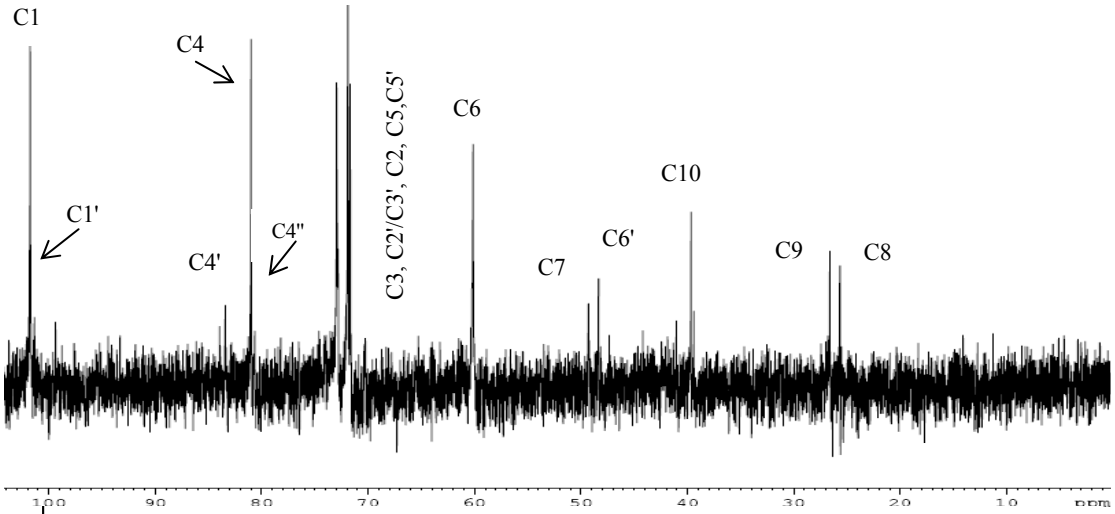

IR

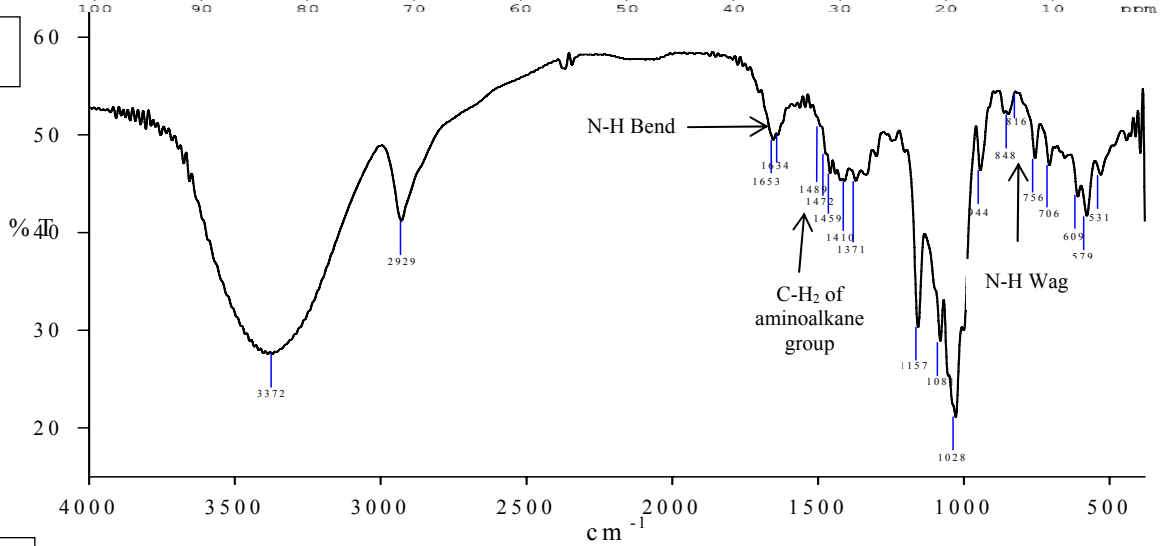

Raman

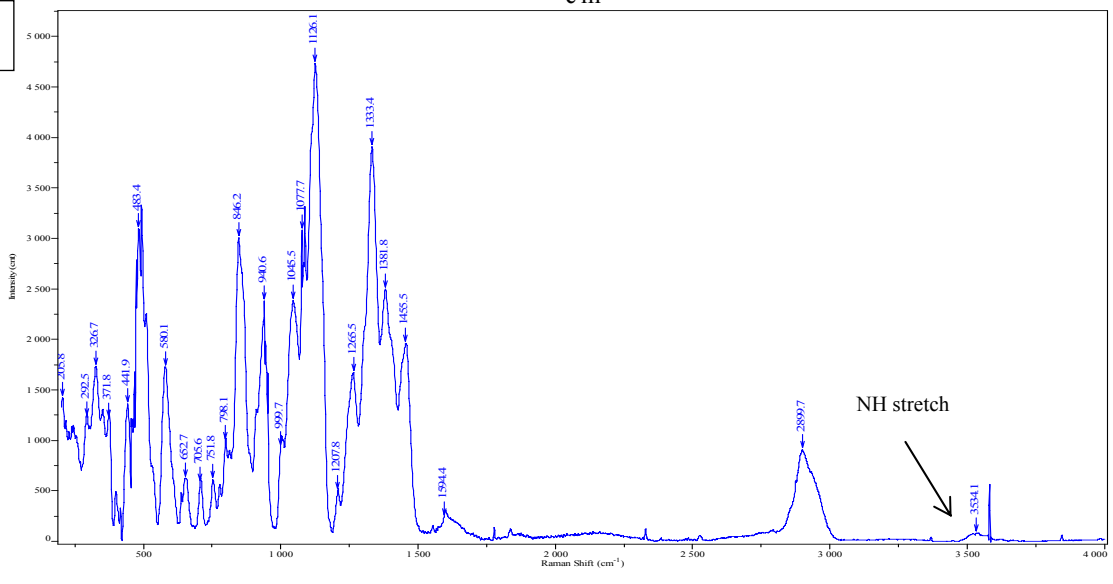

7.4 References

[1] S.E. Brown, J.H. Coates, D.R. Coglan, C.J. Easton, S.J. van Eyk, W. Janoski, A. Lepore, S.F. Lincoln, Y. Luo, B.L. May, D.S. Schiesser, P. Wang and M.L. Williams: *Aust. J. Chem*. **46**, (1993) 953

[2] C. Bertolla, L. Pochet and B Masereel: *Proceedings of the 12th International Cyclodextrin Symposium*, Montpellier, France, May 2004.

[3] N. Zhong, H.S. Byun and R. Bittman: *Tet. Lett*. **39**, (1998) 2919

[4] B. Brady, N. Lynam, T. O' Sullivan, C. Ahern and R. Darcy: *Org. Syn*. **77**, (2000) 220

[5] H.S Byun, N. Zhong and R. Bittman: *Org. Syn*. **77**, (1999) 225

[6] C.J. Easton and S.F. Lincoln: *Modified Cyclodextrins; Scaffolds and Templates for Supramolecular Chemistry*, Imperial College Press, London (1999)

[7] A.P. Singh, P.R. Cabrer, E. Alvarez-Parrilla, F. Meijide and J.V. Tato: *J. Incl. Phenom. Macro:* **35**, (1999) 335

[8] C.F. Potter, N.R. Russell and M. McNamara: *J. Inclusion Phenom. Macrocyclic Chem.* **56**, (2006) 395

[9] Y. Matsui, T. Yokoi and K. Mochida: *Chem. Lett.* **10,** (1976) 1037

[10] A. Capretta, R.B. Maharajh and R.A. Bell: *Carbohydr. Res.* **267**(1), (1995) 49

8. Appendix

8.1 Electronic Spectroscopy

1

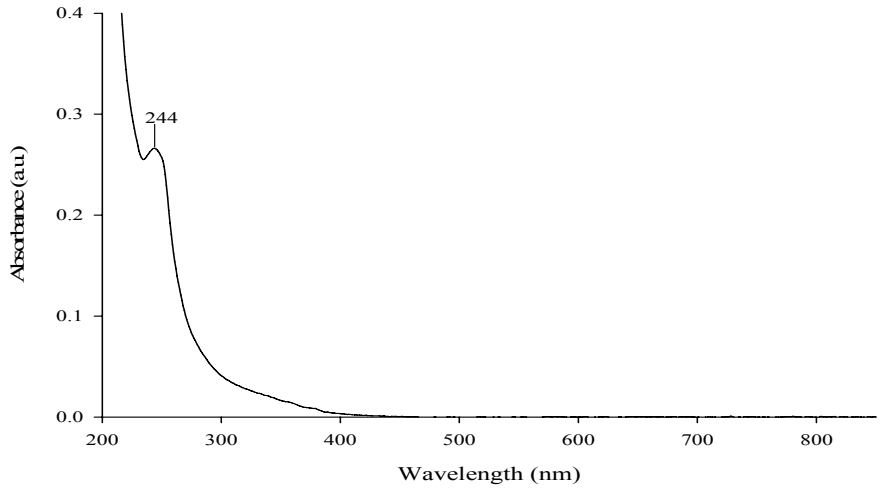

2

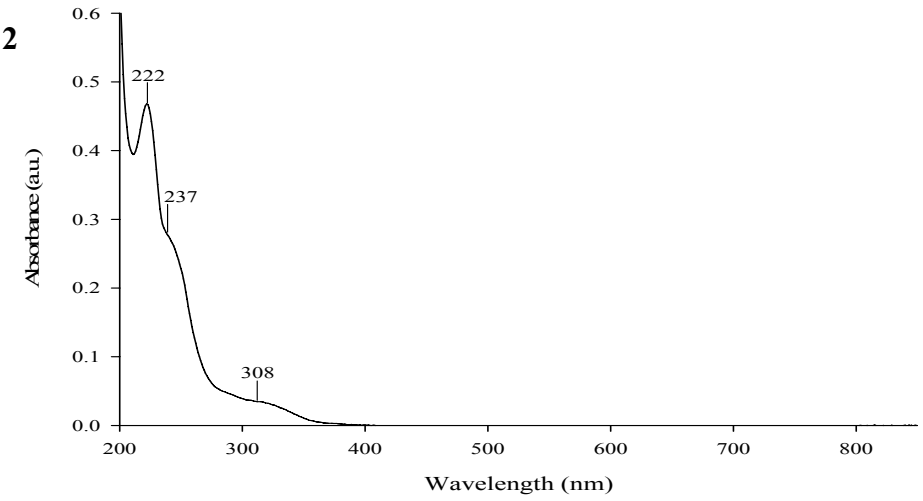

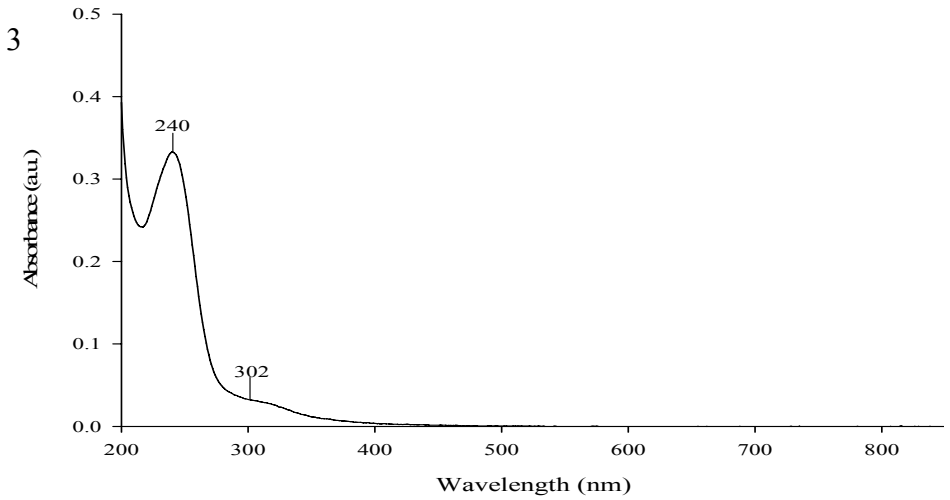

Figure 8.1 Electronic spectra of 1) CDEn, 2) CDPn and 3) CDBn 0.002 M in 0.01 M phosphate buffer pH 7.2 (10 mm cell)

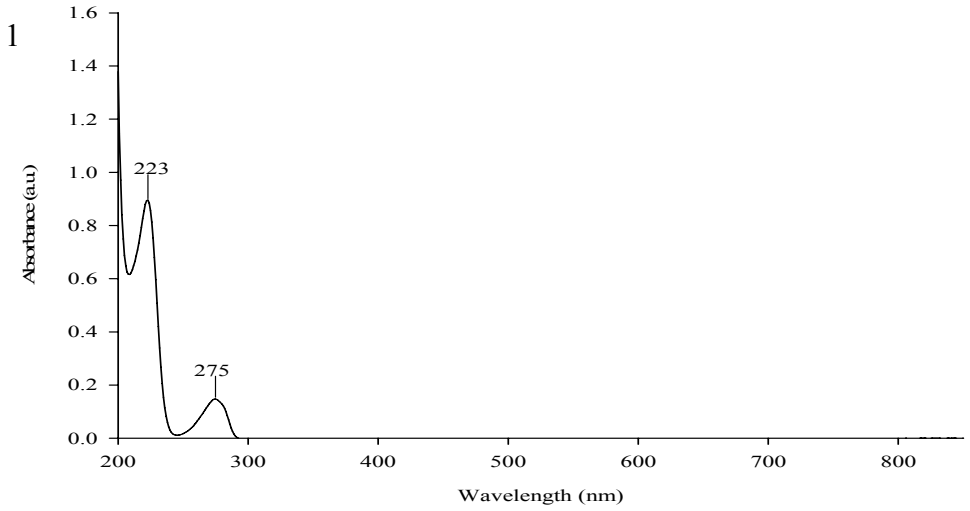

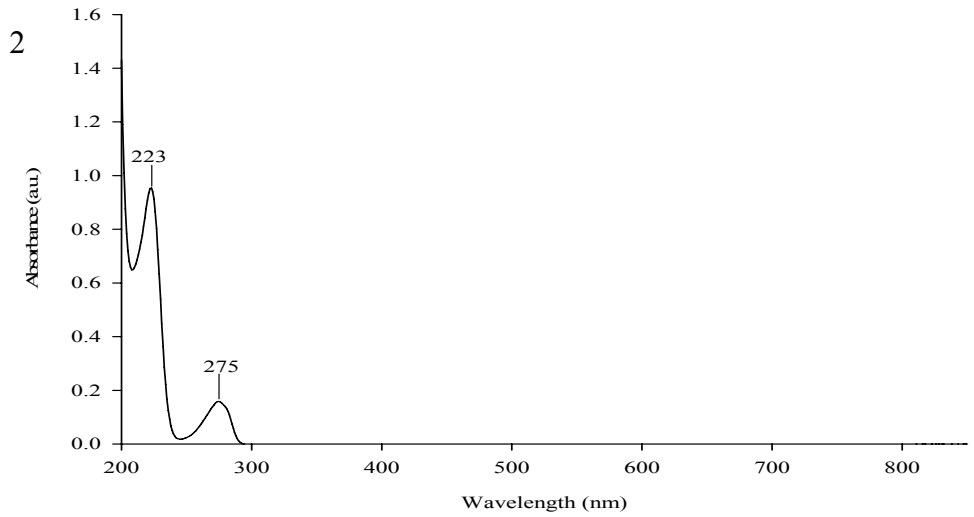

Figure 8.2 Electronic spectra of 1) L-tyrosine and 2) D-tyrosine 0.001 M in 0.01 M phosphate buffer pH 7.2 (1mm cell)

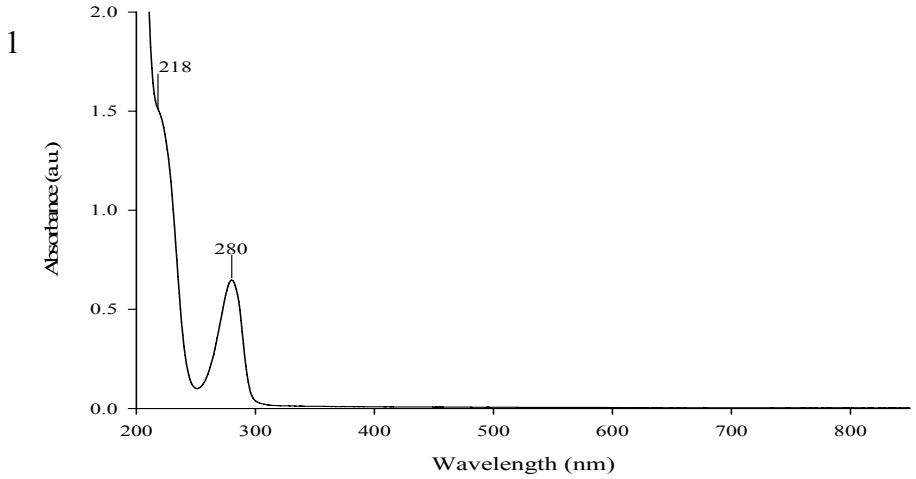

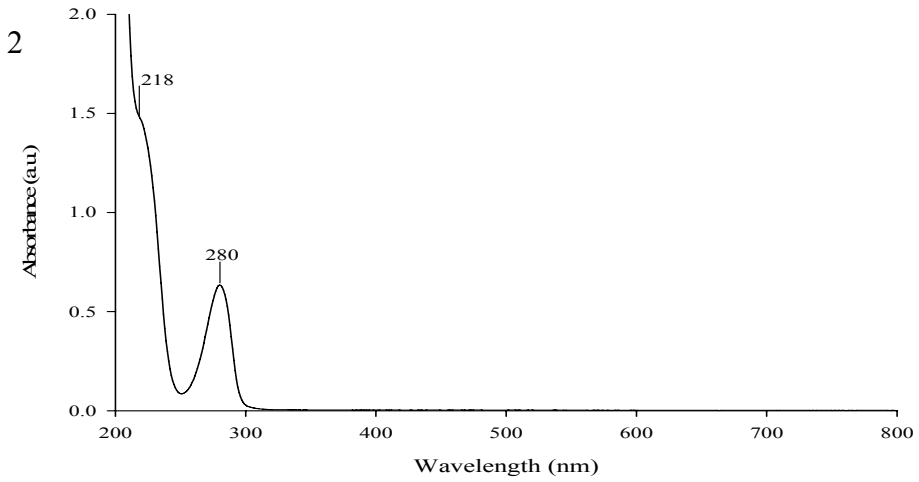

Figure 8.3 Electronic spectra of 1) L-DOPA and 2) D-DOPA 0.002 M in 0.01 M phosphate buffer pH 7.2 (1mm cell)

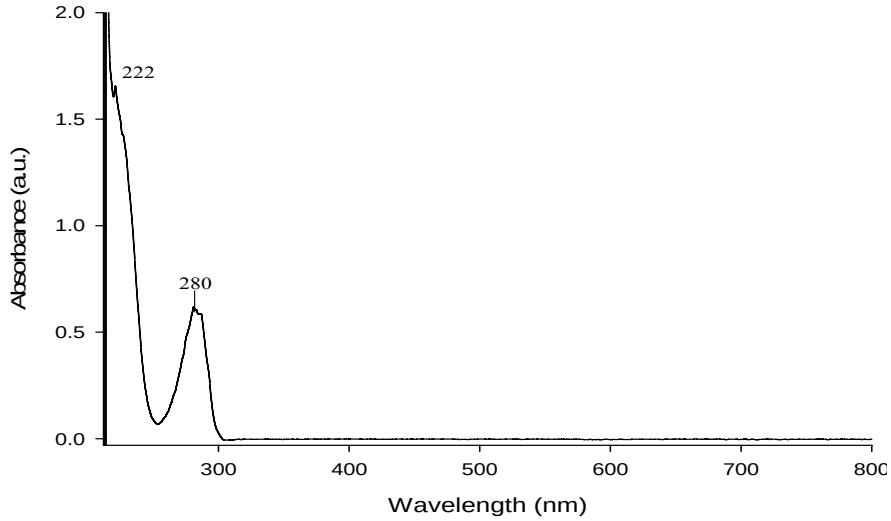

Figure 8.4 Electronic spectrum of L-carbidopa 0.002 M in 0.01 M phosphate buffer pH 7.2 (1mm cell)

Table 8.1 λ_{max} and ε values for the CD derivatives, guests and binary complexes at pH 7.2

Host	**λ_{max} (nm)**	**ε (mol^{-1} dm^3 cm^{-1})**
CDEn	244	27
CDPn	308	4
	237	28
	222	47
CDBn	302	3
	240	33
Ligand/Guest		

L-Tyrosine	275	1477
	223	8966
D-Tyrosine	275	1586
	223	9548
L-DOPA	280	3240
	218	7556
D-DOPA	280	3171
	218	7435
Binary Complex		
$[Cu(CDEn)]^{2+}$	671	69
	254	4557
$[Cu(CDPn)]^{2+}$	716	79
	250	3143
	230	2958
$[Cu(CDBn)]^{2+}$	731	70
	242	2179

8.2 Stoichiometry of Complexes

Table 8.2 Results of spectral titration of Cu(II) with CDEn

Sample	*0.002 M Cu (µl)*	*0.002 M CDEn (µl)*	*Total (µl)*	*Absorbance (650 nm)*	*[Cu]/ [Cu+CDEn]*
1	0	2000	2000	0.0066	0.0
2	100	1900	2000	0.0077	0.05
3	200	1800	2000	0.0190	0.10
4	300	1700	2000	0.0248	0.15
5	400	1600	2000	0.0280	0.20
6	500	1500	2000	0.0325	0.25
7	600	1400	2000	0.0315	0.30
8	700	1300	2000	0.0469	0.35
9	800	1200	2000	0.0499	0.40
10	900	1100	2000	0.0505	0.45
11	1000	1000	2000	0.0526	0.50
12	1100	900	2000	0.0488	0.55
13	1200	800	2000	0.0462	0.60
14	1300	700	2000	0.0394	0.65
15	1400	600	2000	0.0383	0.70
16	1500	500	2000	0.0336	0.75
17	1600	400	2000	0.0289	0.80
18	1700	300	2000	0.0231	0.85
19	1800	200	2000	0.0183	0.90
20	1900	100	2000	0.0120	0.95
21	2000	0	2000	0.0080	1.0

Table 8.3 Results of spectral titration of Cu(II) with D-Tyr

Sample	*0.002 M Cu (µl)*	*0.002 M D-Tyr (µl)*	*Total (µl)*	*Absorbance (250 nm)*	*[Cu]/ [Cu +D-Tyr]*
1	1500	0	1500	0.0000	0
2	1200	300	1500	0.0328	0.2
3	1050	450	1500	0.0487	0.3
4	900	600	1500	0.0612	0.4
5	750	750	1500	0.0730	0.5
6	600	900	1500	0.0851	0.6
7	450	1050	1500	0.0828	0.7
8	300	1200	1500	0.0687	0.8
9	0	1500	1500	0.0000	1

Table 8.4 Results of spectral titration of Cu(II) with L-Tyr

Sample	*0.002 M Cu (µl)*	*0.002 M D-Tyr (µl)*	*Total (µl)*	*Absorbance (250 nm)*	*[Cu]/ [Cu +D-Tyr]*
1	1500	0	1500	0.0000	0
2	1200	300	1500	0.0245	0.2
3	1050	450	1500	0.0362	0.3
4	900	600	1500	0.0405	0.4
5	750	750	1500	0.0552	0.5
6	600	900	1500	0.0654	0.6
7	450	1050	1500	0.0730	0.7
8	300	1200	1500	0.0545	0.8
9	0	1500	1500	0.0000	1

Table 8.5 Results of spectral titration of CuCDEn with D-Tyr

Sample	*0.002 M Cu (µl)*	*0.002 M D-Tyr (µl)*	*Total (µl)*	*Absorbance (250 nm)*	*[Cu]/ [Cu +D-Tyr]*
1	1500	0	1500	0.0000	1
2	1350	150	1500	0.0205	0.9
3	1200	300	1500	0.0323	0.8
4	1050	450	1500	0.0657	0.7
5	900	600	1500	0.0692	0.6
6	750	750	1500	0.0656	0.5
7	600	900	1500	0.0559	0.4
8	450	1050	1500	0.0379	0.3
9	300	1200	1500	0.0204	0.2
10	150	1350	1500	0.0000	0.1
11	0	1500	1500	0.0000	0

Table 8.6 Results of spectral titration of CuCDEn with L-Tyr

Sample	*0.002 M Cu (µl)*	*0.002 M L-Tyr (µl)*	*Total (µl)*	*Absorbance (250 nm)*	*[Cu]/ [Cu +L-Tyr]*
1	1500	0	1500	0.0000	1
2	1200	300	1500	0.0149	0.8
3	900	600	1500	0.0624	0.6
4	750	750	1500	0.0647	0.5
5	600	900	1500	0.0696	0.4
6	450	1050	1500	0.0550	0.3
7	300	1200	1500	0.0347	0.2
8	0	1500	1500	0.0000	0

Table 8.7 Results of spectral titration of Cu(II) with D-DOPA

Sample	*0.002 M Cu (µl)*	*0.002 M D-DOPA (µl)*	*Total (µl)*	*Absorbance (709 nm)*	*[Cu]/ [Cu +DOPA]*
1	0	2000	2000	6.5700e-4	0
2	100	1900	2000	6.4142e-3	0.05
3	200	1800	2000	0.0103	0.1
4	300	1700	2000	0.0209	0.15
5	400	1600	2000	0.0158	0.2
6	500	1500	2000	0.0203	0.25
7	600	1400	2000	0.0212	0.3
8	700	1300	2000	0.0299	0.35
9	800	1200	2000	0.0302	0.4
10	900	1100	2000	0.0315	0.45
11	1000	1000	2000	0.0306	0.5
12	1100	900	2000	0.0319	0.55
13	1200	800	2000	0.0306	0.6
14	1300	700	2000	0.0297	0.65
15	1400	600	2000	0.0276	0.7
16	1500	500	2000	0.0252	0.75
17	1600	400	2000	0.0208	0.8
18	1700	300	2000	0.0177	0.85
19	1800	200	2000	0.0112	0.9
20	1900	100	2000	6.7488e-3	0.95
21	2000	0	2000	0.0000	1

Table 8.8 Results of spectral titration of Cu(II) with L-DOPA

Sample	*0.002 M Cu (µl)*	*0.002 M L-DOPA (µl)*	*Total (µl)*	*Absorbance (709 nm)*	*[Cu]/ [CU+DOPA]*
1	0	2000	2000	1.9020e-3	0
2	100	1900	2000	7.9010e-3	0.05
3	200	1800	2000	9.1300e-3	0.1
4	300	1700	2000	0.0135	0.15
5	400	1600	2000	0.0165	0.2
6	500	1500	2000	0.0159	0.25
7	600	1400	2000	0.0256	0.3
8	700	1300	2000	0.0313	0.35
9	800	1200	2000	0.0365	0.4
10	900	1100	2000	0.0380	0.45
11	1000	1000	2000	0.0401	0.5
12	1100	900	2000	0.0408	0.55
13	1200	800	2000	0.0394	0.6
14	1300	700	2000	0.0392	0.65
15	1400	600	2000	0.0402	0.7
16	1500	500	2000	0.0316	0.75
17	1600	400	2000	0.0300	0.8
18	1700	300	2000	0.0148	0.85
19	1800	200	2000	0.0121	0.9
20	1900	100	2000	5.3850e-3	0.95
21	2000	0	2000	0.0000	1

Table 8.9 Results of spectral titration of CuCDEn with D-DOPA

Sample	*0.002 M D-DOPA (µl)*	*0.002 M CuCDEn (µl)*	*Total (µl)*	*Absorbance (650 nm)*	*[CuCDEn]/ [CuCDEn+D-DOPA]*
1	0	2000	2000	0.0000	1
2	100	1900	2000	0.0213	0.95
3	200	1800	2000	0.0387	0.9
4	300	1700	2000	0.0524	0.85
5	400	1600	2000	0.0771	0.8
6	500	1500	2000	0.0814	0.75
7	600	1400	2000	0.0903	0.7
8	700	1300	2000	0.0893	0.65
9	800	1200	2000	0.0848	0.6
10	900	1100	2000	0.0880	0.55
11	1000	1000	2000	0.0509	0.5
12	1100	900	2000	0.0406	0.45
13	1200	800	2000	0.0430	0.4
14	1300	700	2000	0.0308	0.35
15	1400	600	2000	0.0266	0.3
16	1500	500	2000	0.0195	0.25
17	1600	400	2000	0.0135	0.2
18	1700	300	2000	8.1920e-3	0.15
19	1800	200	2000	5.8297e-3	0.1
20	1900	100	2000	3.4714e-3	0.05
21	2000	0	2000	0.0000	0

Table 8.10 Results of spectral titration of CuCDEn with L-DOPA

Sample	*D-DOPA (µl)*	*CuCDEn (µl)*	*Total (µl)*	*Absorbance (650 nm)*	*[CuCDEn]/ [L-DOPA]*
1	0	2000	2000	0.0000	1
2	100	1900	2000	0.0182	0.95
3	200	1800	2000	0.0336	0.9
4	300	1700	2000	0.0454	0.85
5	400	1600	2000	0.0700	0.8
6	500	1500	2000	0.0683	0.75
7	600	1400	2000	0.0651	0.7
8	700	1300	2000	0.0666	0.65
9	800	1200	2000	0.0586	0.6
10	900	1100	2000	0.0563	0.55
11	1000	1000	2000	0.0420	0.5
12	1100	900	2000	0.0365	0.45
13	1200	800	2000	0.0301	0.4
14	1300	700	2000	0.0289	0.35
15	1400	600	2000	0.0160	0.3
16	1500	500	2000	0.0225	0.25
17	1600	400	2000	9.1800e-3	0.2
18	1700	300	2000	0.0152	0.15
19	1800	200	2000	3.8900e-3	0.1
20	1900	100	2000	7.5950e-3	0.05
21	2000	0	2000	0.0000	0

Table 8.11 Results of spectral titration of Cu with L-carbidopa

Sample	*0.002 M Cu (µl)*	*0.002 M carbidopa (µl)*	*Total (µl)*	*Absorbance (500 nm)*	*[Cu]/ [Cu+carbidopa]*
1	2000	0	2000	0.0000	1
2	1900	100	2000	0.1266	0.95
3	1800	200	2000	0.1704	0.90
4	1700	300	2000	0.2310	0.85
5	1600	400	2000	0.2492	0.80
6	1500	500	2000	0.2610	0.75
7	1400	600	2000	0.2662	0.70
8	1300	700	2000	0.2706	0.65
9	1200	800	2000	0.2864	0.60
10	1100	900	2000	0.2824	0.55
11	1000	1000	2000	-	0.50
12	900	1100	2000	0.2638	0.45
13	800	1200	2000	0.3079	0.40
14	700	1300	2000	0.2769	0.35
15	600	1400	2000	0.2241	0.30
16	500	1500	2000	0.1769	0.25
17	400	1600	2000	0.1468	0.20
18	300	1700	2000	0.1437	0.15
19	200	1800	2000	0.1035	0.10
20	100	1900	2000	0.0497	0.05
21	0	2000	2000	0.0000	0

Table 8.12 Results of spectral titration of CuCDEn with L-carbidopa

Sample	*L-carbidopa (µl)*	*CuCDEn (µl)*	*Total (µl)*	*Absorbance (450 nm)*	*[CuCDEn]/ [L-carbidopa]*
1	0	2000	2000	0.00E+00	1
2	100	1900	2000	2.59E-02	0.95
3	200	1800	2000	4.42E-02	0.9
4	300	1700	2000	4.40E-02	0.85
5	400	1600	2000	5.05E-02	0.8
6	500	1500	2000	6.10E-02	0.75
7	600	1400	2000	5.43E-02	0.7
8	700	1300	2000	5.53E-02	0.65
9	800	1200	2000	5.40E-02	0.6
10	900	1100	2000	5.05E-02	0.55
11	1000	1000	2000	4.82E-02	0.5
12	1100	900	2000	4.30E-02	0.45
13	1200	800	2000	4.22E-02	0.4
14	1300	700	2000	4.26E-02	0.35
15	1400	600	2000	3.63E-02	0.3
16	1500	500	2000	2.98E-02	0.25
17	1600	400	2000	2.22E-02	0.2
18	1700	300	2000	2.01E-02	0.15
19	1800	200	2000	1.37E-02	0.1
20	1900	100	2000	8.10E-03	0.05
21	2000	0	2000	0.00E+00	0

8.3 Circular Dichroism

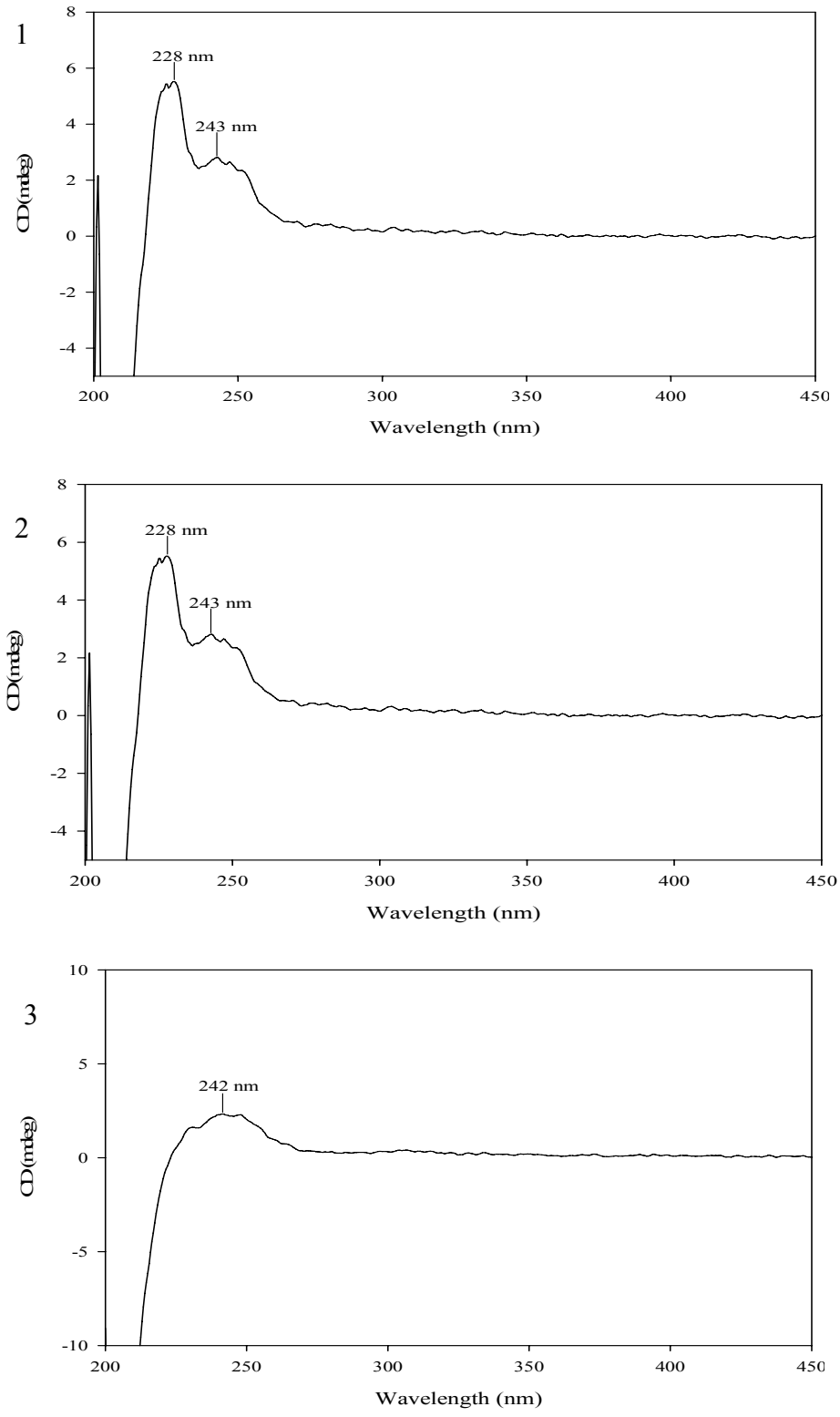

Figure 8.5 Circular dichroism spectra of 1) CDEn, 2) CDPn and 3) CDPn 0.002 M in phosphate buffer pH 7.2

1)

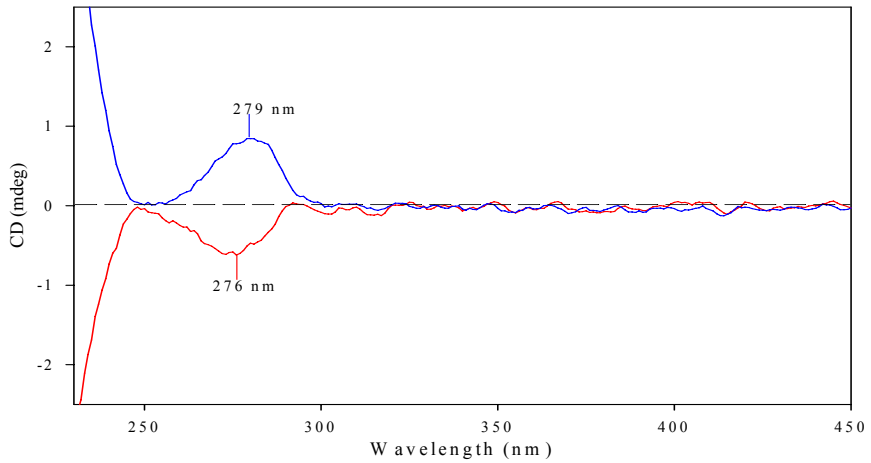

2)

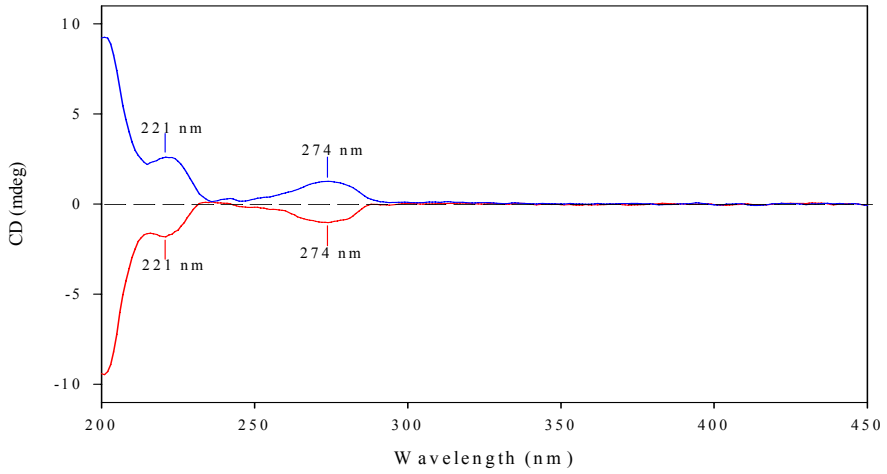

Figure 8.6 Circular dichroic spectra of 1) L,D- tyrosine (0.001 M) and 2) L,D-DOPA (0.002 M) in phosphate buffer pH 7.2